Using Magneto-Rheological Dampers in Semiactive Tuned Vibration Absorbers to Control Structural Vibrations

by

Jeong-Hoi Koo

Dissertation submitted to the Faculty of the

Virginia Polytechnic Institute and State University

in partial fulfillment of the requirements for the degree of

Doctor of Philosophy

in

Mechanical Engineering

Approved:

_____

Dr. Mehdi Ahmadian, Co-Chairman

_____ _____

Dr. Mehdi Setareh, Co-Chairman Dr. Thomas M. Murray

_____ _____

Dr. Donald Leo Dr. Mary Kasarda

July 23, 2003

Blacksburg, Virginia

Keywords: Magnetorheological, Magneto-Rheological, MR Damper, Tuned Mass Damper, TMD, Tuned Vibration Absorber, TVA, Groundhook, Semiactive, Semiactive Control, Vibrations, Floor Vibrations, Human Vibrations, Jeong-Hoi Koo

Using Magneto-Rheological Dampers in Semiactive Tuned Vibration Absorbers to Control Structural Vibrations

by
Jeong-Hoi Koo

Abstract

Since their invention in the early 1900s, Tuned Vibration Absorbers (TVAs) have shown to be effective in suppressing vibrations of machines and structures. A vibration absorber is a vibratory subsystem attached to a primary system. It normally consists of a mass, a spring, and a damper. Mounted to the primary system, a TVA counteracts the motions of the primary system, "absorbing" the primary structure's vibrations. A conventional passive TVA, however, is only effective when it is tuned properly, hence, the name "tuned" vibration absorber. In many practical applications, inevitable off-tuning (or mistuning) of a TVA occurs because of the system's operating conditions or parameter changes over time. For example, the mass in a building floor could change by moving furnishings, people gathering, etc., which can "off-tune" TVAs. When TVAs are off-tuned, their effectiveness is sharply reduced. Moreover, the off-tuned TVAs can excessively amplify the vibration levels of the primary structures; therefore, not only rendering the TVA useless but also possibly causing damage to the structures. Off-tuning is one of the major problems of conventional passive TVAs.

To cope with these problems, this study proposes a novel semiactive TVA, which strives to combine the best features of passive and active TVA systems. The semiactive TVA in this study includes a Magneto-Rheological (MR) damper that is used as a controllable damping element, for providing the real-time adjustability that is needed for improving the TVA performance.

This study is conducted in two phases. The first phase provides a numerical investigation on a two-degree-of-freedom (2-DOF) numerical model in which the primary structure is coupled with a TVA. The numerical investigation considers four semiactive control methods to regulate damping in the MR TVAs. Using numerical optimization techniques, the semiactive and equivalent passive TVA models are optimally tuned for equal comparison of their performance. Moreover, these tuned systems then serve as the basis for numerical parametric studies for further evaluation of their dynamic performance. The parametric study covers the effects of damping, as well as system parameter variations (off-tuning). The results indicate that semiactive TVAs are more effective in reducing the maximum vibrations of the primary structure and are more robust when subjected to off-tuning. Additionally, the numerical study identifies the "On-off Displacement-Based Groundhook control (on-off DBG)" as the most suitable control method for the semiactive TVA among control methods considered in this study.

For the second phase of this study, an experimental study is performed on a test setup, which represents a 2-DOF structure model coupled with an MR TVA. Using this setup, a series of tests are conducted in the same manner as the numerical study to evaluate the performance of the semiactive TVA. The primary purpose of the experiment is to further evaluate the most promising semiactive control methods. Furthermore, the

experiment serves as a "proof-of-concept" for the effectiveness of MR TVAs in floor vibration applications. The results indicate that the semiactive TVA with displacement-based groundhook control outperforms the equivalent passive TVA in reducing the maximum vibrations of the primary structure. This confirms the numerical result that identifies on-off DBG control method as the "best" control method for the MR TVA among the four semiactive control schemes considered. An experimental off-tuning study is also conducted, focusing on the dynamic performance of both the passive and the semiactive TVAs when the mass of the primary system changes (mass off-tuning). The mass of the primary system varied from –23 % to +23 % of its nominal value by adding and removing external mass. The experimental results show that the semiactive TVA is more robust to changes in the primary mass than the passive TVA.

Results of this research justify the benefits of the use of semiactive MR TVAs in controlling structural vibrations, such as building floor vibrations. The off-tuning analysis further suggests that, in practice, semiactive TVAs should be tuned slightly less than their optimum in order to compensate for any added mass to the structure. Additionally, the lessons learned from the experimental study have paved the way for implementing the semiactive MR TVA on a full-scale floor.

Acknowledgements

I would like to thank my advisors Dr. Mehdi Ahmadian and Dr. Mehdi Setareh for their patience and guidance throughout my time as a Ph.D. student. Their enthusiasm and interest in the work of all their students is encouraging. I would also like to thank to Dr Thomas Murray, Dr. Donald Leo, and Dr. Mary Kasarda for serving on my graduate committee. The financial support by the National Science Foundation and the generous contributions by Lord Corporation are greatly appreciated.

I would like to thank Fernando Goncalves, ,Jim Poynor, Dave Simon, for their contributions to my work. Each of them offered a valuable bit of assistance for which I am truly grateful. I am thankful to all my current and former AVDL labmates for their companionship and memories.

I would like to thank my family and friends for their love and support. I would like to express my deepest gratitude to my parents, ChungSeo Koo and KaeJa Choi, and my parents-in-law, SaeKeun Yook and YoungJoo Kwon. Brothers and sisters in Korean Baptist Church of Blacksburg deserve my thanks for their prayers and love. I would especially like to thank my wife, Eunsun, for her encouragement, patience, and friendship. Most importantly, I would like to give all my thanks to God who loves me.

Contents

List of Figures

List of Tables

Chapter 1 Introduction

This chapter begins with the motivation for the work that is presented in this dissertation. After stating the objectives and approach to this research, it covers the contributions of this study. The chapter ends with an outline of this dissertation.

1.1 Problem Statement

Excessive floor vibrations are becoming common problems in offices, apartments, shopping centers, etc. They are not only annoying to the occupants, but also cause an unsuitable environment for sensitive equipment. Excessive floor vibrations can be characterized as too large for sensitive equipment or too large for occupant comfort. Because humans are sensitive to vibrations, floor vibrations in the order of 1 mm can be annoying. These can occur in a system that is perfectly sound from a strength standpoint. Therefore, controlling these floor motions is a serviceability or human comfort issue, rather than a safety issue [1].

Most floors with excessive vibrations have low natural frequencies, generally less than 10 Hz [2]. According to human comfort studies for automobiles and aircraft, humans are more sensitive to the vibrations in the frequency range of 4 and 8 Hz [3], which coincides with the human body's mid-section resonant frequency. Recently, low frequency floors have become common because of the use of lighter, higher strength building materials, and new design methods. Moreover, because today's virtually paperless electronic offices require less heavy office furniture, such as bookcases and file cabinets, the effective mass of floors has decreased. These lighter floors have less inherent damping. Another reason that low frequency floors have become more common is increased floor span length. Additionally, fewer full-height partitions decrease damping, which add to the problems. More recently, serious floor vibration problems have occurred because of increasing rhythmic activities (for example, aerobics, dancing, and indoor jogging), as well as the mixed use of modern buildings (for instance, an office area combined with a health club, areas for handling goods and even transportation terminals).

Floor vibrations can result from a variety of sources, including machinery and occupants. These problematic floor systems can be resonated by dynamic forces induced by human activities, such as walking and jumping. While steady-state vibrations from machinery can be eliminated using isolation techniques, transient vibrations caused by occupants cannot be isolated. Thus, human motion is the main source of excessive floor vibrations, and remedial methods for reducing unwanted floor vibrations are crucial. Figure 1-1 is adapted from the TechWatch section in the January 2002 issue of *Popular Mechanics*. This issue introduces human-induced floor vibrations as a growing serviceability problem, and discusses some corrective methods for this problem.

Figure 1-1. Correcting Human-Induced Floor Vibration Problems [4]

Remedial measures for problematic floor systems can be disruptive, difficult, and costly. Traditional methods, such as installation of full height partitions or damping posts, framing member stiffening, and mass reduction are costly, limited, and can be disruptive if the structure is already occupied. There have been several attempts to use tuned mass dampers (TMDs) to address this problem. However, floor vibration applications have had limited success because conventional passive TVAs are effective only in a narrow frequency band, and tend to off-tune as the dynamic characteristics of floor systems vary with time. Active control systems have been considered as a means to reduce floor vibrations, but disadvantages such as cost and the need for frequent maintenance limit their use. In general, there has been limited success in finding corrective measures for floor vibration problems.

This research proposes a new semiactive TVA as an alternative means for reducing excessive floor vibrations. Typically, semiactive systems have provided excellent solutions in many engineering problems because they combine the simplicity of passive systems with the real-time control and adaptability of active systems. This study will use a versatile Magneto-Rheological (MR) damper in a conventional TVA to realize a semiactive TVA system.

1.2 Research Scope and Objectives

The nature of this research is multidisciplinary because it deals with a mechanical engineering component (semiactive MR TVA) as well as a civil engineering component (floor system). The scope of the current study is to perform this research in a mechanical engineering perspective. In other words, this study will focus on the development of the semiactive MR system and the dynamic evaluation of the system, which will support the civil engineering aspect of floor vibration research (full-scale laboratory floor tests).

Therefore, this research intends to develop a new class of semiactive TVA that uses an MR damper, which surpasses the performance of a passive TVA. It also intends to assess the comprehensive dynamics of the new system. The primary objectives of this study can be summarized as follows:

(1) evaluate, both analytically and experimentally, the dynamics of semiactive MR TVAs with various semiactive control polices that can provide better performance than conventional passive TVAs,

(2) investigate the ability of semiactive MR TVAs to robustly adapt to primary structures' parameter changes, which is critical in determining the effectiveness of semiactive TVAs to structural vibration control, and

(3) suggest effective guidelines for the use of MR semiactive TVAs in floor vibration applications.

1.3 Approach

There are two distinct phases in this investigation. The first phase is a numerical investigation, which is performed on a two-degree-of-freedom (2-DOF) numerical model in which the primary structure is coupled with a TVA. The numerical investigation considers four different control polices for the semiactive TVA and an equivalent passive TVA. These numerical models are optimally tuned using numerical optimization techniques to equally compare each TVA system. These tuned systems then serve as the basis for numerical parametric studies for further evaluation of the dynamic performance. The parametric study covers the effects of damping parameter changes, as well as system off-tuning.

The second phase of this study is an experimental investigation. A test apparatus is used to represent a single-degree-of-freedom (SDOF) structure model coupled with an MR TVA. Using this test setup, a series of tests evaluate the effectiveness of the semiactive TVA in the same manner as the numerical investigation. The purpose of the experiment is to validate the analytical study and to serve as a "proof-of-concept" of the effectiveness of this MR TVA for floor vibration applications.

1.4 Contributions

The findings of this research will contribute to the development of a new class of semiactive TVAs for reducing vibrations in structures and mechanical systems. This semiactive MR TVA demonstrates superior performance in reducing the primary structure's vibration levels and proves to be more robust to system parameter changes than a passive TVA. Moreover, the semiactive MR TVA is more cost-effective and maintenance-free than a comparable active control system. Therefore, the current research is anticipated to contribute to broader applications of the semiactive MR system to mechanical and structural systems other than building floor structures.

More specific contributions of this research include:

- This research demonstrates optimal tuning of semiactive TVAs by using an optimization technique. The numerical optimization method used in this research will enable us to design TVAs and predict their performance.
- This study, numerically and experimentally, evaluated various semiactive control methods to identify a suitable semiactive control policy for TVA applications. Based on these results, it suggests an adequate control method for a semiactive MR TVA for reducing structural vibrations, such as floor vibrations.
- The experimental results will serve as a valuable "proof-of-concept" of semiactive MR TVAs for full-scale floor tests and field use.
- The outcomes of this research will be the foundation of further research into the use of semiactive TVAs for structural vibration control. Applications of semiactive TVAs with MR dampers can be extended to control wind-induced and earthquake-excited vibrations in buildings and.

1.5 Outline of the Dissertation

The next chapter, Chapter 2, offers the background and literature review. It covers some of past studies on floor vibrations and tuned vibration absorbers. It then discusses the necessary background information on MR dampers and semiactive damping control. Chapter 3 presents the dynamic analysis of semiactive TVAs using numerical models. This chapter investigates the use of numerical models to evaluate system dynamics. In search of a suitable semiactive control policy, four different semiactive control polices are evaluated. In addition, the results of the optimized TVAs will be presented. Chapter 4 further evaluates the dynamics of semiactive TVAs by performing parametric studies. The parametric studies include the effect of on/off-state damping changes, as well as system off-tuning due to changes in system parameters, such as the primary structure's mass. The experimental component of this research begins in Chapter 5 with a description of the test setup. This description includes a detailed description of a SDOF structure coupled with an MR TVA model and its mechanics. Furthermore, the actuation system used to excite the system is discussed, along with a data acquisition system used

to record the dynamic responses of the structure mass. Chapter 6 discusses experimental test results, presented in the same manner as the numerical model results. Finally, chapter 7 provides a summary of the work. Significant results are highlighted, and recommendations for future research are also discussed.

Chapter 2 Literature Review and Background

This chapter reviews earlier studies of floor vibrations and tuned vibration absorbers. In addition to providing a literature review, it also provides needed background information on Magneto-Rheological (MR) fluid dampers. This chapter concludes with an overview of semiactive control systems.

2.1 Floor Vibrations

The problem statement section in chapter 1 gave a brief overview of floor vibrations, discussing their nature and a few examples of corrective methods for them. Thus, this section focuses on summarizing the historical development of human comfort criteria for floor vibrations. It also discusses common remedial measures to reduce excessive floor vibrations.

2.1.1 Human Comfort Criteria

As mentioned earlier, excessive floor vibrations can be characterized as large motions for sensitive equipment or occupant comfort; thus, the problems are serviceability and human comfort issues. Most early studies of floor vibrations tried to outline criteria for human perceptibility to floor vibrations, rather than controlling the vibrations themselves [5]. For many years, researchers have tried to quantify human responses to floor motion. Moreover, determining these permissible levels has comprised an entire research area in itself. Table 2-1 chronologically lists human acceptance criteria for floor vibrations.

Table 2-1. A Chronological List of Human Acceptance Criteria for Floor Vibrations [6]

Year	Reference	Loading	Application	Comments
1931	Reiher and Meister	Steady State	General	Human response criteria
1966	Lenzen	Heel-drop	Office	Design criterion using Modified Reiher and Meister scale
1970	HUD	Heel-drop	Office	Design criterion for manufacturing housing
1974	ISO	Various	Various	Human response criteria
1974	Wiss and Parmelee	Footstep	Office	Human response criteria
1974	McCormick	Heel-drop	Office	Design criterion using Modified Reiher and Meister scale
1975	Murray	Heel-drop	Office	Design criterion using Modified Reiher and Meister scale
1976	Allen and Rainer	Heel-drop	Office	Design criterion using modified ISO scale
1981	Murray	Heel-drop	Office	Design criterion based on experience
1984	Ellingwood and Tallin	Walking	Commercial	Design criterion
1985	Allen et. al.	Crowds	Auditorium	Design criterion related to ISO scale
1986	Ellinwood et.al.	Walking	Commercial	Design criterion
1988	Ohsson	Walking	Residential/ Office	Lightweight Floors
1989	ISO 2231-2	Various	Buildings	Human response criteria
1989	Clifton	Heel-drop	Office	Design criterion
1989	Wyatt	Walking	Office/Residential	Design criterion based on ISO 2631-2
1990	Allen	Rhythmic	Gymnasium	Design criterion for aerobics
1993	Allen and Murray	Walking	Office/Commercial	Design criterion using ISO 2631-2

More recently, Murray et al. [6] published, *Floor Vibrations Due to Human Activity*, as part of The American Institute of Steel Construction's Steel Design Guide Series. In this design guide, they proposed a broader use of walking excitation criteria in modern buildings. Figure 2-1 shows their recommended peak acceleration limits for human comfort. This design guide also provides basic principles and simple analytical tools for evaluating steel framed floor systems and footbridges. Moreover, it offers

guidance on developing remedial measures for problematic floors, which will be discussed in the next section.

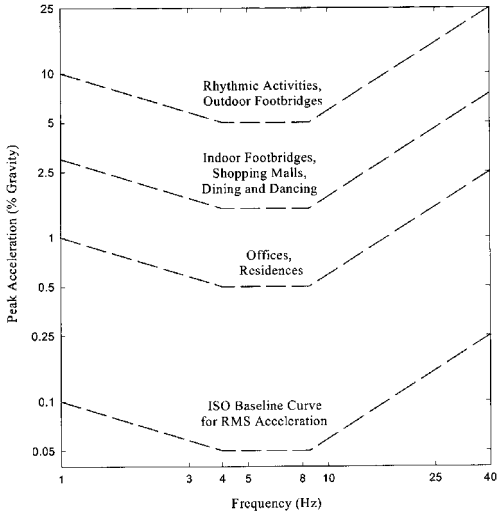

Figure 2-1. Recommended Peak Acceleration for Human Comfort for Vibrations due to Human Activities (Allen and Murray 1993; ISO 2631-2:1989)

2.1.2 Remedial Methods

Although structural engineers have many scales and criteria for evaluating floor designs before construction, there are still many floors with excessive levels of vibration. This section summarizes common remedial measures designed to mitigate unwanted floor vibrations based on the Design Guide [6].

2.1.2.1 Relocation

Relocation of the vibration source and/or a sensitive occupancy or sensitive equipment is the easiest and potentially cheapest corrective methods. Relocation examples include placing "vibration source facilities," such as a gym, in a ground floor instead of on the top floor of buildings and locating sensitive equipment near columns or walls where vibrations are less severe than at a mid-bay. However, these methods are not always possible.

2.1.2.2 Stiffening

Increasing structural stiffness can reduce human-induced vibrations, such as walking or rhythmic activities, because it increases the floor's natural frequency. Examples of stiffening include adding new column supports, adding cover plates or rods to the supporting joists and girders, and so on. These stiffening techniques are restricted by the layout of the structures and the space available in the structures. The Design Guide suggests welding or clamping a queen post hanger to the bottom flange of a beam or joist to effectively increase structural stiffness. It also presents more detailed techniques and examples with figures.

2.1.2.3 Damping Increase

Increasing the damping of the floor system can improve floor vibrations. It is effective only if damping is small in the existing floor system. Damping in existing floors depends primarily on the presence of non-structural components, such as partitions, ceilings, mechanical service lines, furnishings and on the number of people on the floor. Additions of these components provide some added damping to floors.

2.1.2.4 Passive Control

The use of tuned mass dampers (TMDs)* or tuned vibration absorbers (TVAs) is the best example of passive control. A TMD is effective only if its natural frequency is tuned to the frequency of the troublesome mode of floor vibration. However, TMDs, which are initially tuned, can become out-of-tune or off-tune due to changes in the floor's natural frequencies resulting from the addition or removal of materials, as well as presence of occupants. Thus, passive control of floors through TMDs has met with varying degrees of success. Nonetheless, TMDs are probably the least obtrusive of the remedial measures discussed so far because they can often be installed in ceilings or closets. Examples of TMDs to reduce floor vibrations will be discussed in more detail in the next section.

---

* This dissertation will use this term interchangeably with Tuned Vibration Absorbers (TVAs)

2.1.2.5 Active Control

According to Murray et al. [6], the active control of floor systems is in its developmental stage. Although the concept has been successfully demonstrated, no permanent installations yet exist. There are two reasons for this. The first is the relatively high initial cost. The second is that active control requires continuous electrical power and periodic maintenance. Webster and Vaicaitis [7] rejected the use of active mass damper systems to control vibrations of composite floor systems because of high installation cost and need for regular maintenance, which could not be ensured over the life of the structure. In spite of these shortcomings, Hanagan and Murray [8-10] successfully implemented active control to reduce vibration levels in lightweight floor systems. They developed a velocity feedback scheme, in which an electromagnetic proof-mass actuator was used to impart control forces on a floor system to reduce the amplitudes of the floor motion. For the laboratory floor experiments, their active system improved the floor response at the center of the floor, reducing the maximum velocity about by a factor of ten. Based on in-situ floor experiments, Hanagan and Murray concluded that the active system was less effective when the fundamental frequency of a floor system was below 5-6Hz.

In summary, several technologies are available but each one has the pros and cons. The "best" method to control floor vibrations requires cost-effectiveness and the least alteration to the original use of floors. One of the promising methods that can fulfill these demands is the use of semiactive control methods because they can surpass performance of passive systems without the disadvantages of active systems, such as high cost, and periodic maintenance. However, very little research on the use of semiactive systems has been done to correct floor vibration problems.

2.2 Tuned Vibration Absorbers

This section provides a general discussion of TVAs, including their concept and historical development. It also provides some applications of TVAs to structures, such as floors, footbridges, and buildings, to control human-induced, wind-induced, and earthquake-induced vibrations.

2.2.1 Overview of Tuned Vibration Absorbers

Among all vibration control devices, research on tuned vibration absorbers (TVAs) is, perhaps, the richest in terms of the total number of investigations and the time devoted to these investigations. Since their invention in the early 1900s, TVAs have effectively suppressed vibrations of machines and structures. A TVA is a vibratory subsystem attached to a primary system. It normally consists of a mass, a spring, and a damper. Mounted on the primary system, a TVA counteracts its motions by "absorbing" its vibrations. However, a conventional passive TVA is only effective when it is tuned properly, hence, the name "tuned" vibration absorber. Tuned mass damper (TMD) is another name for tuned vibration absorbers (TVAs) that is commonly used in civil engineering.

Tuned vibration absorbers have attracted the special and continued attention of many researchers and practitioners because of their ability to control vibrations caused by different types of forces. Den Hartog described the working principle of the device in his monograph [11], providing simple formulas to obtain the optimum tuning and damping parameters of a tuned vibration absorber to control the displacement of an undamped single-degree-of-freedom system subjected to a harmonic force. Warburton [12], among others, extended the Den Hartog's solution by considering the control of several other cases of excitation and responses. He also discussed the use and limitation of TVAs for multiple-degree-of-freedom systems. Among other researchers, Tsai and Lin [13] have extended the classical solution to a damped primary system. Using curve fitting, they have provided formulas to obtain the optimal parameters.

In many practical applications, off-tuning of a TVA occurs because of the inheritance of a system's operating conditions and system parameter changes over time. To cope with these problems, extensive studies over the past two decades have attempted to develop new designs and concepts for passive TVAs. These designs include adaptive, semiactive, and active TVAs. A comprehensive review of configurations, developments, and applications of TVAs can be found in the papers by Sun et al. [14], Housner et al. [15], Symans and Constaninou [16], and Soong and Spencer [17].

The application of TVAs has been extended to civil engineering structures, such as floors, tall buildings, and bridges. In such applications, the goal is to attenuate the vibrations due to human excitations in floors, and wind and seismic excitations in tall buildings and bridges [18-20]. Considerable attention has been given to the use of semiactive MR dampers in both vehicle and civil engineering applications, due to their low power requirements and failure-safe advantages [21-24]. Subsequent sections will review selected examples of TVAs to civil engineering applications.

2.2.2 Use of TVAs for Floor Vibration Control

The first use of TMDs for floor vibration applications was reported by Lenzen [25]. The absorber mass was simply tuned so that the natural frequency of the TMD was about 1.0 Hz less than that of the floor to be damped. Tests using the absorbers showed that the TMDs could reduce the vibration level from annoying to entirely satisfactory.

Allen and Swallow [26] used TVAs to reduce floor vibrations due to walking. The TVAs consisted of steel boxes, loaded with concrete blocks, and supported at each corner by a commercial compression spring and housing. They also reported on the use of damper posts, which simply involved connecting two successive floors with a special post. The construction was such that any relative motion between the two floors caused shearing of the rubber clamped between tongue and yoke, and consequently generated high damping.

Allen and Pernica [27] considered the problem of walking vibrations on an existing long-span floor structure. They proposed a special and simple TVA, consisting

of a wooden plank or layered system of planks with weights on top. The planks were supported by the bottom cords of steel joists or by the bottom flanges of steel beams.

Thornton et al. [28] reported the use of TVAs to control floor motions from gymnasium activities in a high school building. The gymnasium was located on the third floor of the building, and strongly perceptible floor motions were common for the second and third floors. This was because the frequency of a typical forcing function, which is about 2-2.5Hz, generated by synchronous activity (such as jumping jacks or aerobic dancing) nearly coincided with the natural frequency of the floor, resulting in an "almost-resonant" condition. Dynamic measurements showed that the first four modes of the third floor occurred at frequencies of 4.0, 4.6, 5.3, and 6.2 Hz, and the damping ratio was 1.7% for the first mode, and 0.9% for the second mode. Eight TVAs were designed to treat these four modes of vibration. The eight units were suspended from the concrete T-beams of the gym floor. Subsequent tests showed that the accelerations in the second and third floors were reduced by more than a factor of two.

Thornton et al. [28] also explored several remedial schemes to vibration problems in a seven-story college building. The building contained two bay areas: a fifth floor, double-height gym, and a ground floor, swimming pool, at the base of a double-height lobby. A pedestrian bridge over the pool served as the main entrance to the lobby. The second floor was used as office space, and the third floor was for locker rooms and showers. An exercise room and an aerobic dance studio were located in the fourth floor. Directly above the gym was the seventh floor, which served as offices and a large meeting room. The occupants reported excessive vibrations from the second floor up, especially during the high-impact aerobic sessions. Analysis and field-testing confirmed that the main vibration frequency of the structure were 4.75Hz. Moreover, the natural frequencies of the floors were close to 4.75 Hz. This frequency was excited by aerobic exercise, resulting in an almost-resonant condition.

To fix this problem, Thornton et al. developed four remedial schemes. Schemes 1 and 2 were to increase girder stiffness. The first scheme considered adding a steel truss below each girder; the second scheme used two diagonal members from the second to the first floor, shortening the girder spans. Remedial schemes 3 and 4 consisted of the use of

TMDs, which could minimize obstruction. The scheme 3 was installing several small TMD units at strategic locations throughout the building. Some units were placed on the floor or others were suspended from the beams below the fifth-floor gym. The scheme 4 was a partial solution, dealing only with seventh floor with two or more TMDs. This example illustrates that fixing floor vibration problems is complex because one must consider the building structure as a whole, not just the floor structure. Moreover, corrective measures are constrained because of many factors, such as cost and space available.

A series of papers by Setareh and Hanson [29-31] presented the design and implementation of TMDs on a balcony in an auditorium. During rock concerts, excessive vibrations occurred in the balcony section because of resonance of its first natural frequency. They used the Component Mode Synthesis (CMS) method to compute the response of the floor-TMD system using only a few natural modes of the floor. The CMS method was also used to tune TMDs for multiple-degree of freedom systems. They found that tuning parameters obtained using the CMS method ensured optimal TMDs' parameters regardless of closeness of the natural frequencies of the system. Finite element analysis was performed using SAP 80. Based on simulation results, three 4,000 lb TMDs were designed to control the first mode of vibrations and two 2,000 lb were designed to control the second mode of vibrations. They were both implemented onto the balcony. With the TMDs in place, the amplitudes of vibration were reduced by about 78%.

Webster and Vaicaities [32] used TVAs to control the floor vibration of a long-span cantilevered, composite floor system at the Terrace on the Park building in New York City. The floor was used as dining and dancing halls, and guests complained about the structure's vibrations. Preliminary vibration tests performed during dance events showed that the peak acceleration was 7% g (gravity), and the peak displacement was 0.13 inches. These were "unacceptable" for dining and dance floors, based on the human comfort criteria. The vibration tests further found that the first natural frequency was 2.3 Hz, which corresponds to the beat of music. The damping for the first mode ranged from 2.8% to 3.6%, and the TVA mass was 4.6% of the structure mass. They were placed at the four corners of the building, as close to the cantilevered ends as possible. The results

showed that the TMDs reduced the floor accelerations during dance events by at least 60%. Webster and Vaicaities commented the cost of constructing the four TMDs was less than 15% of the estimated construction cost of structural stiffening (with new columns between the ballroom floors and the ground).

In another case, prior to the completion of a museum building, the owner raised concerns with excessive floor vibrations caused by human footfall-induced excitation. The problematic floor, which was a gallery space, had a long span and open on two sides. Bell [33] used a TMD to fix this problem. Initial measurements of the floor response due to heel-drop impact indicated that the floor natural frequency was 3.7 Hz, the damping ratio was 1%, and the peak displacement was 0.2 mm. The TMD used to control the floor vibration had a mass ratio of 3.78%. Bell used fluid dashpots for damping and solid concrete blocks for the mass tuning. The installation of the TMD on the steel framing below the slab increased the damping by 580%. Bell reported that there were no complaints associated with floor vibrations after the museum was open.

Shope and Murray [34] reported the use of TMDs to improve the vibration characteristics of a laboratory and an office floors. The damping device was multi-celled, liquid filled TMD. The TMD consisted of a steel plate as the spring element, two stacks of steel plates which were used to adjust TMD's frequency. Instead of conventional dashpots, multi-celled, liquid filled bladders confined in two rigid containers were used as the damping element. For the laboratory floor experiments, they used four TMDs to control first two modes of vibrations that occurred at 7.3 Hz and 17 Hz. These TMDs almost eliminated vibrations caused by heel-drop impacts. When the floor was excited by a person walking along the mid-span, the TMDs reduced average peak accelerations from 0.06 g to 0.01 g. Shope and Murray also used fourteen TVAs to control several modes of vibration in the second floor of a new office building. The steel joist-concrete slab floor vibrated at frequencies ranging from 5.13 Hz to 6.5 Hz at the center of the bay. TMDs were installed to control the two most significant modes of vibrations. A major improvement in the floor response was shown by the acceleration time histories of the uncontrolled versus controlled floor vibrations. The authors reported that the occupants' responses were very positive to the effectiveness of the TMDs.

Rottmann [35] used TMDs to control three modes of vibration of various floors. For laboratory floor experiment, three prototype TMDs were used to control modes of vibration occurring at frequencies of 7.38 Hz, 9.38 Hz, and 16.75 Hz. The prototype TMDs decreased root-mean-square (RMS) accelerations that were caused by people walking perpendicular to the joists by a factor of 3.7; they decreased RMS accelerations that were caused by people walking parallel to the joists by a factor of 5.5. Prototype TMDs were also used to control anywhere from one to three modes of vibration on three different bays of an office floor. The frequencies that were of concern on those bays ranged from 4.25 Hz to 8 Hz. TMDs decreased RMS accelerations caused by walking by factors ranging from 1.23 to 1.75. Rottmann concluded that TMDs were more effective when the natural frequencies are well spaced (that is, at least 2 Hz between adjacent frequencies) or there was relatively small damping in a floor. Closely spaced natural frequencies (less than 2 Hz between adjacent frequencies) were difficult for the TMDs to control effectively.

In general, passive TVAs or TMDs have been used with varying degrees of success to mitigate unwanted floor vibrations. The next section provides applications of TVAs to other civil engineering structures.

2.2.3 Use of TVAs for Other Structures

In addition to floor applications, TVAs have been used in many civil engineering structures such as footbridges and buildings, where they suppress human-induced and wind-excited vibrations. They can also protect building structures from seismic hazards.

Several investigators have studied the use of TVAs for reducing annoying vibrations in footbridges. Matsumoto et al. [36] studied five footbridges that had problematic vibrations caused by foot traffic. Their results showed considerable reduction in the amplitude of vibrations. Bachmann and Weber [37] also reported the use of TVAs on a four span girder footbridge. They used two TVAs to control the fundamental mode of vibration. Their results showed that the acceleration due to walking was reduced by a factor of five; and the acceleration due to running was reduced by a factor of 2.9.

Although tuned vibration absorbers have been quite successfully used in several structures to control wind-induced vibrations, their use for seismic response control has received mixed reports from different investigators. Some investigators (Wirsching and Campbell [38]; Kitamura, et al [39]; Clark [40]; Soto-Brito and Ruiz [41]) have shown that tuned vibration absorbers can help control seismic responses, yet others (Gupta and Chandrasekaren [42]; Kaynia, et al, [43]; Sladek and Klinger [44]) disagreed. Chowdhury et al. [44] even claim that a single tuned vibration absorber could amplify higher mode vibrations. Without scrutinizing the details of these studies, it is not easy to identify the precise reason (or reasons) for these conflicting conclusions. However, Villaverde and his associate (Villaverde [46]; Villaverde and Koyama, [47]; Villaverde, [48]) offer, perhaps, the most convincing argument for these different findings. They observe that the primary reason for TVAs' ineffectiveness is the use of classical solutions that are not necessarily optimal for the particular situation under study. Optimal is the key word here. They suggest that the vibration absorber parameters must be tuned to increase the damping ratios of the dominant modes. For this, the absorber must be in resonance with its supporting structure, and its damping ratio must be equal to the structural damping ratio plus a term that depends on the generalized mass ratio and the modal displacement at the point where the damper is attached (Villaverde and Koyama [47]). To show the effectiveness of this tuned vibration absorber design procedure, Villaverade and Koyama offered several numerical results.

Sadek et al [49], however, further examined the approach suggested by Villaverde and Koyama [47] with an example of a tuned vibration absorber attached to a single-degree-of-freedom system. They observed that, except for very small mass ratios, Villaverde and Koyama's approach usually leads to unequal damping ratios in the two modes of the combined system, which is not as efficient as having two equal damping ratios in these modes. Based on an exhaustive numerical search of the eigenvalues of the state matrix of the combined structure and damper system for different values of the system parameters, they were able to identify the optimum tuning and damping ratio parameters that would produce two modes with nearly equal damping ratios. By curve fitting, they developed simple formulas to calculate these optimum parameters in terms of

the mass and damping ratios of the primary mass. They present several sets of numerical results to demonstrate the effectiveness of their design procedure.

Although several studies claim the effectiveness of passive tuned vibration absorbers for seismic applications, the main issue seems to be their ability to obtain optimal absorber parameters. Since seismic input is not as sustained as harmonic inputs, for which the absorbers can be precisely tuned, special arrangements are necessary to keep the system tuned to maintain its effectiveness.

In summary, the potential of TVAs are imminent. TVAs have been actively studied and installed in numerous structures to protect them from various excitations. Improved TVAs will continue to be adopted in many engineering areas.

2.3 Magneto-Rheological Dampers

This section provides an overview of MR fluids and MR dampers to better explain this research. It begins with brief characteristics of MR fluids, and explains how the fluids operate in dampers. This section also introduces different types of MR dampers.

2.3.1 MR Fluids

Magneto-Rheological fluids ("MR" fluids) are "smart materials" because their characteristics can be controlled through the application of a magnetic field. They are composed of oil (usually mineral or silicone based) and ferrous particles that are on the order of 0.05-10 microns in diameter [50]. Jacob Rabinow at the US National Bureau of Standards developed this fluid in the late 1940s [51]. Although similar in operation to electro-rheological (ER) fluids and ferrofluids, MR fluids are capable of achieving much higher yield strengths [52].

When it is not activated, MR fluid behaves like a free flowing liquid, with a consistency similar to that of motor oil. In the presence of an applied magnetic field, the ferrous particles become magnetic dipoles, which connect to each other along lines of magnetic flux, forming linear chains parallel to the field. This phenomenon solidifies the suspension oil and restricts the fluid movement, developing yield strength. The degree of

change is related to the magnitude of the applied magnetic field, and may occur in less than a few milliseconds.

Figure 2-2 illustrates this process. The ferrous particles are randomly dispersed in the medium when there is no magnetic field applied, as shown in Figure 2-2a. In the presence of a magnetic field, the particles start to move to align themselves along lines of magnetic flux (see Figure 2-2b). Figure 2-2c shows the formation of chains of ferrous particles, creating yield strength. Because this change occurs instantly, MR fluids are attractive for real-time control applications.

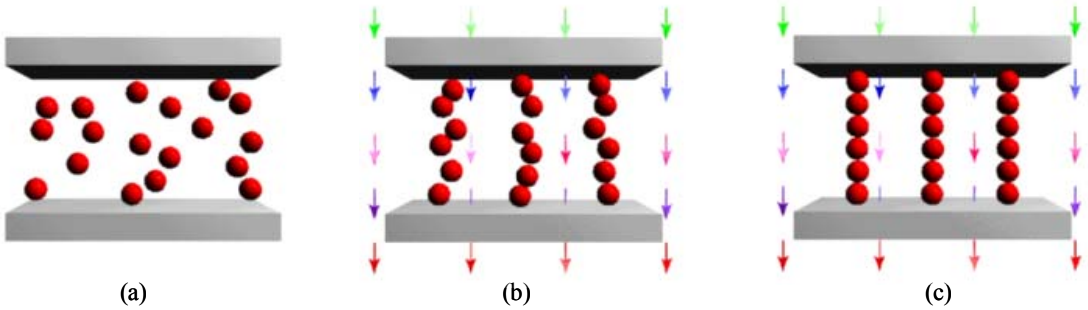

Figure 2-2. Illustration of Activation of MR Fluid: (a) No Magnetic Field Applied, (b) Magnetic Filed Applied, and (c) Ferrous Particles Formed [modified from 52]

2.3.2 Operation of MR fluids in MR dampers

Figure 2-3 shows a cross-section of a typical MR damper to explain the operation of MR fluid dampers. Unlike hydraulic dampers, MR dampers do not require mechanical valves to control flow. Instead, they have electromagnetic coils wound in their pistons, and MR fluid-filled reservoirs. Voltage in the electromagnet coils creates a magnetic field around the fluid gap between the housing and the piston. This study refers to the areas in which MR fluid is exposed to magnetic flux lines as "activation regions."

When the piston rod enters the housing, the MR fluids pass through the annular orifice gap to the other side of the reservoir. As in the damper depicted in Figure 2-3, there are two activation regions, which resist the flow of fluid from one side of the piston to the other when a magnetic field is present.

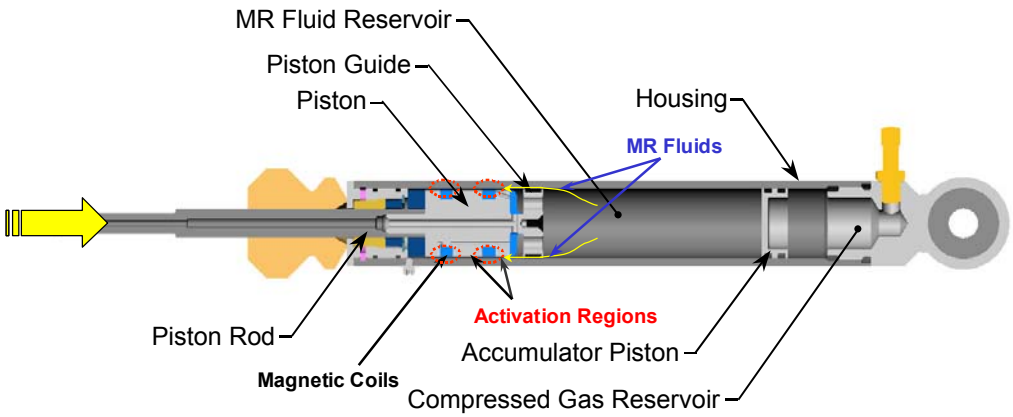

Figure 2-3. Typical MR Damper (modified from [53])

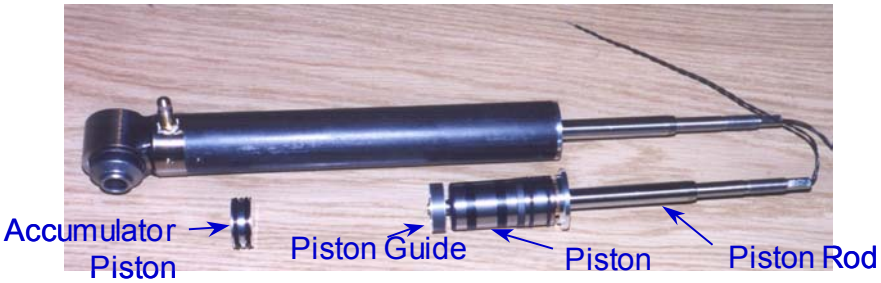

Figure 2-4. Disassembled MR Damper [53]

While the viscosity of the MR fluid remains constant, its "apparent viscosity" changes when it is exposed to a magnetic field. In other words, the MR fluid mixture thickens, and even becomes solid, when it meets a magnetic field. The magnetic field also changes the shear strain rate of the MR fluid, which becomes more sensitive to shearing with an increasing magnetic field. As the magnetic field strength increases, the resistance to fluid flow at the activation regions also increases until it reaches the saturation current. The saturation current occurs when increasing the electric current fails to increase the damping force for a given velocity. The resistance to fluid flow in the activation regions causes the MR dampers to produce force. This mechanism is similar to that of hydraulic dampers, in which force is caused by fluid passage through an orifice. This variable resistance to fluid flow allows us to use MR fluid in electrically-controlled viscous dampers and other devices.

2.3.3 Types of MR Dampers

There are four main types of MR dampers-- mono tube, twin tube, double-ended, and sponge-type. A mono tube MR damper, shown in Figure 2-5, has only one MR fluid reservoir and an accumulator mechanism to accommodate changes in volume resulting from piston rod movement. The accumulator piston provides a barrier between the MR fluid and a compressed gas (usually nitrogen) that accommodates the volume changes that occur when the piston rod enters the housing.

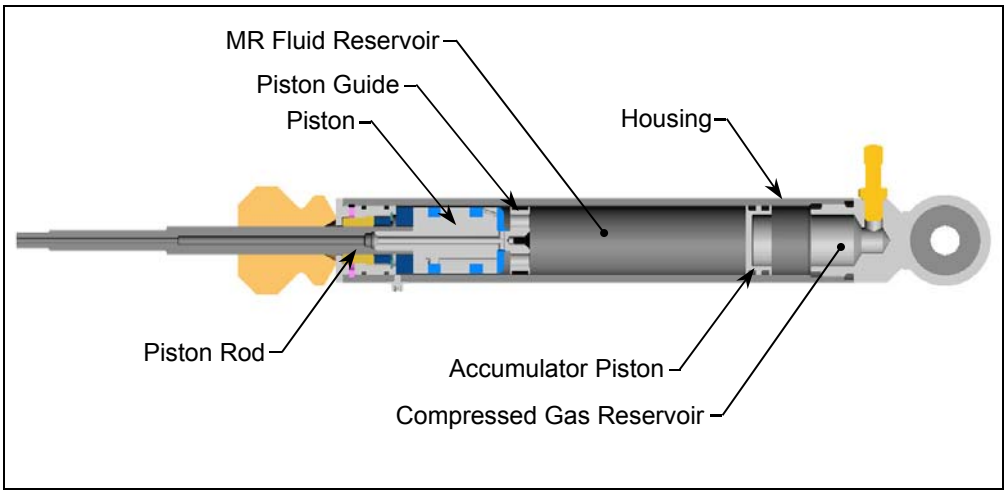

Figure 2-5. Mono Tube MR Damper Section View [53]

The twin tube MR damper has two fluid reservoirs, one inside of the other, as shown in Figure 2-6. In this configuration, the damper has an inner and outer housing. The inner housing guides the piston rod assembly, in exactly the same manner as in a mono tube damper. The volume enclosed by the inner housing is the inner reservoir; the volume that is confined by the space between the inner housing and the outer housing is the outer reservoir. The inner reservoir is filled with MR fluid so that no air pockets exist.

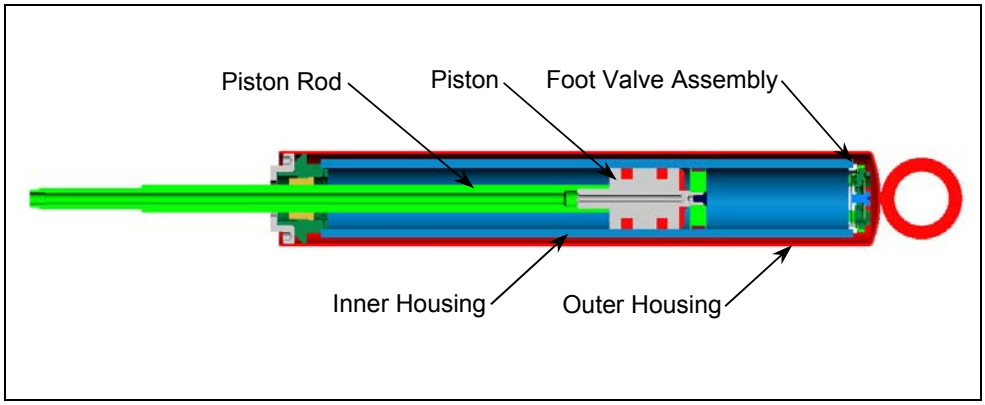

Figure 2-6. Twin Tube MR Damper [53]

An outer reservoir that is partially filled with MR fluid helps to accommodate changes in volume due to piston rod movement. Therefore, the outer tube in a twin tube damper serves the same purpose as the pneumatic accumulator mechanism in a mono tube damper. In practice, a valve assembly, or a "foot valve," is attached to the bottom of the inner housing to regulate the flow of fluid between the two reservoirs. As the piston rod enters the damper, MR fluid flows from the inner reservoir into the outer reservoir through the compression valve, which is part of the foot valve assembly. The amount of fluid that flows from the inner reservoir into the outer reservoir is equal to the volume displaced by the piston rod as it enters the inner housing. As the piston rod withdraws from the damper, MR fluid flows from the outer reservoir into the inner reservoir through the return valve, which is also part of the foot valve assembly.

The third type of MR damper is called a double-ended damper, since a piston rod of equal diameter protrudes from both ends of the damper housing. Figure 2-7 shows a section view of a typical double-ended MR damper. Since there is no change in volume as the piston rod moves relative to the damper body, the double-ended damper does not require an accumulator mechanism. Double-ended MR dampers have been used for bicycle applications [54], gun recoil applications [55], and for controlling building sway motion caused by wind gusts and earthquakes [56].

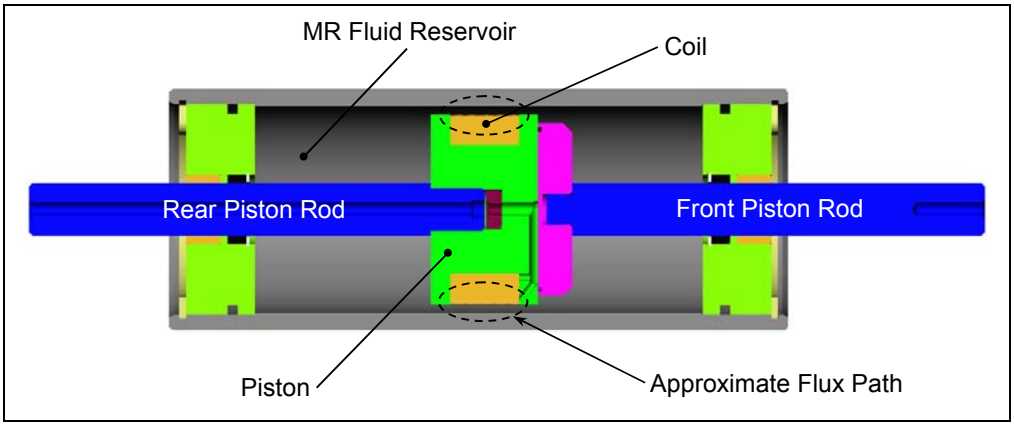

Figure 2-7. Double-Ended MR Damper [53]

The final type of MR damper is called a sponge-type damper. An MR sponge damper contains MR fluid in an absorbent matrix such as sponge, open-celled foam, or fabric. The sponge keeps the MR fluid located in the active region of the device where the magnetic field is applied. The device is operated in a direct shear mode with a minimum volume of MR fluid. Moreover, the MR sponge device does not require high-cost components, such as seals, rod surface finish, and the precision mechanical tolerances that are normally associated with a conventional fluid-filled MR device. Figure 2-8 shows the internal components of the MR sponge damper used in this study. This MR sponge device is appropriate for TVA applications because it provides the necessary on-state damping force when energized and has a reasonably low off-state damping. Lower off-state damping forces (as compared with those of mono-tube type dampers) are possible with MR sponge dampers because they are not pressure charged.

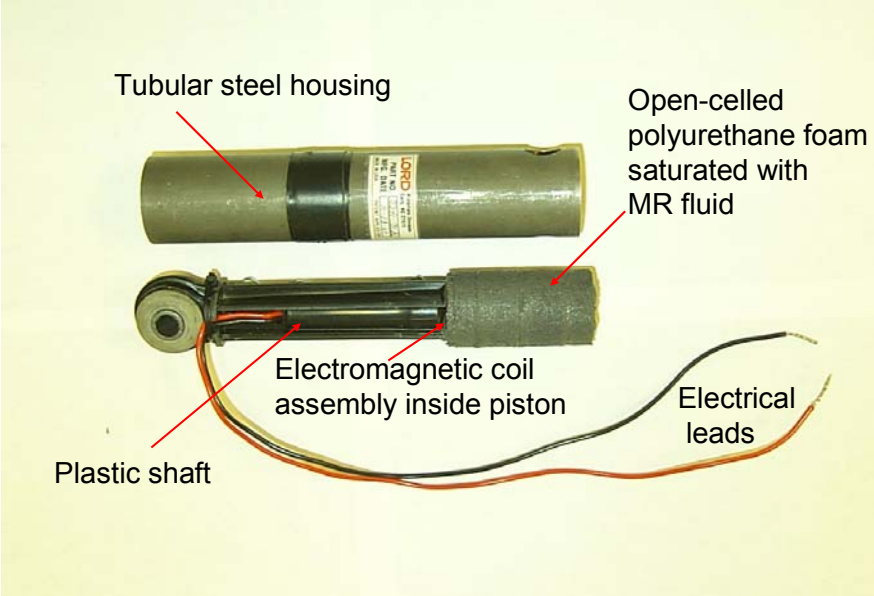

Figure 2-8. Disassembled Sponge-Type MR Damper

2.4 Semiactive Systems

This section discusses semiactive systems, particularly MR semiactive devices and semiactive vibration absorbers. It concludes with background information on the semiactive control methods that this study will use.

2.4.1 MR Semiactive Devices

A semiactive control system typically requires a small external power source for operation. In fact, many can operate on battery power, which is critical when the main power source to the structure fails; for example, seismic events. Moreover, semiactive control systems utilize the motion of the structure to develop the control forces. Therefore, semiactive control systems do not have the potential to destabilize the structure system, unlike active systems. Extensive studies have indicated that semiactive systems perform significantly better than passive devices. A comprehensive review of semiactive control systems can be found in references [57-59]. Because the review of all

the semiactive control systems would be a daunting task, the discussion of semiactive devices will be limited to those that use Magneto-Rheological (MR) dampers.

Recently, the civil engineering community has given considerable attention to the use of MR dampers. There are several reasons for this. First of all, MR dampers offer variable damping, and contain no moving parts other than the piston, which makes them simple and reliable. Furthermore, their ability to generate large damping force makes MR dampers suitable for controlling large structures. Another valuable advantage of MR dampers is their low power requirement (battery operated). A number of pilot studies [60-62] have assessed the effectiveness of MR dampers for reduction of building responses. In these studies, MR devices were used to control earthquake-induced vibrations. Moreover, most efforts were devoted to developing analytical models and optimal control algorithms for MR dampers. Furthermore, MR dampers have mainly been studied in bracing systems or base isolation systems. Unlike TVA systems, MR dampers in these systems are connected between the structural members, and serve as the sole actuators. Thus, generally, larger MR dampers are needed for those systems than for TVA systems, which can utilize the inertial force of TVA masses.

Hiemenz et al. [63] conducted an analytical and experimental study with a semiactive MR damper installed in a brace system. They evaluated a "skyhook" control and a "clipped" continuous sliding mode (CSM) control scheme, and confirmed the effectiveness of the semiactive MR brace system. In their study, the CSM controller seemed to outperform the skyhook controller. However, the superior performance of the CSM method came at a cost of more consumed energy. They concluded that these semiactive controllers performed considerably well both numerically and experimentally, and showed great potential for the use of MR dampers as semiactive braces in building structures.

Yi et al. [64] showed the effectiveness of multiple MR devices for seismic control of civil engineering structures. They used four parallel-plate, shear-mode MR dampers to control a six-story test structure. The control devices were installed in the test structure between the base and first floor, and two were installed between the first floor and second floor. For multi-input/multi-output controls, a nonlinear system identification procedure

was developed to identify the system model, and two semiactive control algorithms (Lyapunov algorithm and clipped-optimal algorithm) were used. The results indicated that the performance of the semiactive systems was significantly better than that of comparable passive systems under various excitations.

A smart isolation system for the base-isolated, two-degree-of-freedom structural model employing MR dampers was investigated experimentally by Yoshioka, Ramallo, and Spencer [65]. They used the Bouc-Wen hysteresis model for an analytical MR damper and a modified clipped-optimal control strategy for controlling the system. As compared with the MR damper's passive mode, the smart base isolation system achieved significant acceleration reductions over the entire range of earthquake intensities.

In summary, several investigators have confirmed the effectiveness of MR dampers as semiactive devices. Many of these investigations have examined the installation of MR devices in structural braces to apply forces directly to the structural mass.

2.4.2 Semiactive Tuned Vibration Absorbers

Another mode of applying control forces is through tuned vibration absorbers. Several studies have confirmed the effectiveness of semiactive TVAs, and shown that performances of TVAs were further improved by making them semiactive. Several investigators [66-72] confirmed that semiactive TVAs performed significantly better than equivalent passive TVAs. Those studies were mostly intended for applications in wind or earthquake engineering, and they generally evaluated the performance of semiactive systems numerically.

Agrawal and Yang [73] proposed device-specific, semiactive algorithms for protection of seismic-excited structures subjected to near-field earthquake ground motions. They considered two types of semiactive control devices, namely "Semiactive Stiffness Damper (SASD)'" and "Semiactive Electromagnetic Friction Damper (SAEMFD)." After deriving the device-specific algorithms for the two devices, the control algorithms were applied to investigate a 5-story building that was subjected to

various near-field earthquakes. The numerical results clearly indicated a superior performance of these two devices.

Abe and Igusa [74] developed an analytical theory for optimal control algorithms for semiactive absorbers. They confirmed that semiactive vibration absorbers were suitable for controlling the impulse response of the structure, and were substantially more effective than conventional passive vibration absorbers.

Hidaka et al. [75] performed one of a few experiments of variable damping dynamic absorbers. They investigated the performance of a variable-damping dynamic absorber using ER fluid. They constructed a prototype variable-damping dynamic absorber and placed it on the top floor of a miniature, three-story structure model. The objective of their study was to reduce several modes of vibrations with a single variable-damping dynamic vibration absorber. They proposed an adaptive neural network algorithm to control damping of the dynamic absorber. According to their time domain experimental results, the dynamic absorber tuned to the first natural frequency of the structure reduced the displacement of the third floor by 67% when the structure was excited at the 2^{nd} natural frequency. Moreover, the controlled dynamic absorber achieved a 36% reduction when the 3^{rd} natural frequency of the structure was excited.

Pinkaew and Fujino [76] studied the control effectiveness of a semiactive tuned mass damper (STMD) with variable damping under harmonic excitation. They investigated the response of a SDOF structure coupled with an STMD by employing the numerical technique and the optimal control theory. Under harmonic excitation, the vibration suppression by a STMD was significantly superior to that of a conventional passive TMD in both transient and steady-state responses. The improvement of STMDs over passive TMDs was equivalent to a four-fold increase of the TMD's mass.

In summary, although several studies exist on semiactive TVAs, very little research has been done on variable damping semiactive TVAs that use MR dampers.

2.4.3 Semiactive Damping Control

This section intends to provide background information on semiactive, groundhook control policies, which will be used for this research. Karnopp and Crosby [77-79] introduced the use of semiactive dampers in vehicles' primary suspension systems. Since the development of the well-known "skyhook" control policy for semiactive dampers over two decades ago, several other semiactive control polices, such as groundhook and hybrid control, have evolved [80-81].

For vehicle applications, skyhook control reduces the vibration of the sprung mass, the portion of mass supported by the suspension, as shown in Figure 2-9, to increase ride comfort. On other hand, groundhook control attempts to reduce the vibration of the unsprung mass, the tire-axle assembly, for the stability of a vehicle. Hybrid control provides the combined effects of skyhook and groundhook.

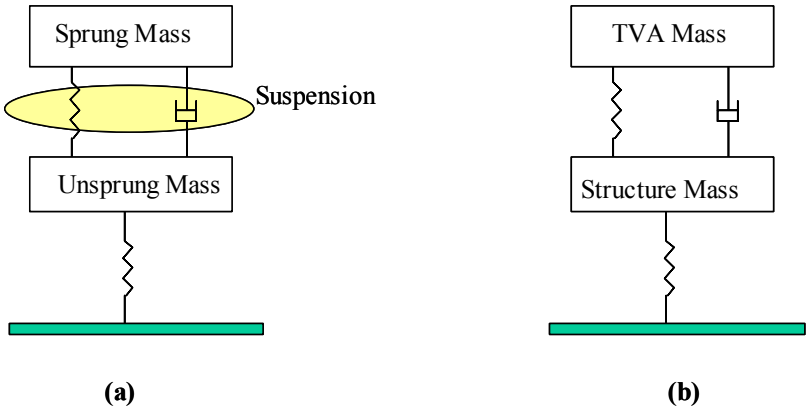

Figure 2-9. Similarities Between Base-excited Vehicle Suspension and TVA Models: (a) Vehicle Suspension Model and (b) TVA Model

Figure 2-9 illustrates the similarity between one quarter of a vehicle and a 2-DOF TVA model; as it shows, the structure mass in the TVA model is analogous to the unsprung mass of a vehicle model. Because of this similarity, the groundhook control policy is more desirable for TVA applications, as it focuses on control of the structure. Therefore, the most commonly used groundhook control policy will be used as an initial control method for the semiactive system in this study.

In on-off groundhook control, the damper is controlled by two damping values referred to as on-state and off-state damping, as shown in Figure 2-10. The determination of whether the damper is to be adjusted to either state depends on the product of the relative velocity across the damper and the absolute velocity or displacement of the primary structure. In continuous groundhook control, damping levels are not limited to the two damping states. They can be any value within the two boundaries, as shown in Figure 2-10. These values are governed by the absolute velocity or displacement of the structure and the relative velocity across the damper. The next chapter will explain the relevance of this policy for TVA applications.

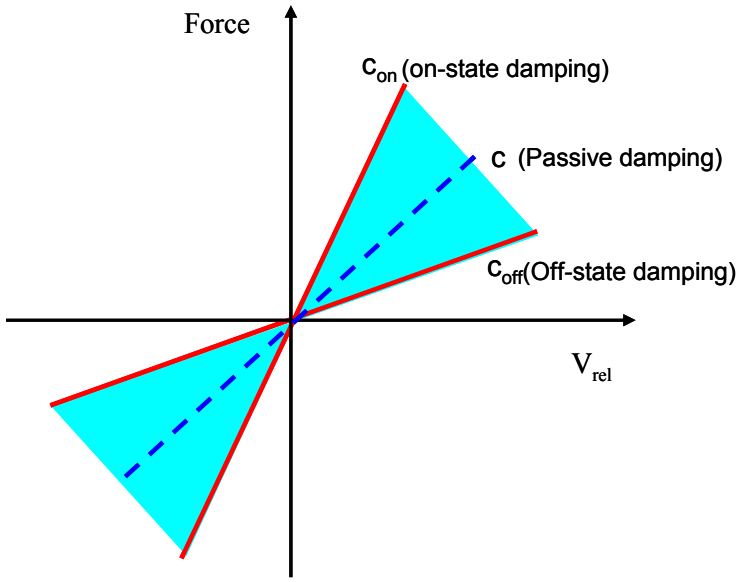

Figure 2-10. Force versus Velocity Curve for Semiactive Dampers

Chapter 3 Numerical Models and Optimal Tuning

This chapter offers a description of the proposed semiactive TVA, along with a dynamic analysis of the TVA that is based upon numerical simulations (optimal tuning). Before introducing the proposed TVA, this chapter describes a conventional passive TVA to help distinguish the two systems. Following the comparisons, this chapter discusses the controller development for the proposed system. It then presents numerical models of the semiactive TVA with different controllers and the equivalent passive TVA along with simulation and system parameters. These numerical models are optimally tuned using numerical optimization techniques to compare each TVA system. Finally, this chapter summarizes the dynamic performance of the tuned systems and suggests the best control method for the proposed semiactive system, based upon the optimization results.

3.1 Conventional Passive TVA Model

As described in Chapter 2, a conventional passive tuned vibration absorber (TVA) is a vibratory subsystem attached to a primary system. It normally consists of a mass, a spring, and a damper. Mounted on the primary system, it counteracts the motions of the primary system, effectively suppressing unwanted vibrations in many mechanical and structural systems. This section discusses the mathematical models of passive TVAs, which will be compared with the proposed semiactive TVA models.

Figure 3-1 shows two 2-DOF, passive TVA models: a base-excited model (Figure 3-1a), and a force-excited model (Figure 3-1b). In both models, the primary structure is coupled with a conventional passive TVA, and the mass of the structure and absorber are defined by m_1 and m_2, with their corresponding displacements as x_1 and x_2, respectively. The absorber's spring (k_2) and damper (c_2) are mounted on the structure. The stiffness and damping of the structure are represented by k_1 and c_1, respectively.

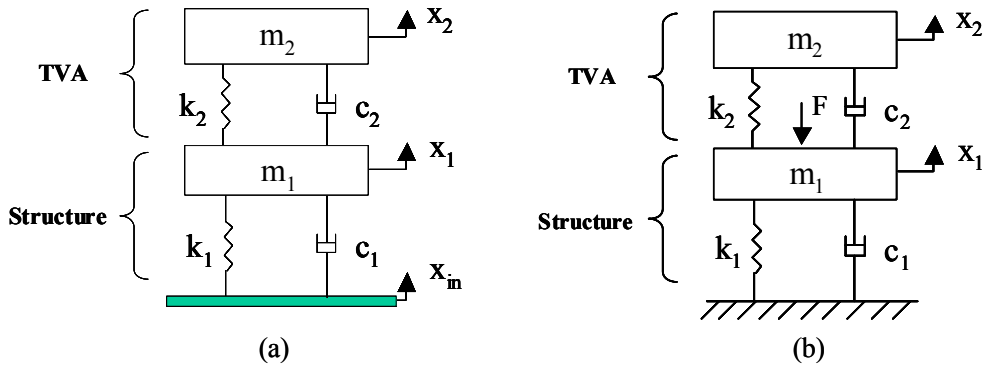

Figure 3-1. Conventional Passive TVA Models: (a) Base-Excited Model and (b) Force-Excited Model

Although the force-excited model, shown in Figure 3-1b, is more suitable for floor vibration analysis, this study will adopt the base-excited model as its baseline system for the numerical analysis. There are two main reasons for this. First of all, the experimental setup for this study is a base-excited system, so it is necessary to use the consistent model. Moreover, the focus of this research is to design TVAs, which are essentially the same for the base-excited and force-excited systems, and to evaluate their performance.

The equations of motion of each model are derived along with their transmissibility equations to show that tuning the TVA is the same for each model. Moreover, the equations of motion of the base-excited model will be transformed into a numerical model in a later section for further numerical analysis. The mathematical representation of the base-excited TVA begins below with the equations of motion in matrix form.

$$\begin{bmatrix} m_1 & 0 \\ 0 & m_2 \end{bmatrix}\begin{Bmatrix} \ddot{x}_1 \\ \ddot{x}_2 \end{Bmatrix}+\begin{bmatrix} c_1+c_2 & -c_2 \\ -c_2 & c_2 \end{bmatrix}\begin{Bmatrix} \dot{x}_1 \\ \dot{x}_2 \end{Bmatrix}+\begin{bmatrix} k_1+k_2 & -k_2 \\ -k_2 & k_2 \end{bmatrix}\begin{Bmatrix} x_1 \\ x_2 \end{Bmatrix}=\begin{bmatrix} c_1\dot{x}_{in}+k_1x_{in} \\ 0 \end{bmatrix} \tag{3.1}$$

Assuming

$$x_1 = X_1 e^{st} \tag{3.2a}$$

$$x_2 = X_2 e^{st} \tag{3.2b}$$

$$x_{in} = X_{in} e^{st} \tag{3.2c}$$

where $s = j\omega$ and ω is the driving frequency. Substituting equations (3.2a - 3.2c) into equation (3.1) yields

$$\begin{bmatrix} m_1 s^2 + (c_1 + c_2)s + k_1 + k_2 & -c_2 s - k_2 \\ -c_2 s - k_2 & m_2 s^2 + c_2 s + k_2 \end{bmatrix} \begin{Bmatrix} X_1 \\ X_2 \end{Bmatrix} = \begin{Bmatrix} (c_1 s + k_1) X_{in} \\ 0 \end{Bmatrix} \tag{3.3}$$

Using Cramer's Rule, the amplitudes X_1 and X_2 can be solved for as

$$X_1 = \frac{\begin{vmatrix} (c_1 s + k_1) X_{in} & -c_2 s - k_2 \\ 0 & m_2 s^2 + c_2 s + k_2 \end{vmatrix}}{\det A} = \frac{(c_1 s + k_1) X_{in} (m_2 s^2 + c_2 s + k_2)}{\det A} \tag{3.4}$$

$$X_2 = \frac{\begin{vmatrix} m_1 s^2 + c_2 s + k_1 + k_2 & (c_1 s + k_1) X_{in} \\ -c_2 s - k_2 & 0 \end{vmatrix}}{\det A} = \frac{(c_1 s + k_1) X_{in} (c_2 s + k_2)}{\det A} \tag{3.5}$$

where,

$$\det A = (m_1 s^2 + c_1 s + c_2 s + k_1 + k_2)(m_2 s^2 + c_2 s + k_2) - (c_2 s + k_2)^2$$

Therefore, the transmissibility equations become

$$\frac{X_1}{X_{in}} = \frac{(c_1 s + k_1)(m_2 s^2 + c_2 s + k_2)}{(m_1 s^2 + (c_1 + c_2)s + k_1 + k_2)(m_2 s^2 + c_2 s + k_2) - (c_2 s + k_2)^2} \tag{3.6}$$

$$\frac{X_2}{X_{in}} = \frac{(c_1 s + k_1)(c_2 s + k_2)}{(m_1 s^2 + (c_1 + c_2)s + k_1 + k_2)(m_2 s^2 + c_2 s + k_2) - (c_2 s + k_2)^2} \tag{3.7}$$

In order to rewrite equations (3.6) and (3.7), the following parameters are introduced:

$$\omega_{n1} = \sqrt{\frac{k_1}{m_1}}, \qquad \omega_{n2} = \sqrt{\frac{k_2}{m_2}},$$

$$\zeta_1 = \frac{c_1}{2\omega_{n1} m_1}, \qquad \zeta_2 = \frac{c_2}{2\omega_{n2} m_2},$$

$$\mu = \frac{m_2}{m_1}, \qquad r = \frac{\omega}{\omega_{n1}},$$

$$g = \frac{\omega_{n2}}{\omega_{n1}},$$

where

ω_{n1} = natural frequency of structure,

ω_{n2} = natural frequency of TVA,

ζ_1 = damping ratio of structure,

ζ_2 = damping ratio of TVA,

μ = mass ratio (TVA mass/structure mass),

r = forced frequency ratio, and

g = natural frequency ratio.

With these parameters, equations (3.6) and (3.7) can be rewritten in a non-dimensionalized form as:

$$\frac{X_1}{X_{in}} = \frac{(1+2\zeta_1 rj)(g^2 - r^2 + 2\zeta_2 grj)}{(-r^2 + 2\zeta_1 rj + 2\zeta_2 \mu grj + 1 + \mu g^2)(-r^2 + 2\zeta_2 rgj + g^2) - \mu(2\zeta_2 grj + g^2)^2} \tag{3.8}$$

$$\frac{X_2}{X_{in}} = \frac{(1+2\zeta_1 rj)(g^2 + 2\zeta_2 grj)}{(-r^2 + 2\zeta_1 rj + 2\zeta_2 \mu grj + 1 + \mu g^2)(-r^2 + 2\zeta_2 rgj + g^2) - \mu(2\zeta_2 grj + g^2)^2} \tag{3.9}$$

For the force-excited model, the equations of motion in matrix form are

$$\begin{bmatrix} m_1 & 0 \\ 0 & m_2 \end{bmatrix}\begin{Bmatrix} \ddot{x}_1 \\ \ddot{x}_2 \end{Bmatrix}+\begin{bmatrix} c_1+c_2 & -c_2 \\ -c_2 & c_2 \end{bmatrix}\begin{Bmatrix} \dot{x}_1 \\ \dot{x}_2 \end{Bmatrix}+\begin{bmatrix} k_1+k_2 & -k_2 \\ -k_2 & k_2 \end{bmatrix}\begin{Bmatrix} x_1 \\ x_2 \end{Bmatrix}=\begin{bmatrix} F \\ 0 \end{bmatrix} \tag{3.10}$$

Assuming

$$F = F_0 e^{st} \tag{3.11a}$$

$$F_0 = k_1 \delta_{st} \tag{3.11b}$$

where δ_{st} is the static deflection. Following the same procedures as the base-excited case, the final transmissibility equations for the force-excited system become:

$$\frac{X_1}{\delta_{st}} = \frac{(g^2 - r^2 + 2\zeta_2 grj)}{(-r^2 + 2\zeta_1 rj + 2\zeta_2 \mu grj + 1 + \mu g^2)(-r^2 + 2\zeta_2 rgj + g^2) - \mu(2\zeta_2 grj + g^2)^2} \tag{3.12}$$

$$\frac{X_2}{\delta_{st}} = \frac{(g^2 + 2\zeta_2 grj)}{(-r^2 + 2\zeta_1 rj + 2\zeta_2 \mu grj + 1 + \mu g^2)(-r^2 + 2\zeta_2 rgj + g^2) - \mu(2\zeta_2 grj + g^2)^2} \tag{3.13}$$

The transmissibility equations (3.8 and 3.12) provide the means of tuning TVAs using optimization techniques. The goal of the techniques is to minimize the maximum transmissibility. In these equations, the denominators are identical, and the only difference is the term $1 + 2\zeta_1 rj$. This term does not contain the TVA parameters.

From equation 3.8 for the base-excited model and equation 3.12 for the force excited model, the TVA for each system can be tuned. The resulting TVAs would provide similar performance to their respective systems. Furthermore, if the force transmissibility for the force-excited system is scaled by the stiffness of the structure, this transmissibility would match that of the base-excited system. Therefore, there is no difference between the tuning of a base-excited system and a force-excited system, which justifies our emphasis on using the base-excited model for this study's baseline system.

3.2 Proposed Semiactive TVA Model

The proposed TVA model replaces a passive damping element with a controllable damping element, which distinguishes it from the conventional passive system. Figure 3-2 shows a conventional passive TVA model (Figure 3-2a) and the proposed semiactive TVA model (Figure 3-2b). A controllable damper, such as an MR damper, is the key element for the new system. It can provide a wide dynamic force range, can offer a real-time control environment at low power, and can be quite cost-effective. Incorporating this versatile damper into the proposed model will significantly enhance its performance, combining the benefits of both passive and active systems. The new system is anticipated to surpass the performance of conventional passive TVAs in reducing the maximum vibration levels of the primary structure and robustly adapt to the primary system's parameter changes.

Figure 3-2b is used to derive the dynamic equations of motion for the semiactive model. The equations of motion that describe this system are:

$$\begin{bmatrix} m_1 & 0 \\ 0 & m_2 \end{bmatrix} \begin{Bmatrix} \ddot{x}_1 \\ \ddot{x}_2 \end{Bmatrix} + \begin{bmatrix} c_1 + c_{controllable} & -c_{controllable} \\ -c_{controllable} & c_{controllable} \end{bmatrix} \begin{Bmatrix} \dot{x}_1 \\ \dot{x}_2 \end{Bmatrix} + \begin{bmatrix} k_1 + k_2 & -k_2 \\ -k_2 & k_2 \end{bmatrix} \begin{Bmatrix} x_1 \\ x_2 \end{Bmatrix} = \begin{bmatrix} c_1 \dot{x}_{in} + k_1 x_{in} \\ 0 \end{bmatrix} \quad (3.14)$$

Equation (3.14) will be used in the development of the numerical model of the semiactive TVA in a later section.

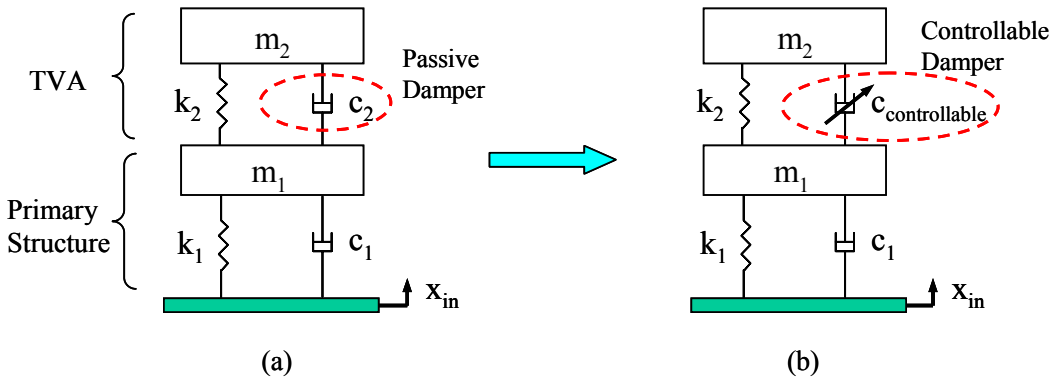

Figure 3-2. Passive TVA versus Semiactive TVA; (a) Passive Model and (b) Semiactive Model

Figure 3-3 illustrates how a controllable damper can provide a wide range of damping force. At a given velocity, V_g, the corresponding damper force for the passive damper is a constant force, F_{pa}. On the other hand, the controllable damper offers a damper force ranging from F_{off} to F_{on}. This controllable damper, which provides a wide dynamic force range, significantly improves the dynamic performance of the semiactive TVA with proper control methods. This will be discussed in the next section. For experimental purposes, this study will employ an MR damper as a controllable damper.

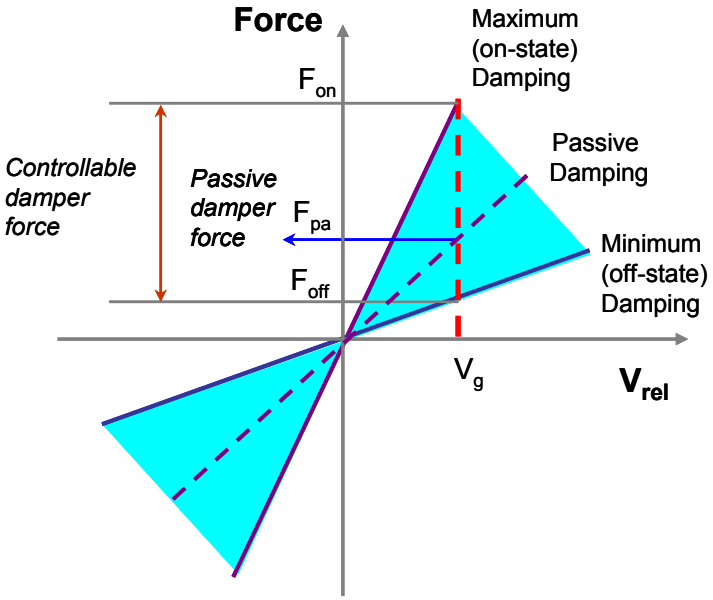

Figure 3-3. Force Velocity Curve

3.3 Controller Development

This section presents several methods for controlling the damper in our proposed semiactive TVA system. This study employs a "groundhook" control policy as an initial method to regulate the controllable damper in the semiactive TVA. The groundhook control policy is suitable for the semiactive system because of its similarity to a quarter car model, which was discussed in Chapter 2. This control policy has been extensively studied at the Advanced Vehicle Dynamics Laboratory at Virginia Tech, and has been successfully implemented in semiactive systems, such as automotive suspension applications. After an overview of the goal and logic of the basic groundhook control,

this section will discuss variant groundhook control policies. This study will examine a total of four groundhook control schemes in order to identify which of these four control methods best suits the semiactive TVA application. The four strategies include:

- Velocity-based, on-off groundhook control (On-off VBG)
- Velocity-based, continuous groundhook control (Continuous VBG)
- Displacement-based, on-off groundhook control (On-off DBG)
- Displacement-based, continuous groundhook control (Continuous DBG)

Figure 3-4a shows the ideal groundhook configuration of a two-degree-of-freedom TVA model. A passive damper hooks the structure to the "ground," hence, the name "groundhook" [82]. However, this ideal groundhook configuration cannot be realized in practice because the damper cannot be fixed to a non-moving inertia frame. For practical applications, a semiactive TVA model, shown in Figure 3-4b, can realize the ideal model, incorporating a controllable damper. The controllable damper implements the groundhook control. The objective of developing a controller is to represent the ideal groundhook damping force with the configuration shown in Figure 3-4b. In other words, the controllable damper in the semiactive model with groundhook control emulates the ideal groundhook force in the ideal configuration model.

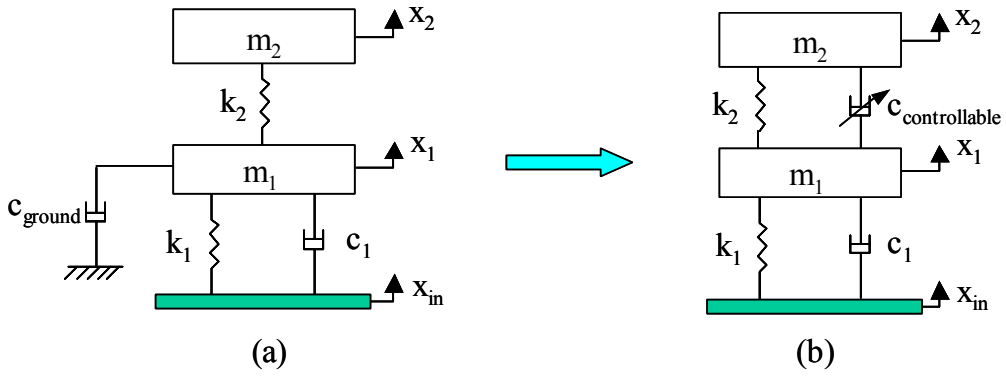

Figure 3-4. Lumped-Parameter Models of Groundhook TVAs;
(a) Ideal Configuration and (b) Semiactive TVA Model

The most comprehensive way to determine the equivalent groundhook damping force is to examine the forces acting on the structure mass under several conditions. First, we must define certain parameters and conventions. Referring to Figure 3-4b, the relative velocity, v_{12}, is the velocity of the structure mass (m_1) minus the velocity of the TVA mass (m_2). When the two masses separate, v_{12} is negative. For all other cases, up is positive and down is negative. With these definitions, we may consider a case in which the structure mass moves upwards and the two masses separate. Under the groundhook equivalent configuration, there is tension placed on the damper, and the damper force pulls up the structure mass from its equilibrium position. For this reason, minimum damping is desired, as it minimizes the damper force on the structure mass.

Next, let us consider a case in which both v_1 and v_{12} are positive. Because the damper is compressed, the damper force pushes the structure mass down to its equilibrium position. In this case, a maximum damping level maximizes damper force. If the structure mass moves downwards and the two masses separate. The semiactive damper applies force to the structure mass in the positive direction, creating tension on the damper. Thus, maximum damping maximizes the force, pulling the structure mass up to its equilibrium position. The final case to consider is one in which the structure mass moves downwards and the two masses come together. Again, the damper is in compression, and the damper force pushes the structure mass down. Thus, minimum damping and damper force are desired.

Summarizing these four conditions, the on-off VBG groundhook control policy is derived:

$$\begin{aligned} v_1 v_{12} \geq 0 \qquad & c_{controllable} = c_{on} \\ v_1 v_{12} < 0 \qquad & c_{controllable} = c_{off} \end{aligned} \tag{3.15}$$

Table 3-1 illustrates the above discussion.

Table 3-1. Illustrations of Groundhook Control Logic

Illustrations	Sign Conventions	Direction of Damping Force Acting on m_1	Desired Damper Force Damping State
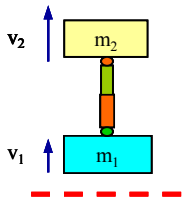	$v_1 > 0$ $v_1 - v_2 < 0$	 Damper is in Extension Pulling up m_1 from Equilibrium	**Minimum Damper Force** Off-State
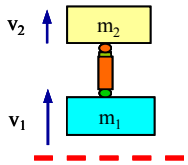	$v_1 > 0$ $v_1 - v_2 > 0$	 Damper is in Compression Pushing down m_1 to Equilibrium	**Maximum Damper Force** On-State
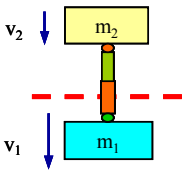	$v_1 < 0$ $v_1 - v_2 < 0$	 Damper is in Extension Pulling up m_1 to Equilibrium	**Maximum Damper Force** On-State
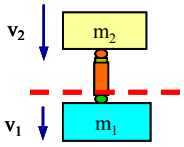	$v_1 < 0$ $v_1 - v_2 > 0$	 Damper is in Compression Pushing down m_1 from Equilibrium	**Minimum Damper Force** Off-State

The on-off VBG groundhook control policy can be evolved to the on-off DBG groundhook control policy by changing v_1 to x_1 in equation (3.3). While the damping force for on-off VBG is determined by the product of structure mass velocity and the relative velocity across the damper, the damping force for on-off DBG is based on the product of floor mass displacement and the relative velocity. The formulation of on-off DBG is:

$$\begin{aligned} x_1 v_{12} \geq 0 \qquad & c_{controllable} = c_{on} \\ x_1 v_{12} < 0 \qquad & c_{controllable} = c_{off} \end{aligned} \tag{3.16}$$

The on-off groundhook control policies can be extended to continuous groundhook control policies. As discussed in an earlier section, for on-off groundhook control the damper switches back and forth between two possible damping states, on and off-state. For continuous groundhook control, however, the damper continuously changes the damping level between on and off-state damping levels. Comparing the ideal and the equivalent groundhook configurations, the controllable damping can be formulated as follows:

$$c_{controllable} = \frac{Gv_1}{v_1 - v_2} \tag{3.17}$$

$$c_{controllable} = \frac{Gx_1}{v_1 - v_2} \tag{3.18}$$

for continuous VBG and continuous DBG, respectively. The parameter 'G' represents a constant gain that can adjust the overall damping of the TVA. These formulations bypass the conventional switching logic, which is common to groundhook control systems.

3.4 Simulation Models and Parameters

This section explains the development of simulation models, which will be tuned along with the selected semiactive control policies and used to study the effect of parameter variation. It also defines the simulation and system parameters for the numerical study.

The simulation models are developed by joining the controllers and the mathematical models that were discussed earlier. The actual realization of these simulation models is done with Matlab. The Simulink toolbox within Matlab is used to build block diagrams for each of these simulation models. Figure 3-5 shows an example of a Simulink block diagram for a semiactive model (on-off VBG model). Table 3-2

shows the system parameters of simulations, which represent a physical model for experiments.

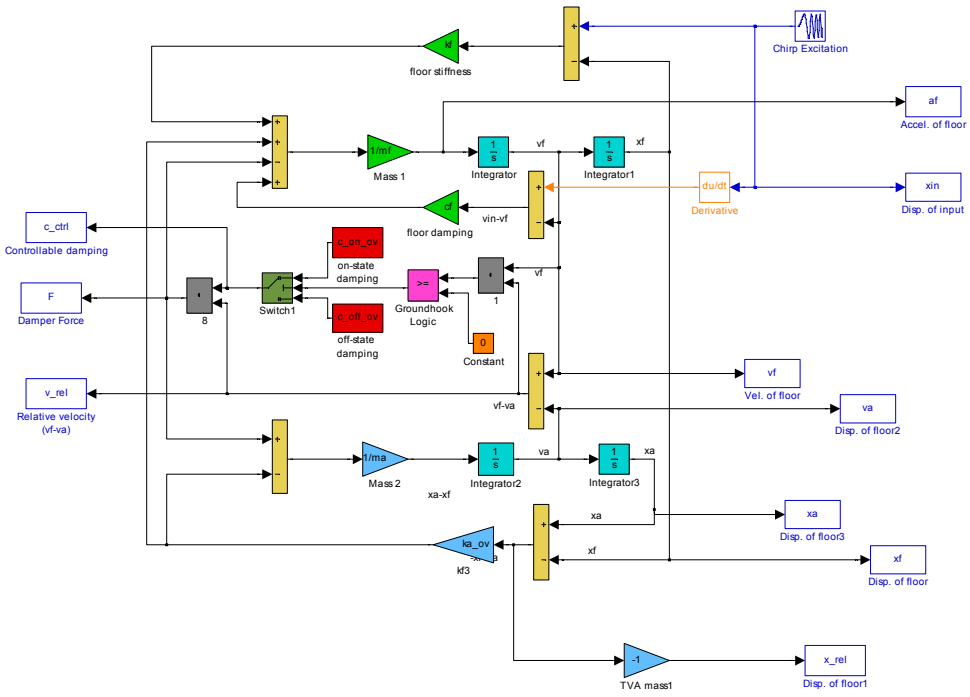

Figure 3-5. Simulink Block Diagram for the On-Off Velocity Based Groundhook Model

Table 3-2. System Parameters

Parameter	Value
Structure Mass (m_1)	575 lb
TVA Mass (m_2)	32 lb
Structure Stiffness (k_1)	1909 lb/in
Structure Damping Ratio (ζ_1)	3 %

This numerical study uses a chirp signal as its simulation input. It is applied to the numerical models for identifying the dynamics of the systems in the frequency domain. To determine an initial and a target frequency for the chirp input, the natural

frequency of the system needs to be calculated. From the parameters given in Table 3-2, the natural frequency of the structure can be calculated as:

$$\omega_{n1} = \sqrt{\frac{k_1}{m_1}}$$

Using this, the natural frequency of the primary structure is found to be 5.1 Hz. The frequency ranges for a chirp should include this frequency and also account for TVA frequencies, which is close to the structure's natural frequency. Considering this aspect, the chirp used in this study sweeps frequency ranges from 0.5 Hz to 10 Hz in 150 seconds. This slow sweeping chirp signal preserves the low frequency dynamics. **Table 3-3** shows a summary of the simulation parameters used in the Simulink.

Table 3-3. Numerical Parameters Used in Simulink Models

Simulation Input	Initial Frequency	Target Frequency	Simulation Time	Equation Solver	Fixed-step Size
Chirp	0.5 Hz	10 Hz	150 sec	Runge-Kutta	1/100

3.5 Optimal Tuning

This section presents the optimal tuning of simulation models and evaluates the performance of the tuned systems. The tuned systems provide for an equal comparison of system performance and, thus, identification of the best model. The simulation models are tuned by using a numerical optimization technique, which is necessary for the models because of the presence of damping in the primary system and the non-linearity of semiactive control. The goal of the optimization is to find the TVA parameters, such as on/off-damping ratios (ζ_{on} and ζ_{off}), stiffness (k_2), and gains (G), which generate the "best" performance of each model. The optimization routine uses a minimization of the maximum value of transmissibility as an optimization criterion. After describing the optimization routine, this section will conclude with a summary and discussion of the optimization results.

3.5.1 Optimization Routine

Figure 3-6 shows the flow chart for the optimization routine. Running within Matlab, the execution of the optimization routine involves three steps. In the main program, the system parameters are defined, along with the initial values and ranges of the simulation parameters. The main program calls the Simulink numerical models, which are responsible for generating the peak transmissibilities. These peak transmissibilities are then sent to the optimization function, "fmincon.m", where the minimum values of the peak transmissibilities are returned, along with the corresponding simulation parameters.

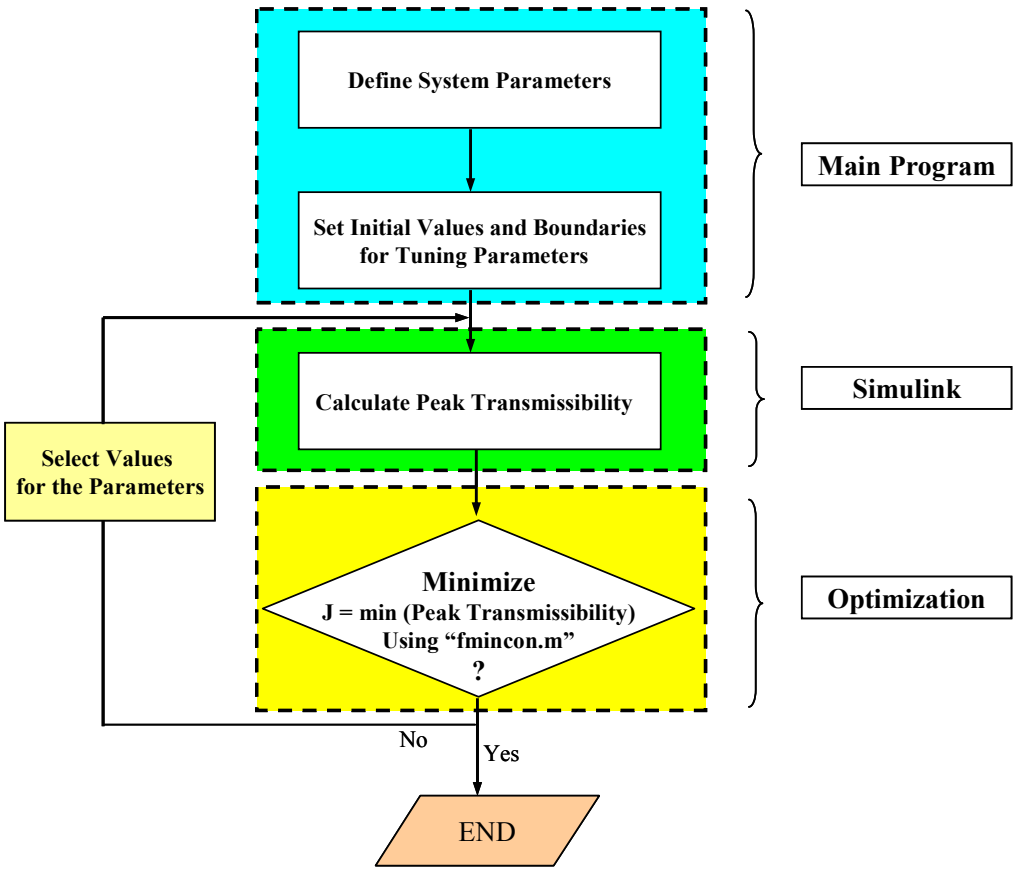

Figure 3-6. Flow Chart for Optimization Routine

Table 3-4 summarizes the simulation parameters and their ranges used for the optimization routine. Note that large numbers are selected for upper limits of on-state damping ratios in order to obtain theoretically achievable optimization results. In other words, taking advantage of computer simulations, this study examines a wide range of parameters and cases, greater than what would be reasonable with a physical system.

Table 3-4. Summary of Initial Values and Parameter Ranges for Optimization Routine

Model	Parameter	Initial Value	Parameter Range
Passive	Damping Ratio	0.15	$0.1 \le \varsigma_{pa} \le 1.5$
	TVA Stiffness (lb/in)	75.3	$10000 \le k_{a\_pa} \le 100000$
On-off VBG	On-state Damping Ratio	0.18	$0.1 \le \varsigma_{on\_ov} \le 1$
	Off-state Damping Ratio	0.09	$0.01 \le \varsigma_{off\_ov} \le 0.099$
	TVA Stiffness (lb/in)	89.5	$10000 \le k_{a\_ov} \le 100000$
On-off DBG	On-state Damping Ratio	4.69	$0.1 \le \varsigma_{on\_od} \le 100$
	Off-state Damping Ratio	0.5	$0.01 \le \varsigma_{off\_od} \le 10$
	TVA Stiffness (lb/in)	58.8	$10000 \le k_{a\_od} \le 100000$
Continuous VBG	On-state Damping Ratio	0.7	$0.1 \le \varsigma_{on\_cv} \le 10$
	Off-state Damping Ratio	0.07	$0.01 \le \varsigma_{off\_cv} \le 1$
	TVA Stiffness (lb/in)	64.6	$10000 \le k_{a\_cv} \le 100000$
	Gain	1	$1 \le gain_{\_cv} \le 100$
Continuous DBG	On-state Damping Ratio	0.7	$0.1 \le \varsigma_{on\_cd} \le 10$
	Off-state Damping Ratio	0.05	$0.01 \le \varsigma_{off\_cd} \le 1$
	TVA Stiffness (lb/in)	69.3	$10000 \le k_{a\_cd} \le 100000$
	Gain	764	$1 \le gain_{\_cv} \le 1000$

3.5.2 Optimization Results

This section presents the optimization results. Transmissibility plots and percent reduction bar charts are included. The optimization results are summarized in a table at the end of this section.

Figure 3-7 shows the transmissibility of each of the optimally tuned TVA models. A floor system without a TVA is shown as well to highlight the benefits of using TVAs. Figure 3-7 also shows that displacement-based controlled TVAs outperform the passive and velocity-based, semiactive TVAs in reducing the peak transmissibility. Note that the continuous DBG model offers the lowest valley floor because its off-state damping is low.

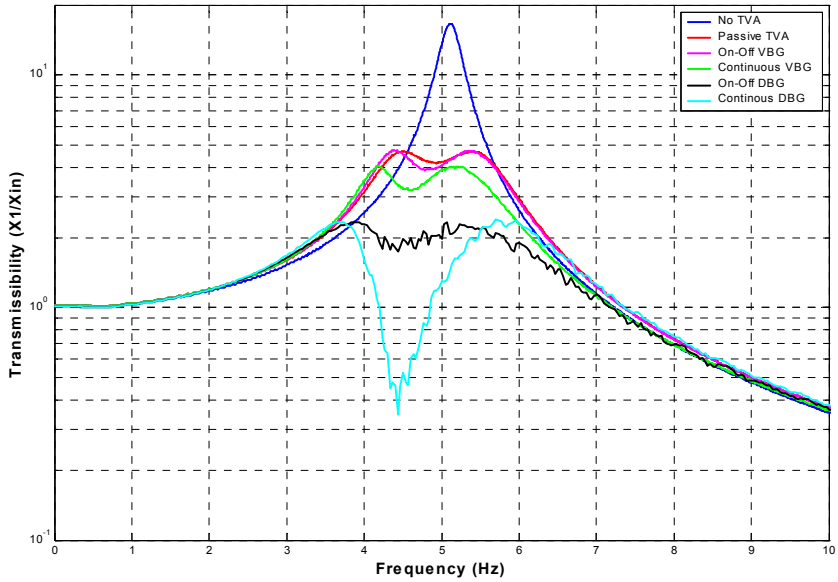

Figure 3-7. Optimally Tuned Transmissibility Results

Figure 3-8 offers another method of quantifying the results of optimization. Here, the percent reduction, with respect to the passive TVA, for each of the semiactive TVA models is plotted to show the relative benefits of the semiactive TVAs. Figure 3-8 shows that the maximum reduction occurs using on-off DBG. This indicates that on-off DBG offers the best performance among the considered TVA models. Another interesting

observation is that on-off VBG performs very close to passive, while on-off DBG performs slightly better than continuous DBG.

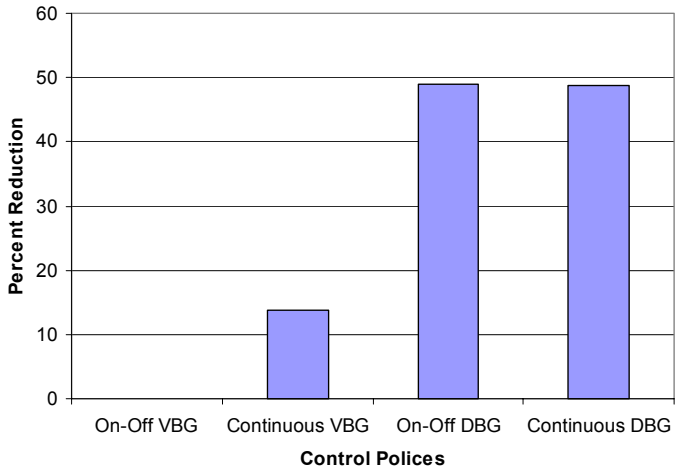

Figure 3-8. Percent Reduction of Peak Vibrations Relative to an Optimally Tuned Passive TVA

The results of the optimization routine are summarized along with the optimal passive parameters in Table 3-5. The optimal on-state damping ratios for passive and on-off VBG are close. However, damping ratios for continuous VBG, on-off DBG, and continuous VBG are too large to achieve in practice because of damping saturations. These optimization results indicate the maximum possible performance of each TVA in terms of reducing vibrations.

Table 3-5. Summary of Optimal TVA Parameters

Parameters	Passive	On-off VBG	Continuous VBG	On-off DBG	Continuous DBG
TVA Stiffness (lb/in)	75.3	72.8	63.4	60.1	66.1
On-state Damping Ratio	0.145	0.165	2.817	4.741	4.880
Off-state Damping Ratio	N/A	0.098	0.073	0.048	0.010
Continuous Gain	N/A	N/A	1.37	N/A	764.34
Passive Reduction	N/A	0.03 %	13.86 %	48.95 %	48.71 %

Chapter 4 Numerical Model Parametric Studies

This chapter uses baseline models as the basis for numerical parametric studies for further evaluation of the dynamic performance of the proposed semiactive TVA. The parametric studies include the effects of changing parameters of the TVA, such as on-state ratios, off-state damping ratios, and control gains. The parametric studies also perform off-tuning analyses by changing the primary system's parameters, namely the mass of the structure (mass off-tuning), the stiffness of the structure (stiffness off-tuning), and the damping ratio of the structure (damping off-tuning). For each parametric study, the parameter that is being evaluated varies, while the rest of the parameters remain fixed at their baseline values.

4.1 Baseline Models for Parametric Studies

In the previous chapter, the TVAs were optimized with a critically large range of damping parameters to investigate the maximum possible performance. In practice, however, the damping force cannot be increased indiscriminately because of the physical limitation of controllable dampers, such as the size of the damper. Thus, this section considers physically reasonable (and realizable) ranges of damping parameters to obtain baseline models, along with their tuning parameters. These baseline models, with their tuned parameters, will then be used for further dynamic analysis of the TVAs by performing parametric studies.

To obtain baseline models and their tuning parameters, this section uses the same numerical models (2-DOF, base-excited models) and optimization routine that were used in Chapter 3. For this case, however, the range of parameters in the optimization routine are constrained such that they represent practical values.

Table 4-1 summarizes the initial values and parameter ranges for this optimization.

Table 4-1. Summary of initial values and parameter ranges

Model	Parameter	Initial Value	Parameter Range
Passive	Damping Ratio	0.1	$0.1 \le \varsigma_{pa} \le 0.7$
	TVA Stiffness (lb/in)	75.3	$10000 \le k_{a\_pa} \le 100000$
On-off VBG	On-state Damping Ratio	0.21	$0.1 \le \varsigma_{on\_ov} \le 0.7$
	Off-state Damping Ratio	0.06	$0.01 \le \varsigma_{off\_ov} \le 0.07$
	TVA Stiffness (lb/in)	69.8	$10000 \le k_{a\_ov} \le 100000$
On-off DBG	On-state Damping Ratio	0.7	$0.1 \le \varsigma_{on\_od} \le 0.7$
	Off-state Damping Ratio	0.07	$0.01 \le \varsigma_{off\_od} \le 0.07$
	TVA Stiffness (lb/in)	71.1	$10000 \le k_{a\_od} \le 100000$
Continuous VBG	On-state Damping Ratio	0.7	$0.1 \le \varsigma_{on\_cv} \le 0.7$
	Off-state Damping Ratio	0.07	$0.01 \le \varsigma_{off\_cv} \le 0.07$
	TVA Stiffness (lb/in)	64.4	$10000 \le k_{a\_cv} \le 100000$
	Gain	1	$1 \le gain_{\_cv} \le 700$
Continuous DBG	On-state Damping Ratio	0.7	$0.1 \le \varsigma_{on\_cd} \le 0.7$
	Off-state Damping Ratio	0.07	$0.01 \le \varsigma_{off\_cd} \le 0.07$
	TVA Stiffness (lb/in)	72.3	$10000 \le k_{a\_cd} \le 100000$
	Gain	700	$1 \le gain_{\_cv} \le 700$

Figure 4-1 shows the optimization results of baseline models. Note that the passive TVA performs slightly better than the on-off VBG TVA in reducing the maximum transmissibility for the range of parameters. The on-off DBG and the continuous DBG models outperform the passive and velocity-based, semiactive systems in reducing the peak transmissibility. Table 4-2 shows a summary of the values of baseline parameters. These results will serve as the baseline values for parametric studies in the subsequent sections.

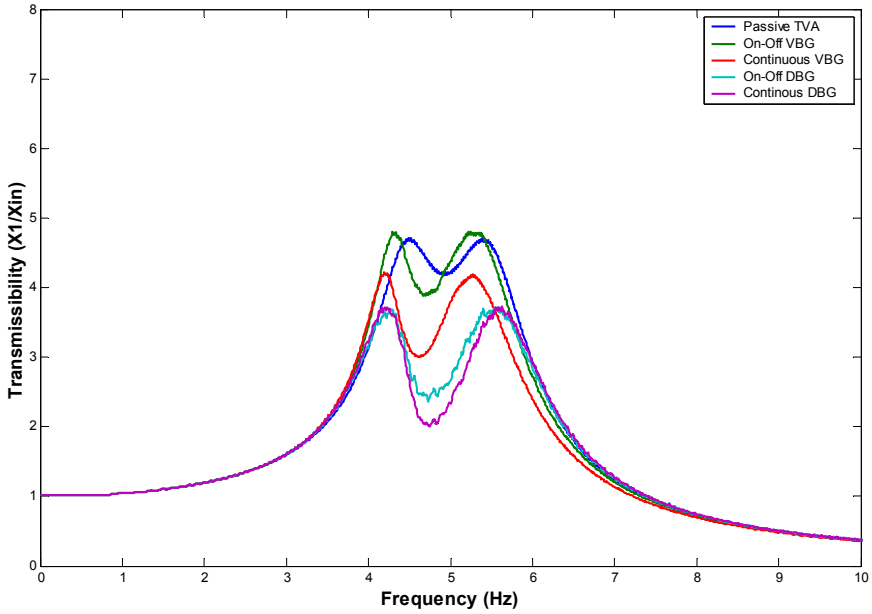

Figure 4-1. Optimization Results for Baseline Models

Table 4-2. Summary of Optimal Parameters for Baseline Models

Parameters	Passive	On-off VBG	Continuous VBG	On-off DBG	Continuous DBG
TVA Stiffness (lb/in)	75.3	69.8	64.4	70.8	71.5
On-state Damping Ratio	0.145	0.211	0.7	0.7	0.7
Off-state Damping Ratio	N/A	0.07	0.07	0.07	0.057
Continuous Gain	N/A	N/A	0.96	N/A	700
Passive Reduction (%)	N/A	-1.99	10.22	20.96	20.82

4.2 Parametric Studies

This section contains the results of the parametric studies performed on the baseline numerical models. The parametric studies examine the effects of on-state and off-state damping ratios, as well as control gains. The primary purpose of these parametric studies is to understand the dynamics of the TVAs as their parameters change within a practical range.

4.2.1 Effect of On-state Damping Ratio

This section of the study examines the effect of changing the on-state damping ratio. To this end, the on-state damping ratio is varied discretely below and above the baseline on-state damping ratio, while other parameters remain fixed at their baseline values. This section uses transmissibility and phase plots to evaluate each TVA's performance. The phase angle analysis adds valuable explanations in analyzing the results.

4.2.1.1 Passive TVA

Figure 4-2a shows the transmissibility, or the ratio between the output and the input displacement of the primary structure, for a passive TVA as the damping ratio (ζ_2) changes from 0.0 to 0.9. When the damping ratio is 0.0, there are two large peaks, and a complete isolation occurs at the valley. Increasing the damping ratio to its baseline value lowers these resonant peaks and widens the valley between the two peaks. However, this has a negative effect; it raises the valley floor. Further increasing the damping ratio above its baseline value gradually causes the two peaks become a single peak. This means that the structure and the TVA become strongly coupled, and function nearly as a single mass, effectively negating any benefits of the TVA. Figure 4-2b shows the phase angles between the TVA mass and the structure mass as the damping ratio increases. The phase plots support the above discussion. When the damping ratio is at its baseline value, the phase angle around the tuned frequency is relatively close to 90 degrees; the TVA effectively counteracts the motions of the structure mass, achieving the minimum transmissibility over the entire frequency range of interest. However, as the damping

ratio increases, the phase angle decreases. When the damping ratio is 0.9, the phase angle drops to about 30 degrees, indicating that the two masses have become strongly coupled. Thus, a single resonant peak forms in the transmissibility plot at this high damping ratio. For the passive system, excessively increasing the damping ratio results in a coupling of the TVA, and effectively renders it useless in reducing the vibrations of the structure mass.

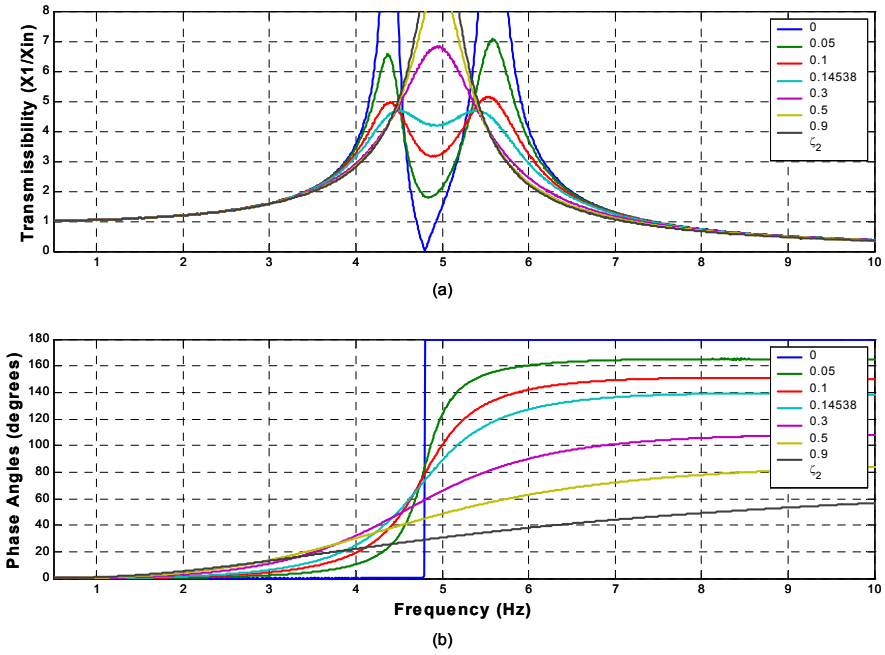

Figure 4-2. Effect of Damping Ratio on Passive TVA Dynamic Performance: (a) Transmissibility (X1/Xin); (b) Phase Angles Between the TVA and the Structure

4.2.1.2 On-off Velocity-Based Groundhook TVA

The effect of changing the on-state damping ratio for the on-off VBG controlled semiactive TVA is shown in Figure 4-3. As the on-state damping ratio ranges from 0.1 to 0.9, the two resonant peaks merge into a single peak, and the peak grows (see Figure 4-3a). These dynamics are similar to those of the passive system. The rate increase of the peak, however, is lower in the on-off VBG case, indicating that the coupling of the two masses occurs slowly. The phase plots, shown in Figure 4-3b, support these findings. Like the passive case, when the damping ratio is at its baseline value, the phase angle around the resonant frequency of the structure mass is close to 90 degrees. Increasing the on-state damping ratio above its baseline value reduces the phase angle below 90 degrees. These behaviors also occur in the passive system. However, when the damping ratio is 0.9, the phase angle around the resonant frequency of the structure is about 45 degrees in on-off VBG, whereas the passive system's phase angle is about 30 degrees (see Figure 4-2b). This confirms that the coupling of the TVA and the structure occurs at a faster rate in the passive system.

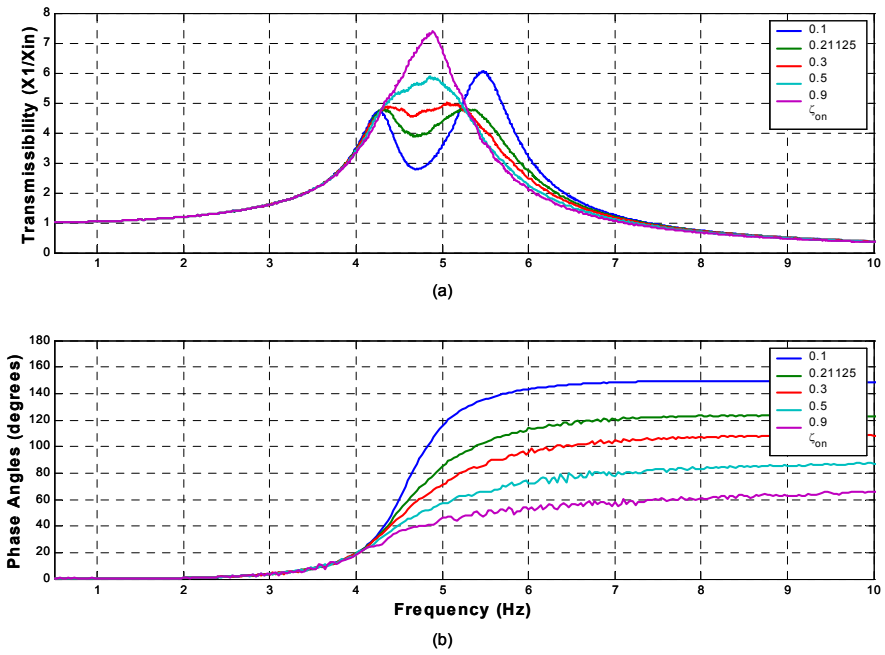

Figure 4-3. Effect of On-State Damping Ratio on the Performance of a Semiactive TVA with On-Off Velocity-Based Groundhook Control: (a) Transmissibility (X1/Xin); (b) Phase Angles Between the TVA and the Structure

4.2.1.3 Continuous Velocity-Based Groundhook TVA

Figure 4-4a shows transmissibility plots of the continuous VBG model as the on-state damping ratio discretely varies from 0.1 to 0.9. When the on-state damping ratio is increased from 0.1 to 0.3, the amplitude of the second peak is reduced significantly, at the expense of slightly raising the first peak and the valley. As the on-state damping ratio is further increased above 0.3, the second peak decreases, and the first peak increases. However, the changes are small, and the transmissibilities are nearly the same when the damping ratios are 0.7 and 0.9. This is because damping forces are dictated by the baseline gain value, which is fixed for this analysis. Note that the on-state damping ratio determines the upper boundary of the controllable damping, and a gain adjusts the damping level between the lower and upper boundaries. Figure 4-4b shows phase plots for this case. Around the frequency where the second peak occurs, the phase angle with the on-state damping ratio of 0.3 is much closer to 90 degrees than that of 0.1. This means that the TVA works more effectively with the damping ratio of 0.3. Consequently, a larger reduction of the second peak is observed in Figure 4-4a when the on-state damping ratio increases from 0.1 to 0.3.

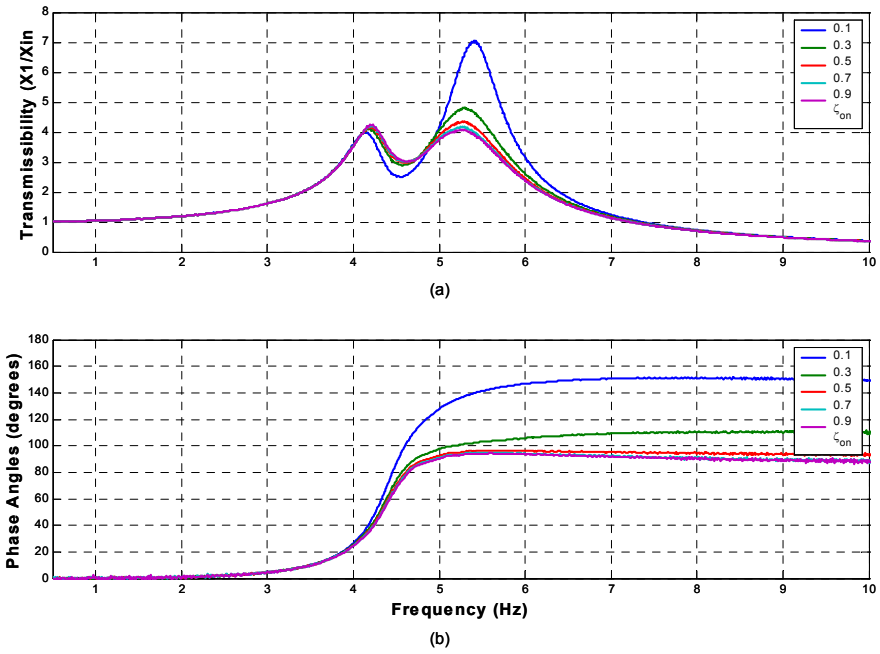

Figure 4-4. Effect of On-State Damping Ratio on the Performance of Semiactive TVA with Continuous Velocity-Based Groundhook Control: (a) Transmissibility (X1/Xin); (b) Phase Angles Between the TVA and the Structure Masses

4.2.1.4 On-off Displacement-Based Groundhook TVA

For the case of on-off DBG, the on-state damping ratio varies from 0.1 to 0.9, with an increment of 0.2. Unlike the passive and the velocity-based systems, the two resonant peaks decrease as the on-state damping ratio increases, without raising the isolation valley (see Figure 4-5a). This indicates that the on-off DBG control keeps the TVA and the structure masses decoupled at the tuned frequency, enabling the TVA to effectively counteract the motions of the structure at a high on-state damping ratio. This is because on-off DBG control policy ensures the minimum (off-state) damping ratio at the valley, independent of the on-state damping ratio, preventing lock-up (coupling of the two bodies). Further analysis of this control policy will be discussed in a later section. This result is one of the key benefits of this semiactive system. Figure 4-5b shows the phase angle changes of the on-off DBG system as the on-state damping ratio increases. The phase angle of at the tuned frequency (valley) stayed close to 90 degrees, regardless of the on-state damping ratio. Thus, the on-off DBG TVA achieved the minimum

transmissibility. Moreover, the phase angles at the two resonant frequencies approach 90 degrees as the on-state damping ratio increases, reducing the resonant peaks, as shown in Figure 4-5a.

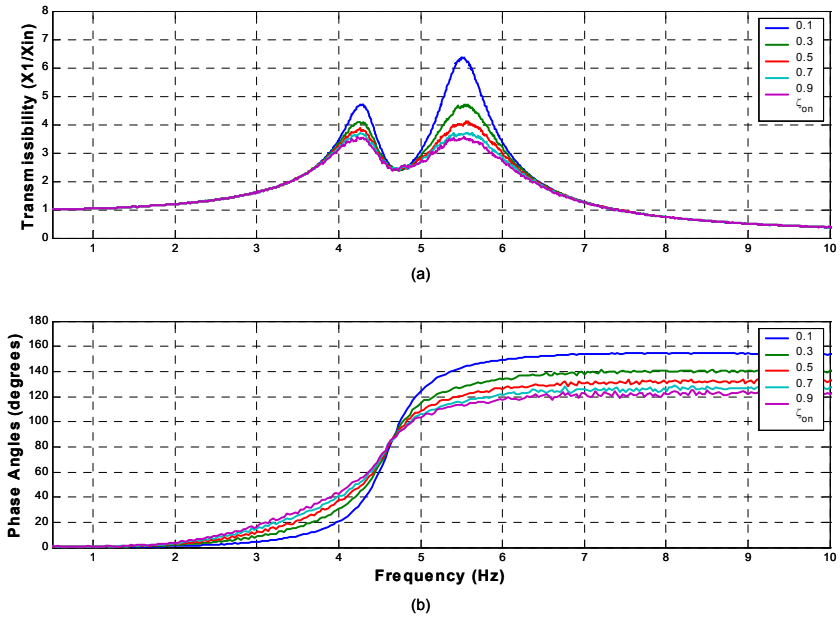

Figure 4-5. Effect of On-State Damping Ratio of the Performance of Semiactive TVA with On-Off Displacement-Based Groundhook Control: (a) Transmissibility (X1/Xin); (b) Phase Angles Between the TVA and the Structure

4.2.1.5 Continuous Displacement-Based Groundhook TVA

This section presents the results of the on-state damping ratio changes of the continuous DBG system (transmissibility and phase plots, respectively). The dynamics of this system are much like those of the on-off DBG system. As the on-state damping ratio varies discretely from 0.1 to 0.9, the two peaks decrease, without increasing the valley floor. Thus, the minimum transmissibility occurs at the valley, regardless of the on-state damping ratio (see Figure 4-6a). Figure 4-6b shows further dynamics of continuous DBG with phase angle changes. Similar to on-off DBG, independent of the on-state damping ratio, the phase angles of the continuous DBG are kept close to 90 degrees at the frequency where the isolation valley occurs. Also, increasing the on-state damping ratio makes the phase angle approaches 90 degrees, reducing the two resonant peaks.

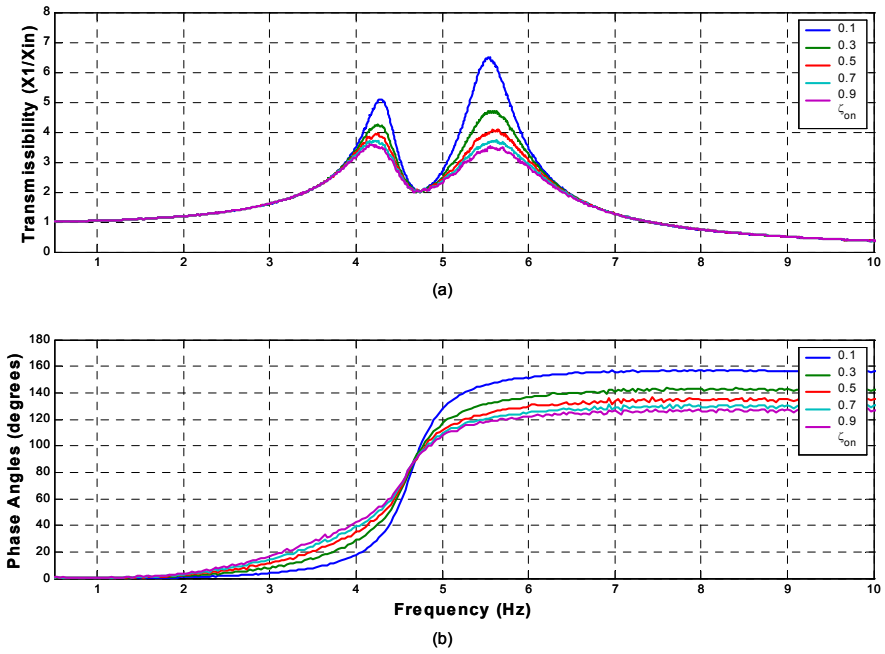

Figure 4-6. Effect of On-State Damping Ratio on the Performance of Semiactive TVA with Continuous Displacement-Based Groundhook Control: (a) Transmissibility (X1/Xin); (b) Phase Angles Between the TVA and the Structure

4.2.2 Effect of Off-state Damping Ratio

This section studies the effect of changing the off-state damping ratio. For this parametric study, the off-state damping ratio varies discretely above and below the baseline off-state damping ratio, while the rest of the simulation parameters remain fixed at their baseline values.

4.2.2.1 On-off Velocity-Based Groundhook TVA

To study the effect of the off-state damping ratio of the On-off VBG control case, the off-state damping ratio is varied. Values for the off-state damping ratio are 0.05, 0.07, 0.09, 0.11, and 0.13. Figure 4-7 shows the transmissibility plots for the on-off VBG when the off-state damping ratio changes. Increasing the off-state damping ratio decreases the first resonant peak at the expense of raising the valley and the second resonant peak. The results imply that increasing the off-state damping ratio to higher than its tuned value degrades the performance the on-off VBG TVA.

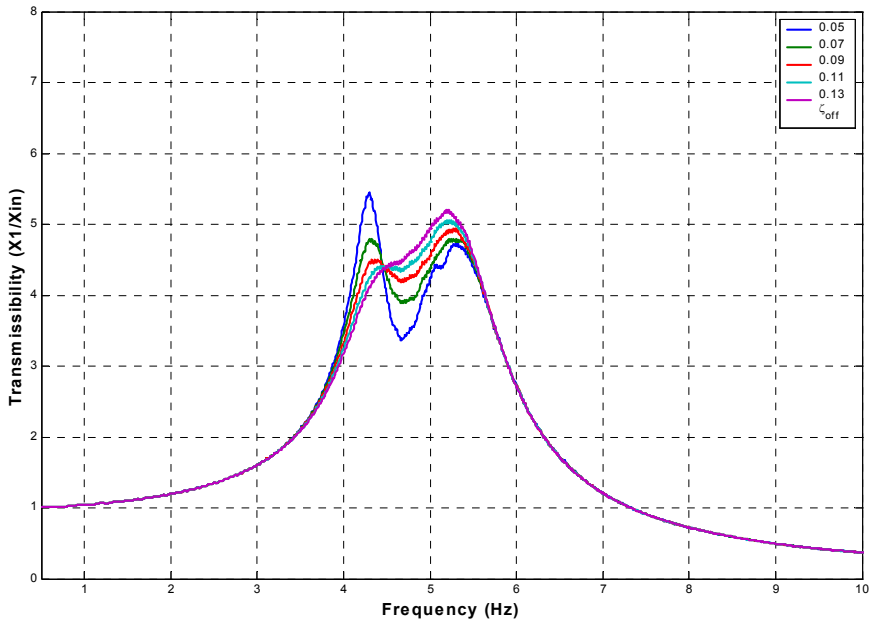

Figure 4-7. Effect of Off-state Damping Ratio on Transmissibility for On-off Velocity-Based Groundhook TVA

4.2.2.2 Continuous Velocity-Based Groundhook TVA

In this section, the off-state damping ratio is varied from 0.05 to 0.13 in order to analyze the effect of different ratios in the continuous VBG case. As with the on-off VBG system, as the off-state damping ratio increases, the second peak increases as shown in Figure 4-8. Moreover, the isolation valley grows. An excessively large off-state damping ratio would couple the TVA and the structure, disabling the TVA.

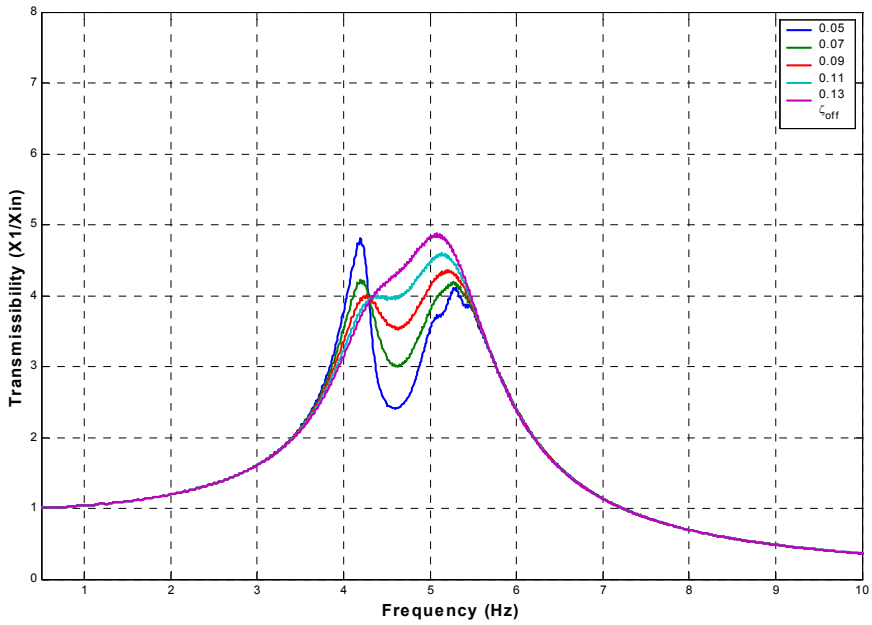

Figure 4-8. Effect of Off-state Damping Ratio on Transmissibility for Continuous Velocity-Based Groundhook TVA

4.2.2.3 On-off Displacement-Based Groundhook TVA

Figure 4-9 shows transmissibility plots of the on-off DBG TVA, as the off-state damping ratio ranges from 0.05 to 0.13. When the off-state damping ratio increases, the valley floor also increases. Moreover, the amplitudes of the two peaks grow, and they tend to become one. This observation indicates that high off-state damping ratios negate the performance of the on-off DBG TVA like velocity-based, semiactive systems. This analysis suggests that the off-state damping ratio should be tuned at its optimal value in order to offer its maximum performance gains.

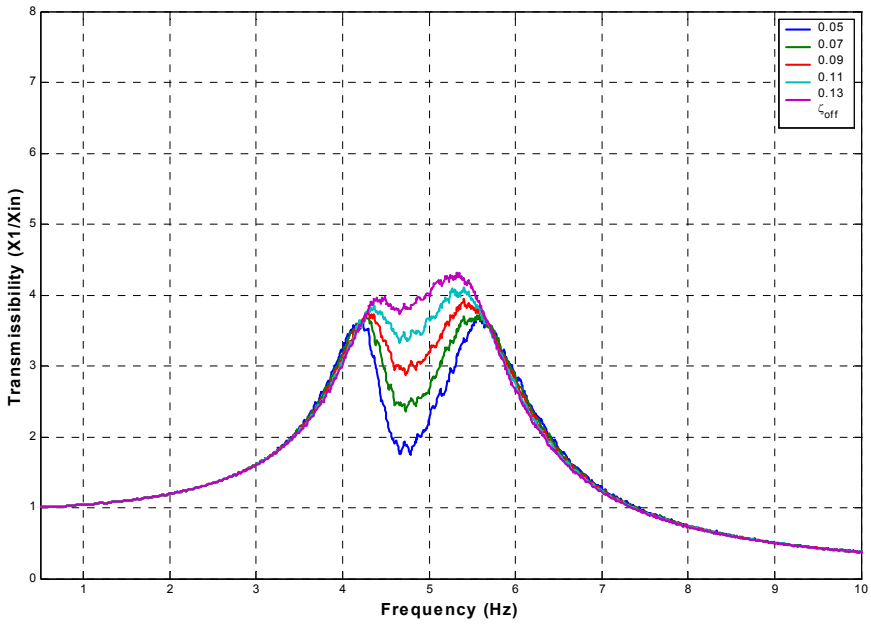

Figure 4-9. Effect of Off-state Damping Ratio on Transmissibility for the On-off DBG TVA

4.2.2.4 Continuous Displacement-Based Groundhook TVA

To study the effect of changing the off-state damping ratio of the continuous DBG case, the damping ratio is varied incrementally from its baseline value (0.057) to 0.13. Figure 4-10 shows the results, which are very similar to those of the on-off DBG case. Increasing the damping ratio raises the magnitudes of the two resonant peaks, as well as the valley floor. Further increase in the off-state damping ratio would eventually couple the two masses. Large off-state damping ratios negate the effectiveness of the continuous DBG system

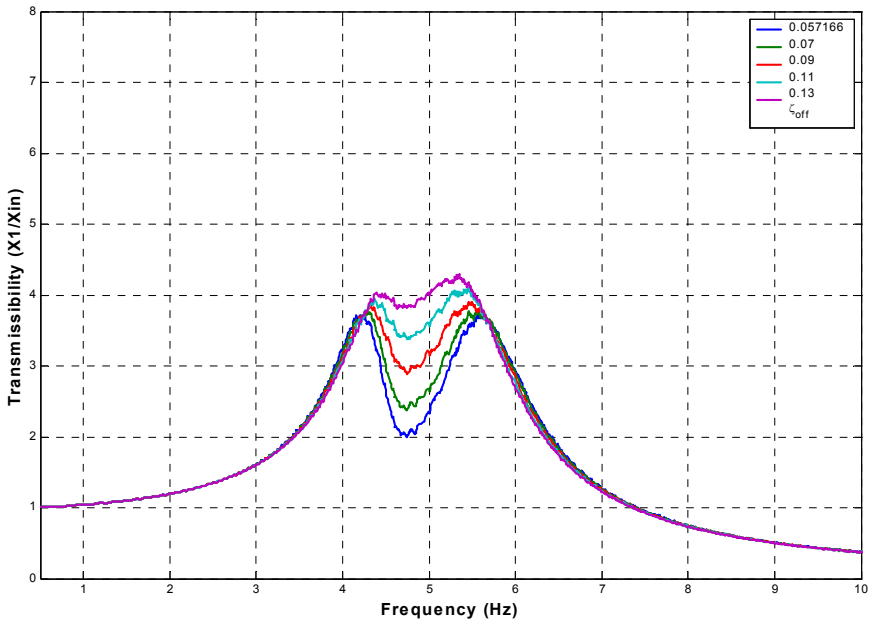

Figure 4-10. Effect of Off-state Damping Ratio on Transmissibility for the On-off DBG TVA

4.2.3 Effect of Gains

This part of the study examines the effect of control gains for continuous semiactive systems, namely continuous VBG/DBG models. Hence, the control gains are varied, while the on-state and off-state damping ratios remain fixed at their baseline values. The control gain, 'G' in equations (3.17) and (3.18), determines the distribution of damping levels between the minimum and maximum damping boundaries of a controllable damper. A small gain distributes the damping level closer to the lower boundary (set by the off-state damping ratio); a large gain places the bias on the damping level to the upper boundary (set by the on-state damping ratio).

4.2.3.1 Continuous Velocity-Based Groundhook TVA

Figure 4-11 shows transmissibility variations as the gain ranges incrementally from 0.5 to 1000 for the continuous VBG model. As the gain increases from 0.5 to 100, the two peaks merge into a single peak and it increases, demonstrating similar dynamics to those of the passive system. This dynamic occurs because the distribution of damping levels is raised close to the maximum damping limit, as the gain increases. Thus, when the gain is 100, the TVA damping becomes quite large, which links the TVA and the structure. When the gain is further increased from 100 to 1000, the transmissibilities are the same because the damping force has reached its dynamic saturation point at its maximum (on-state damping ratio) boundary. Note that damping levels higher than the on-state damping ratio, which limits the upper boundary, are clipped and limited by the boundary. Therefore, as the gain increases excessively, the continuous system approaches the on-off system.

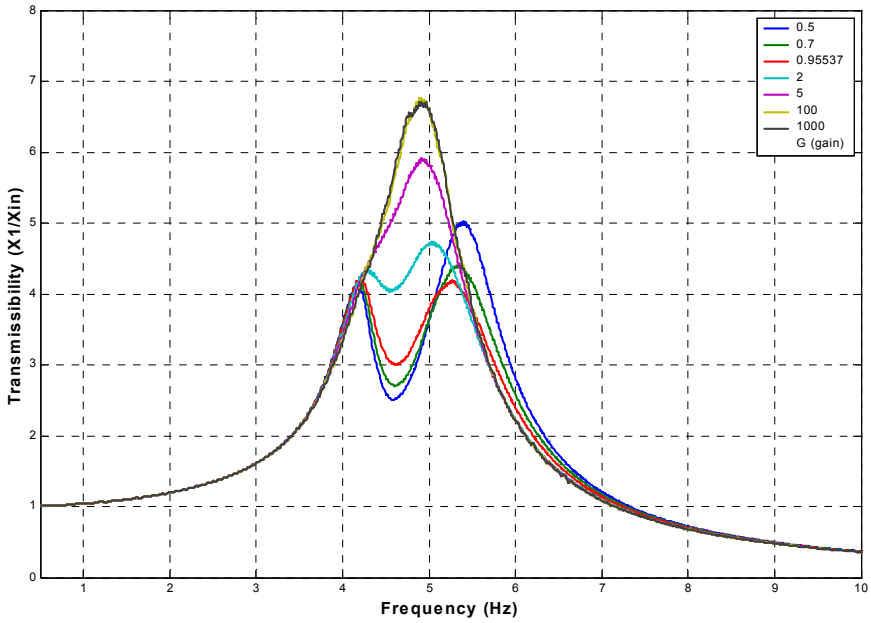

Figure 4-11. Effect of the Control Gain on Transmissibility for the Continuous VBG TVA

4.2.3.2 Continuous Displacement Based Groundhook TVA

Figure 4-12 shows the results for changing the gain for the continuous DBG TVA from 1 to 1000 in several increments. As the gain increases, the two resonant peaks decrease without raising the valley floor. This behavior is similar to that of the on-off DBG system with increase of the on-state damping ratio. When the gains are 700 and higher, the transmissibilites are the same, implying that the damping forces have saturated.

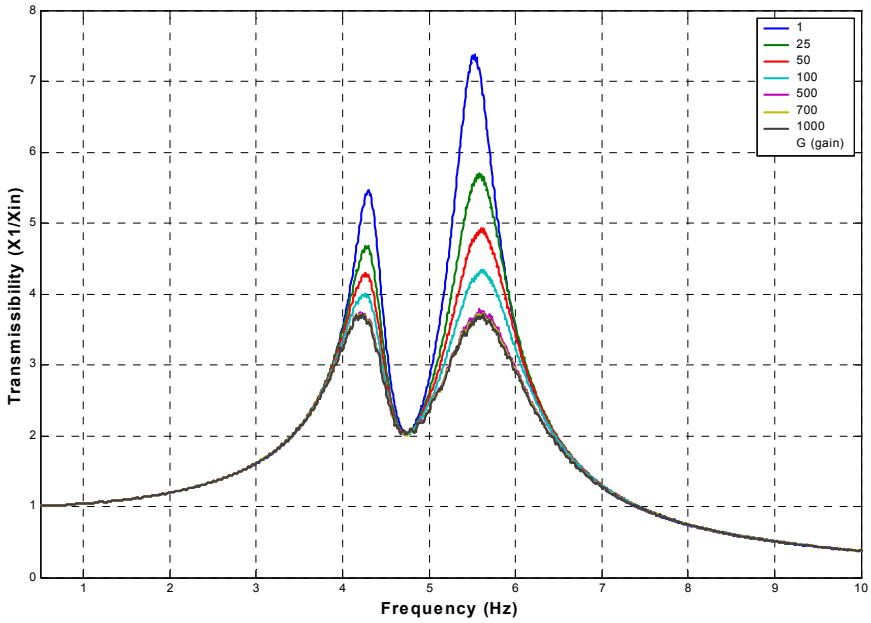

Figure 4-12. Effect of the Control Gain on Transmissibility for the Continuous DBG TVA

4.3 Off-Tuning Analysis

Although passive TVAs can be optimally designed, they only offer benefits when they are accurately tuned. In practice, off-tuning (or mistuning) of TVAs occur due to changes of the primary systems' characteristics or the TVA. Thus, the major problem with using passive TVAs is off-tuning, which sharply reduces the performance and may even cause damage to the main structure. The subsequent sections perform a comprehensive off-tuning analysis of passive and semiactive TVAs due to changes of the primary structure's parameters. The analysis takes into account the effect of the primary system's mass, stiffness, and damping ratio changes (mass off-tuning, stiffness off-tuning, and damping off-tuning, respectively). To justify the benefits of the practical use of semiactive TVAs, the results of these off-tuning analyses show that semiactive TVAs are more robust than the passive systems when subjected to changes in system parameters; this clearly justifies their real-world use. Hence, each off-tuning analysis examines the relative benefits of semiactive TVAs as compared with an equivalent passive system.

4.3.1 Effect of Mass Off-Tuning

This section considers the effect of mass off-tuning due to changes in the structure mass. This mass off-tuning analysis is particularly valuable for building floor systems because their masses and their distributions constantly change due to moving furnishings, people gathering, and so on. This change in mass is responsible for the off-tuning of TVAs. To study the effect of mass off-tuning, this section varies the structure mass below and above its nominal magnitude, while other parameters remain at their respective baseline values. It then presents transmissibility plots to analyze each TVA's performance. Finally, it provides a comparison plot that shows the peak transmissibility changes of each TVA as the structure mass varies 30% below and above its original mass. This plot summarizes the results of the mass off-tuning analysis.

4.3.1.1 Passive TVA

Figure 4-13a shows transmissibility variations of the passive TVA as the structure mass is reduced 10%, 20%, and 30% below its baseline structure mass. In this case, the second resonant peak increases. When the structure mass is discretely increased to 10%, 20%, and 30% above the baseline structure mass, which is 535 lb, the first resonant peak increases, as shown in Figure 4-13b. The increase in the peak transmissibility is notably greater when the structure mass is increased, indicating that the passive TVA is more robust to decreases in the structure mass.

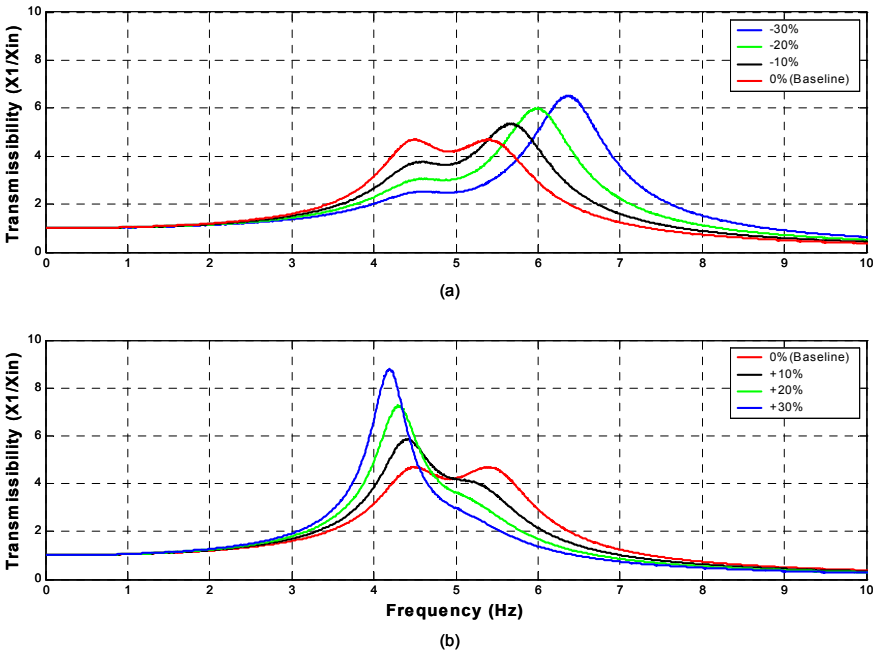

Figure 4-13. Transmissibility Changes of the Passive TVA As the Structure Mass Varies: (a) Subtracting Mass and (b) Adding Mass

4.3.1.2 On-off Velocity-Based Groundhook TVA

Figure 4-14a shows the transmissibility plots of the on-off VBG case, as the structure mass decreases to 30% of its baseline value, with an increment of 10%. Similar to the passive case, the second peak increases as the structure mass decreases. The first resonant peak grows as the structure mass increases to 10%, 20%, and 30% above its baseline mass (see Figure 4-14b). Again, like the passive system, the rate increase of the first peak is higher than that of the second peak in the on-off VBG case, indicating that the on-off VBG controlled, semiactive TVA is also more robust to decreases in the structure mass.

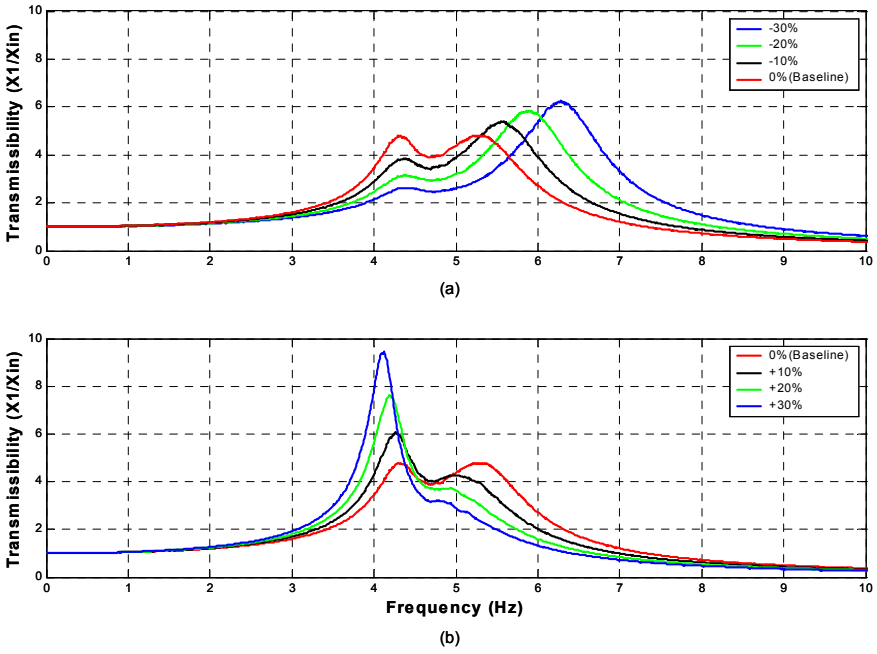

Figure 4-14. Transmissibility Changes of the On-off VBG Case As the Structure Mass Varies: (a) Subtracting Mass and (b) Adding Mass

4.3.1.3 Continuous Velocity-Based Groundhook TVA

For the continuous VBG TVA, the structure mass changes in the same manner as the passive and on-off VBG cases. The second resonant peak increases as the structure mass decreases, as shown in Figure 4-15a. These dynamics are similar to those observed in the passive and on-off VBG systems. However, the rate increase of the peak is lower in the continuous VBG case, implying that the continuous VBG case is more robust to the structure mass increases as compared with the passive and on-off VBG cases. Figure 4-15b shows the transmissibility changes of the continuous VBG case as the structure mass increases. The first resonant peak increases at a lower rate than those of the passive and on-off VBG. This again indicates that the continuous VBG is more robust to increases in the structure mass. Figure 4-15 suggests that the continuous VBG is more robust to decreases of the structure mass because the amplitudes of the first peaks in Figure 4-15b are higher than those of the second peaks in Figure 4-15a.

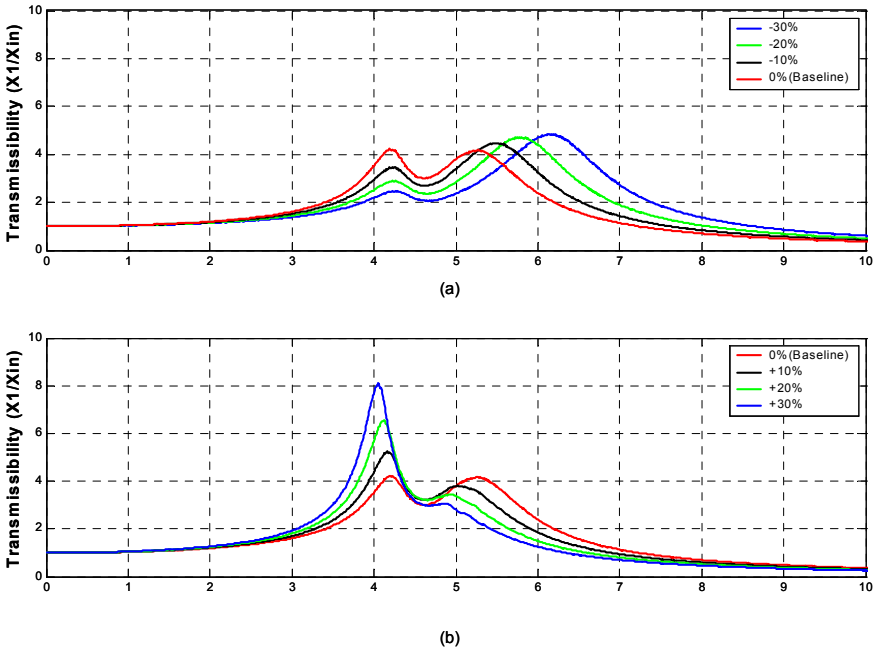

Figure 4-15. Transmissibility Changes of the Continuous VBG Case As the Structure Mass Varies: (a) Subtracting Mass and (b) Adding Mass

4.3.1.4 On-off Displacement-Based Groundhook TVA

This section presents the mass off-tuning analysis of the on-off DBG case. Figure 4-16a shows the transmissibility changes as the structure mass decreases by 10%, 20%, and 30% below its original mass. The second peaks slightly increase as the mass decreases. The first peaks increases as the structure mass discretely increases to 30% above its baseline mass with a 10% increment, as shown in Figure 4-16b. The rate increase of the first peak is higher than that of the second peak, indicating that the on-off DBG case is also robust to decreases in the structure mass.

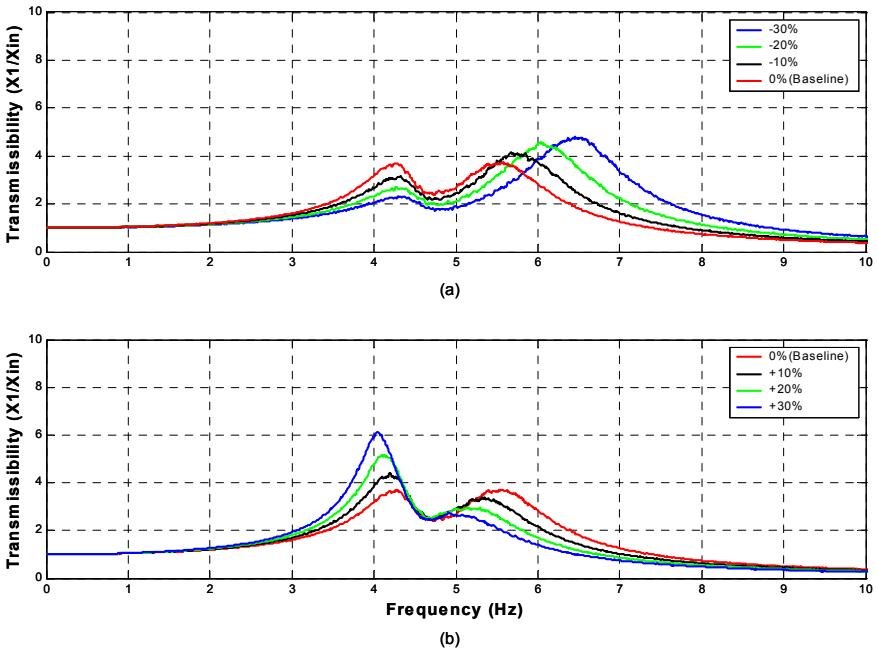

Figure 4-16. Transmissibility Changes of the On-off DBG Case As the Structure Mass Varies: (a) Subtracting Mass and (b) Adding Mass

4.3.1.5 Continuous Displacement-Based Groundhook TVA

Figure 4-17 shows the transmissibility variations as the structure mass decreases and increases, respectively. The dynamics of the continuous DBG case are, in many ways, similar to those of the on-off DBG system. The second peak increases as the mass decreases (see Figure 4-17a), and the first peak increases as the mass increases (see Figure 4-17b). The rate increase of the first peak is higher than that of the second peak, indicating that the continuous DBG is more robust to decreases in the structure mass, which is observed in other cases as well. The next section will compare the peak transmissibility changes of each TVA, summarizing the mass off-tuning analysis.

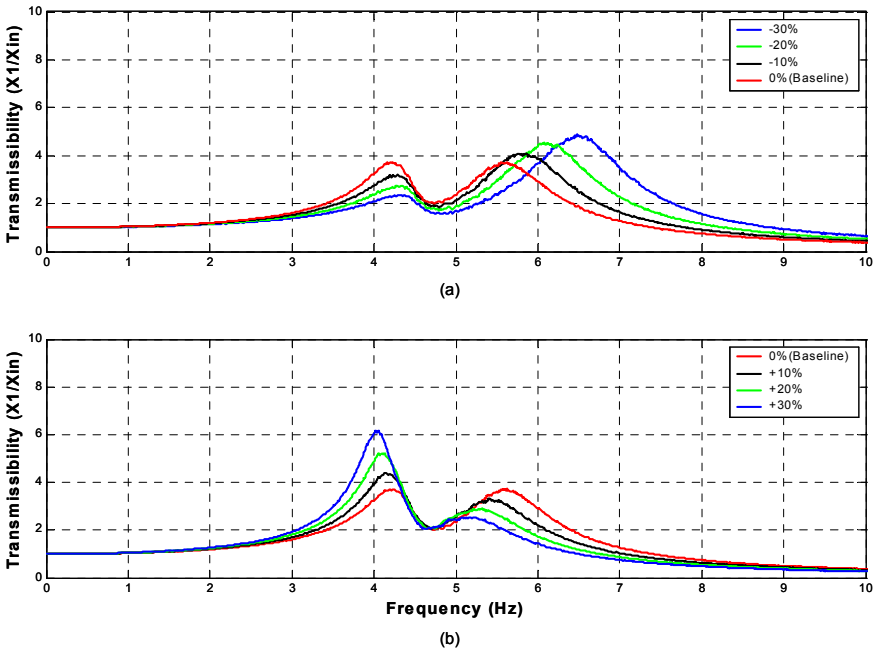

Figure 4-17. Transmissibility Changes of the Continuous DBG Case As the Structure Mass Varies: (a) Subtracting Mass and (b) Adding Mass

4.3.1.6 Comparisons

This section summarizes the performance of TVAs due to changes in the structure mass and analyzes their relative benefits. Figure 4-18 compares peak transmissibility changes of passive and semiactive TVAs as the structure mass varies from –30% to +30% of its original, or baseline, mass. For all cases, the slope of the lines are less when the structure masses are less than the baseline mass, indicating that all TVAs are more robust to decreases in structure mass. The on-off DBG and the continuous DBG cases show very similar performances. When the structure mass increases, the slopes of the passive, on-off VBG, and continuous VBG systems are steeper than those of the on-off DBG and continuous DBG systems, suggesting that the displacement-based, controlled, semiactive systems better adapt to increases in the structure mass. In summary, the results of mass off-tuning analysis indicate that displacement-based control polices are more robust to changes in the structure mass. Hence, they are more suitable for semiactive TVA applications.

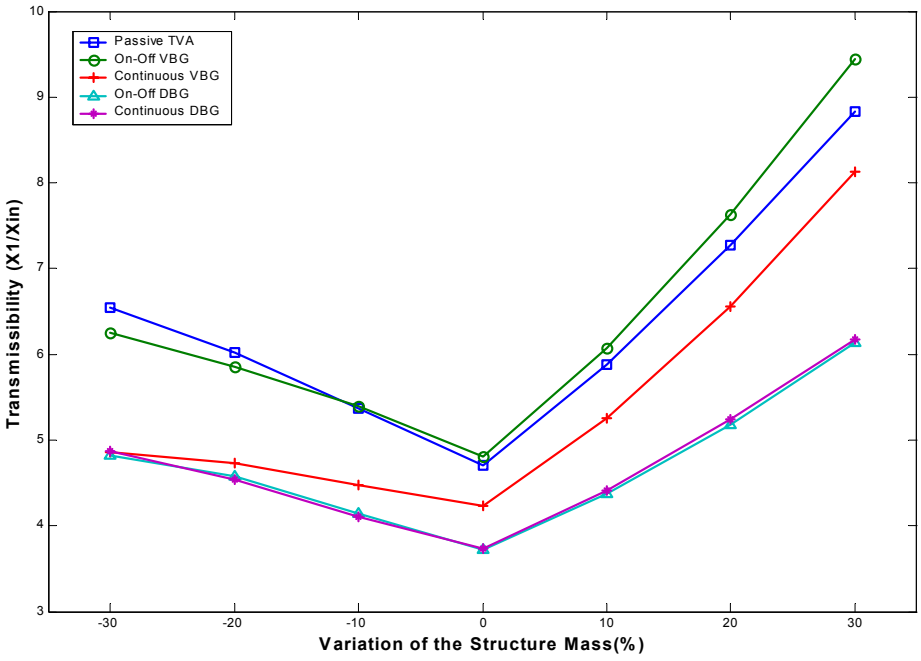

Figure 4-18. Peak Transmissibility Changes as the Structure Mass Varies From -30% to +30% of Its Baseline Value

4.3.2 Effect of Stiffness Off-tuning

In addition to the structure mass, the structure's stiffness can also cause off-tuning of TVAs. In the case of floor systems, changes in the properties of the materials used to provide stiffness can change the systems' stiffness. This section looks into the effect of stiffness off-tuning by changing the structure stiffness. After evaluating each TVA's performance due to stiffness off-tuning, it summarizes the results, providing a plot that shows the peak transmissibility variation in each system.

4.3.2.1 Passive TVA

Figure 4-19a shows the transmissibility plots of the passive case as the structure stiffness decreases to 30 % of its original (baseline) value with an increment of 10 %. Decreasing the stiffness raises the magnitudes of the first peaks. However, increasing the stiffness above its baseline value raises the second resonant peaks. Because the rate increase of the first peaks is slightly higher than that of the second peaks, the passive system is more robust to increases in the structure stiffness.

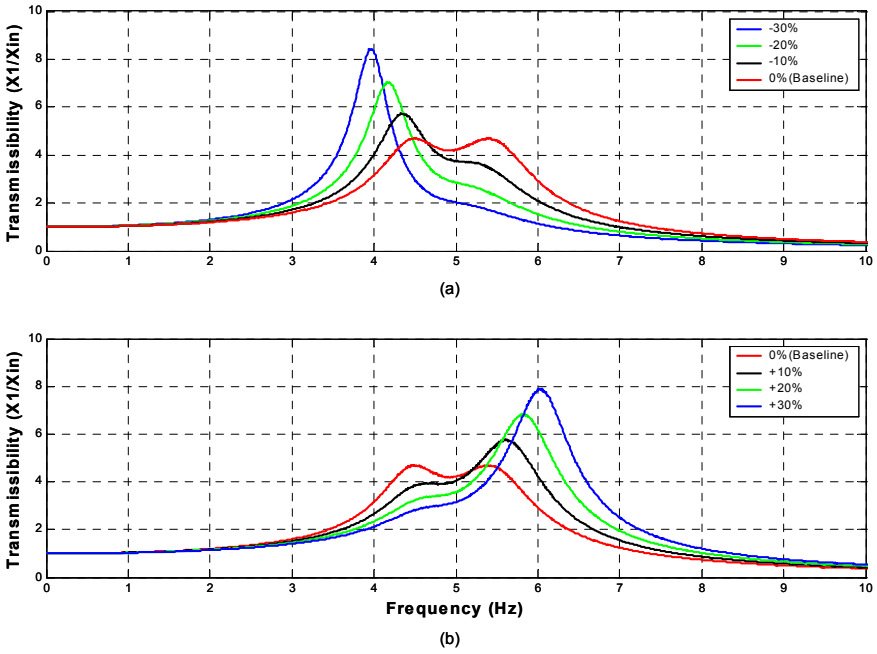

Figure 4-19. Transmissibility Variations of the Passive TVA As the Structure Stiffness Varies: (a) Decreasing Stiffness and (b) Increasing Stiffness

4.3.2.2 On-off Velocity-Based Groundhook TVA

Figure 4-20a shows the transmissibility variations of the on-off VBG model as the structure stiffness is reduced to 10%, 20%, and 30% below its baseline value. In this case, the first resonant peak increases. When the stiffness increases to 10%, 20%, and 30% above its baseline value, the second peak increases, as shown Figure 4-20b. It is observed that the rate increase of the first peak is much higher than that of the second peak, suggesting that the on-off VBG case is more robust to increases in the structure stiffness.

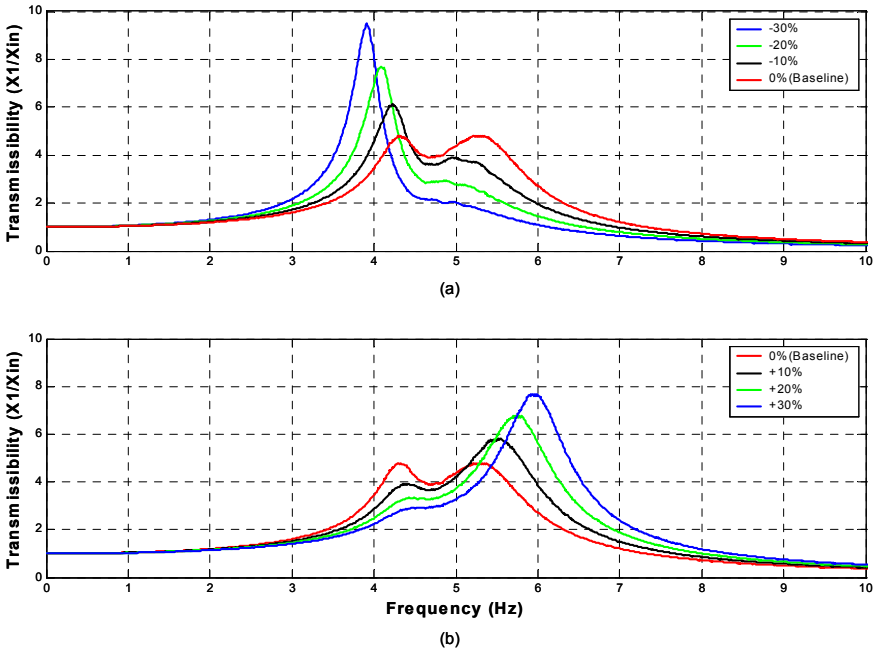

Figure 4-20. Transmissibility Variations of the On-off VBG TVA As the Structure Stiffness Varies: (a) Decreasing Stiffness and (b) Increasing Stiffness

4.3.2.3 Continuous Velocity-Based Groundhook TVA

This section presents the results of the stiffness off-tuning for the continuous VBG model. The structure stiffness varies by 10%, 20%, and 30% below and above its original stiffness. The amplitude of the first peak increases as the structure stiffness decreases, as shown in Figure 4-21a. When the stiffness increases, the magnitude of the second peak also increases. Similar to the on-off VBG case, the rate increase of the first peak is higher than that of the second peak, indicating that the continuous VBG case is also robust to increases in structural stiffness.

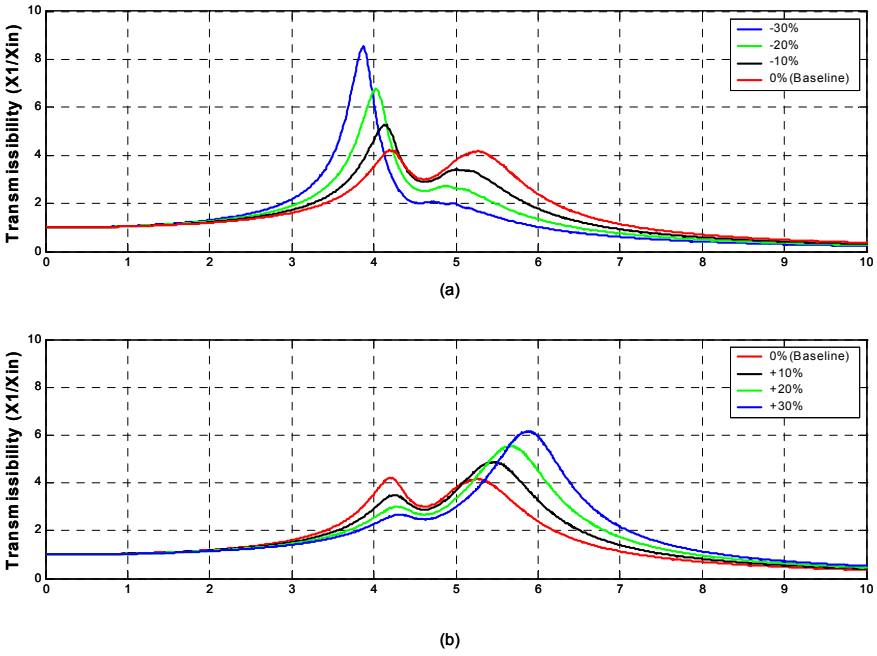

Figure 4-21. Transmissibility Variations of the Continuous VBG TVA As the Structure Stiffness Varies: (a) Decreasing Stiffness and (b) Increasing Stiffness

4.3.2.4 On-off Displacement-Based Groundhook TVA

Figure 4-22a shows the transmissibility variations of the on-off DBG case as the structure stiffness is reduced to 10%, 20%, and 30% below its baseline value. In this case, the first resonant peaks increase. When the stiffness increases to 10%, 20%, and 30% above its baseline value, the second peak grows, as shown in Figure 4-22b. Unlike velocity-based systems, the rate increases of the first and the second peaks are very similar, indicating that the on-off DBG system is equally robust to increases and decreases in structural stiffness.

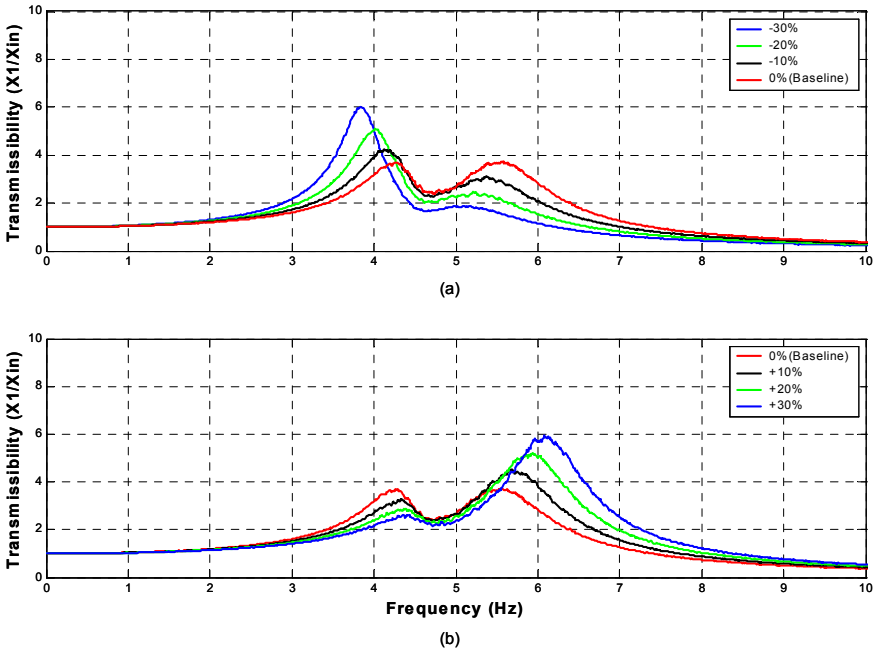

Figure 4-22. Transmissibility Variations of the On-off DBG TVA As the Structure Stiffness Varies: (a) Decreasing Stiffness and (b) Increasing Stiffness

4.3.2.5 Continuous Displacement-Based Groundhook TVA

Figure 4-23 shows the transmissibility variations as the structure's stiffness changes. The dynamics of the continuous DBG case are similar to those of the on-off DBG system. The first peak increases as the stiffness decreases (see Figure 4-23a), and the second peak increases as the stiffness increases (see Figure 4-23b). Also, the growth rates of the two peaks are similar, indicating that the continuous DBG is equally robust to decreases and increases in structural stiffness.

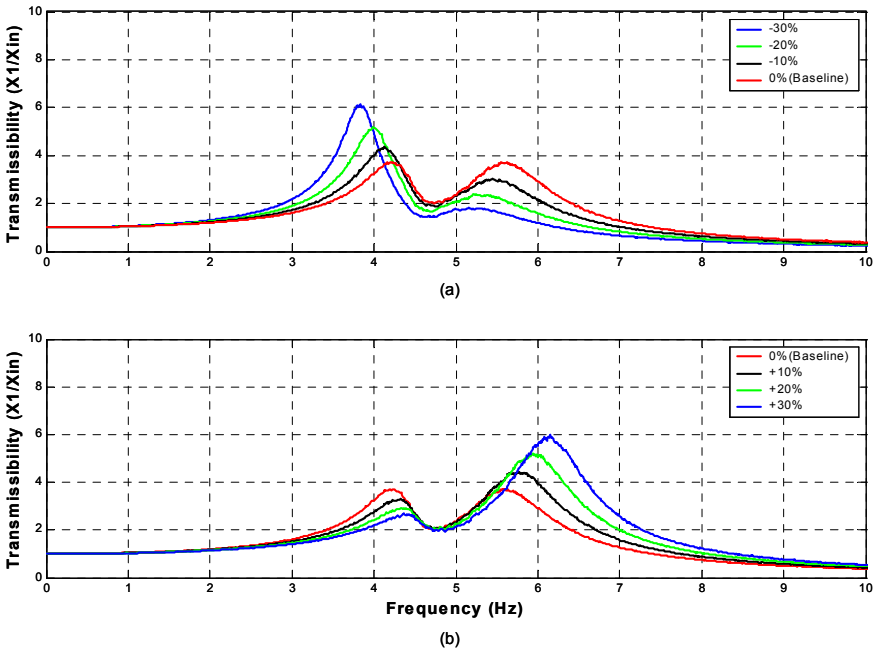

Figure 4-23. Transmissibility Variations of the Continuous VBG TVA As the Structure Stiffness Varies: (a) Decreasing Stiffness and (b) Increasing Stiffness

4.3.2.6 Comparisons

This section compares the results of structural stiffness off-tuning by providing peak transmissibility variations and evaluating the relative benefits of each TVA. Figure 4-24 shows peak transmissibility variations of each TVA as the structure stiffness ranges from -30% to 30% of its baseline value. Velocity-based controlled, semiactive TVAs are more robust to increases in structural stiffness because their slopes are steeper when the stiffness decreases. Moreover, the passive system is slightly more robust to increases in structure stiffness. On the other hand, displacement-based control systems are equally robust to increases and decreases in stiffness. The overall performances of on-off DBG and continuous DBG are nearly the same, but on-off DBG is slightly more robust to decreases in structural stiffness. Further observations reveal that the displacement-based controlled, semiactive systems offer better robustness as structural stiffness decreases. This is because the slopes of on-off DBG and continuous DBG are lower than those of other cases. This stiffness off-tuning study suggests that displacement-based controls are more appropriate for semiactive TVA applications.

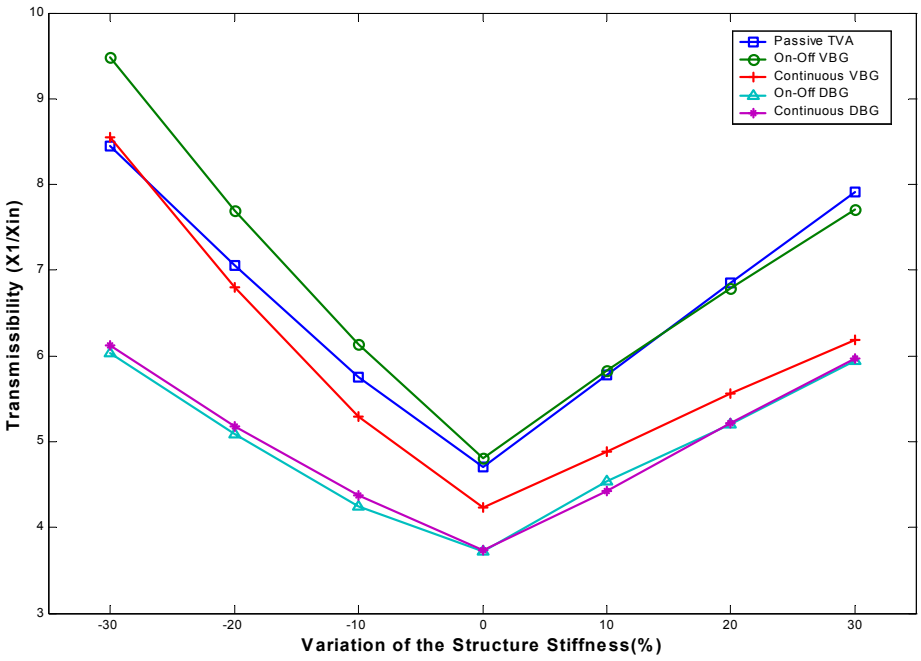

Figure 4-24. Peak Transmissibility Variations As the Structure Stiffness Varies From -30% to +30% of Its Baseline Value

4.3.3 Effect of Damping Off-Tuning

In the case of floor systems, the additions of carpeting and partitions can change damping. Additionally, errors in the estimation of the systems' damping values can off-tune TVAs. This section studies the effects of damping off-tuning by changing the structure damping ratio below and above its baseline value, while other parameters remain at their respective baseline values. It presents the results of each TVA's performance with transmissibility plots. This section concludes with a comparison plot that shows peak transmissibility changes of each TVA.

4.3.3.1 Passive TVA

Figure 4-25 shows the transmissibility plots of the passive system as the structure damping ratio varies from 0.0 to 0.06 with an increment of 0.01. When damping ratios are less than the structure's baseline value (ζ_1=0.03), the amplitude of the second peak is higher than that of the first peak. As the damping ratio increases above the baseline value, the magnitude of the second peak decreases, raising the first peak's amplitude. The overall amplitudes of transmissibilities decrease as the structure damping ratio increases.

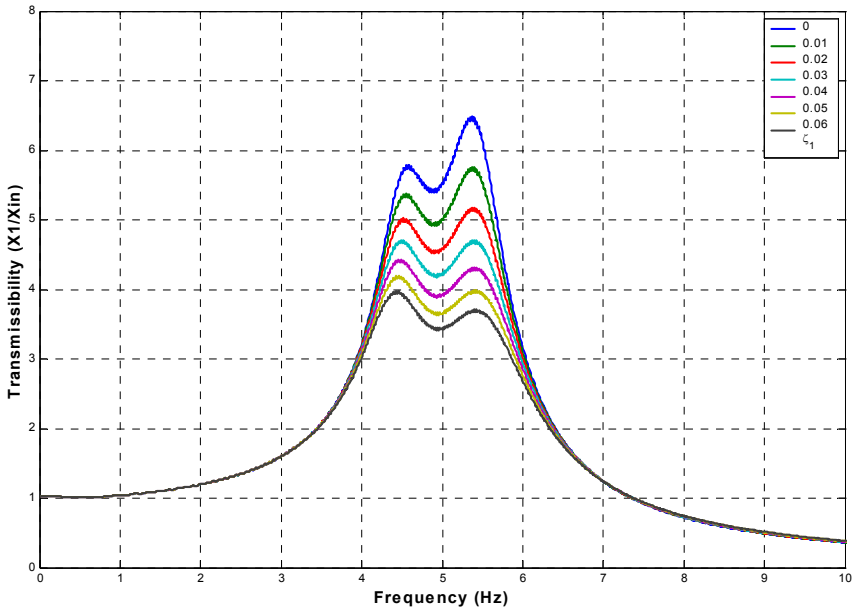

Figure 4-25. Transmissibility Variations of the Passive TVA As the Structure Damping Ratio Varies

4.3.3.2 On-off Velocity-Based Groundhook TVA

This section looks at the effect of changing the structural damping ratio of the on-off VBG TVA. Figure 4-26 shows the results of this case as the damping ratio discretely varies from 0 to 0.06. When the structure damping ratio is 0.0, the TVA is off-tuned because the amplitude of the second peak is larger than that of the first peak. As the damping ratio increases, the overall transmissibility curve decreases, indicating that increasing the damping ratio reduces the overall vibration levels of the system. Trade-offs between the amplitudes of the first peak and the second peak occur as the damping ratio increases. This is also observed in the passive system.

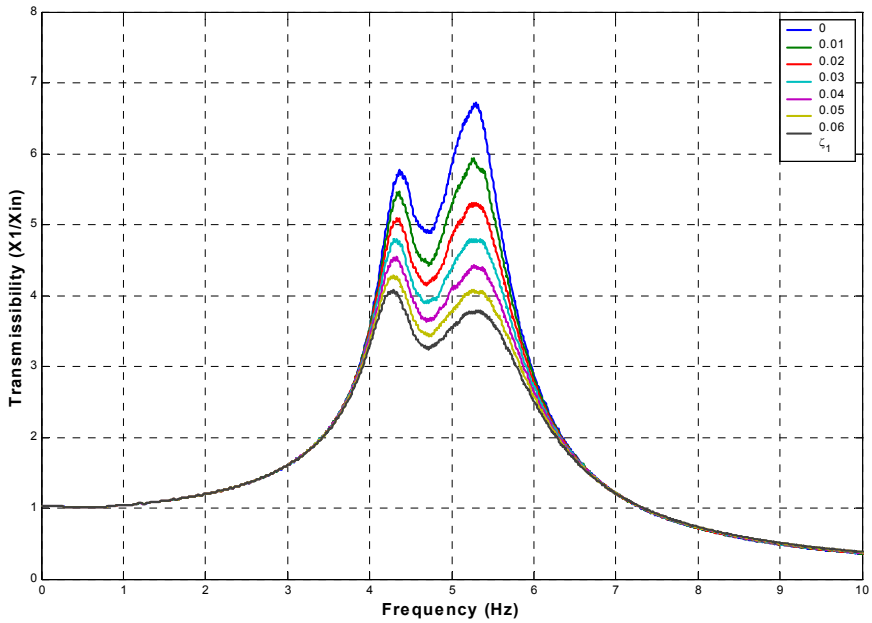

Figure 4-26. Transmissibility Variations of the On-off VBG TVA As the Structure Damping Ratio Varies

4.3.3.3 Continuous Velocity-Based Groundhook TVA

Figure 4-27 shows the transmissibility variations of the continuous VBG model, as the structure damping ratio ranges from 0.0 to 0.06. The dynamics of the continuous VBG system are similar to those of the passive and the on-off VBG systems. As the damping ratio increases, a reduction of transmissibility curves occurs, indicating that the overall vibration levels of the structure decrease as the damping ratio increases.

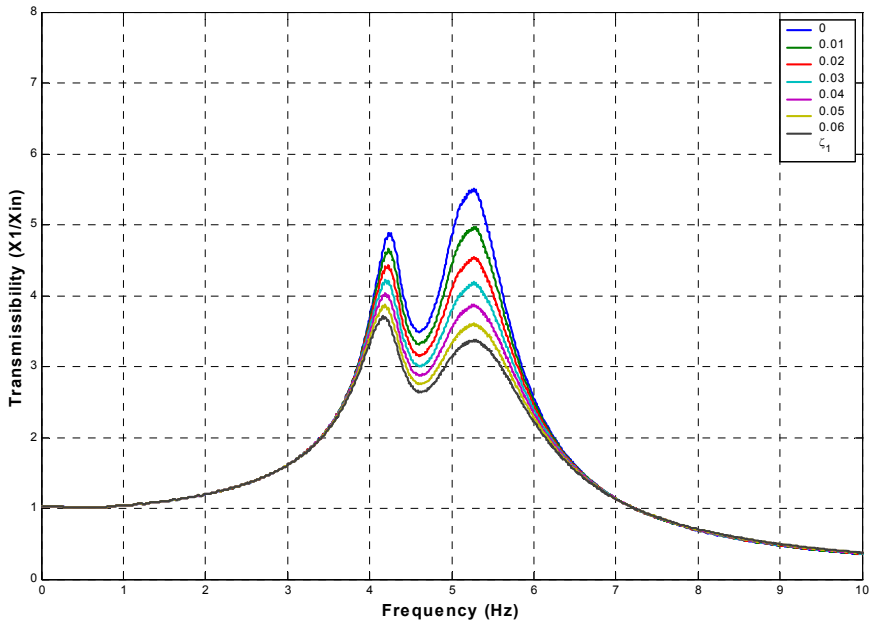

Figure 4-27. Transmissibility Variations of the Continuous VBG TVA As the Structure Damping Ratio Varies

4.3.3.4 On-off Displacement-Based Groundhook TVA

Figure 4-28 shows the transmissibility variations of the on-off DBG model as the structure damping ratio increases to 0.06 with an increment of 0.01. As the damping ratio increases, the amplitude of the second peak decreases, but the magnitude of the first peak increases. This behavior occurs with a reduction of the entire transmissibility curve, indicating that increases in the structural damping ratio result in a reduction of system vibrations.

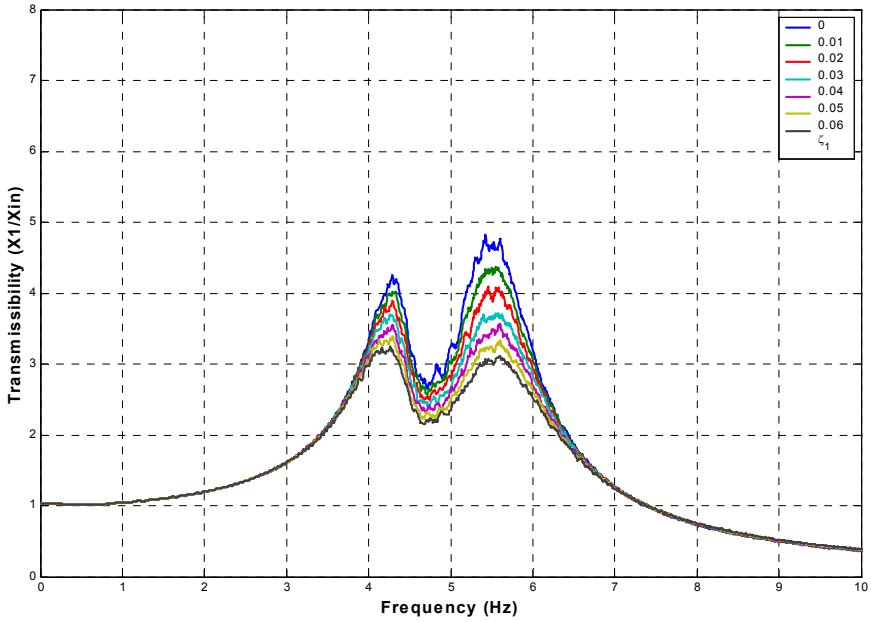

Figure 4-28. Transmissibility Variations of the On-off DBG TVA As the Structure Damping Ratio Varies

4.3.3.5 Continuous Displacement-Based Groundhook TVA

To study the effect of the structural damping ratio of the continuous DBG model, the damping ratio varies in the same way as the other cases. Figure 4-29 shows the transmissibility variations for this model. As observed in other systems, the overall transmissibility curves of the continuous DBG case also reduces as the structure damping ratio increases. Again, this means that increasing the damping ratio reduces the vibration levels of the system.

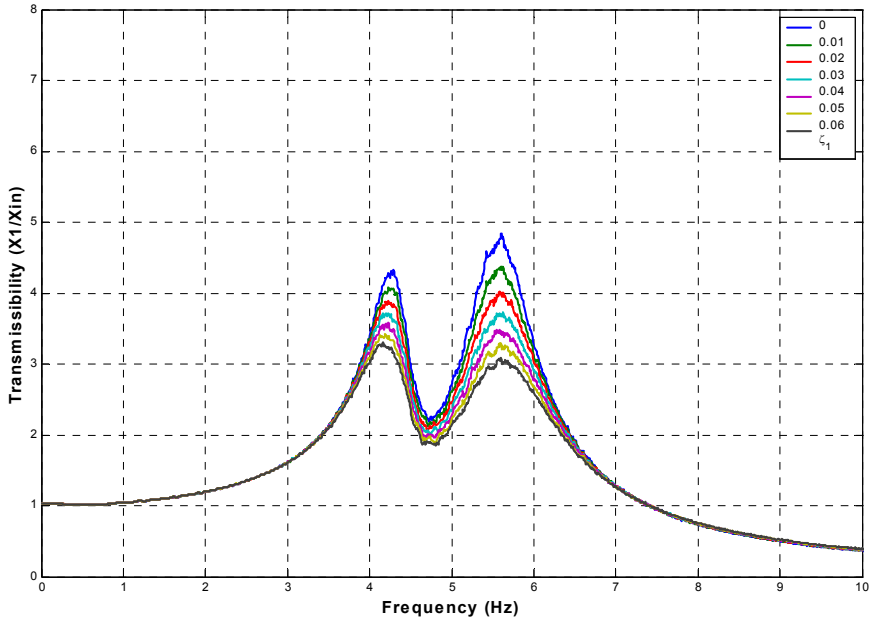

Figure 4-29. Transmissibility Variations of the Continuous DBG TVA As the Structure Damping Ratio Varies

4.3.3.6 Comparisons

This section summarizes the structural damping off-tuning analysis by comparing the peak transmissibility variations of each model. Figure 4-30 shows them as the structure damping ratios range from 0.0 to 0.06 with an increment of 0.01. For all cases, the slopes of the lines are negative, indicating that the transmissibility decreases as the damping ratio increases. In other words, increases in structural damping reduce the vibration levels of the structure. Moreover, as the damping ratio increases, the distance between the lines become narrower, implying that the performance gains of the semiactive systems over the passive system decrease. This observation suggests that semiactive TVAs perform more effectively in structures with lower damping ratios. Typical damping ratios of floor systems, such as offices and residences, ranges from 0.02 (for floors with few non-structural components) to 0.05 (for full-height partitions between floors) [6].

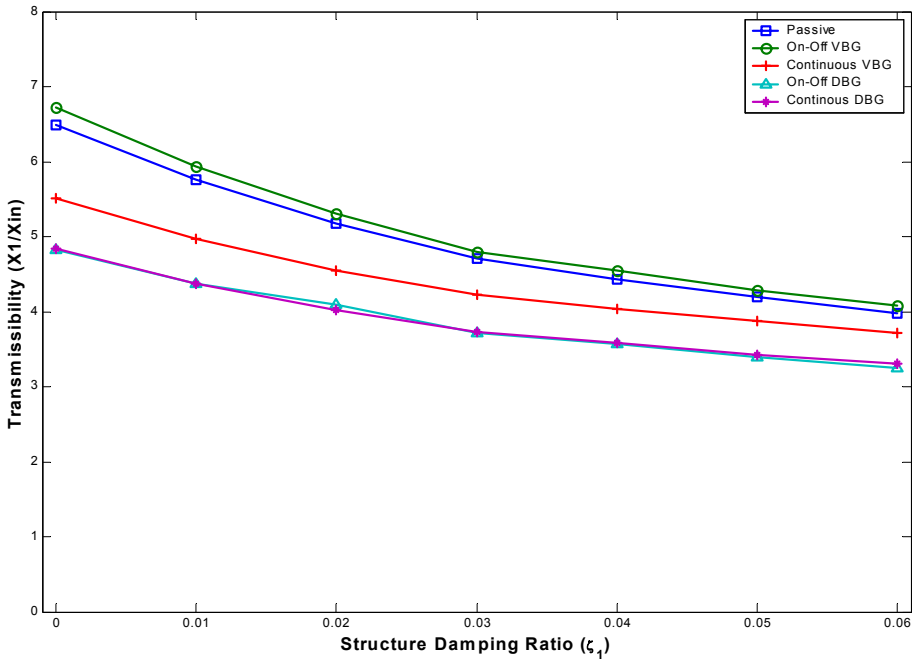

Figure 4-30. Peak Transmissibility Variations As the Structure Damping Ratio Varies

Chapter 5 Experimental Setup and Procedures

Included in this chapter is a detailed description of the test setup for all experiments conducted here. Each aspect of the laboratory testing is discussed: design and mechanics of the test rig, hydraulic actuation system, and data acquisition system. The chapter begins with a description of the test rig and its mechanics. This is followed by a description of the actuation system used to excite the rig. The data acquisition system that consists of both software and hardware components is then explained. A description of the data acquisition system concludes the chapter.

5.1 Design of Test Rig

A 2-DOF test rig was designed to experimentally evaluate the effectiveness of a semiactive TVA that uses an MR damper. The physical representation of the test rig is shown in Figure 5-1, along with 2-DOF mathematical model to show the correlation between simulation and experimental models.

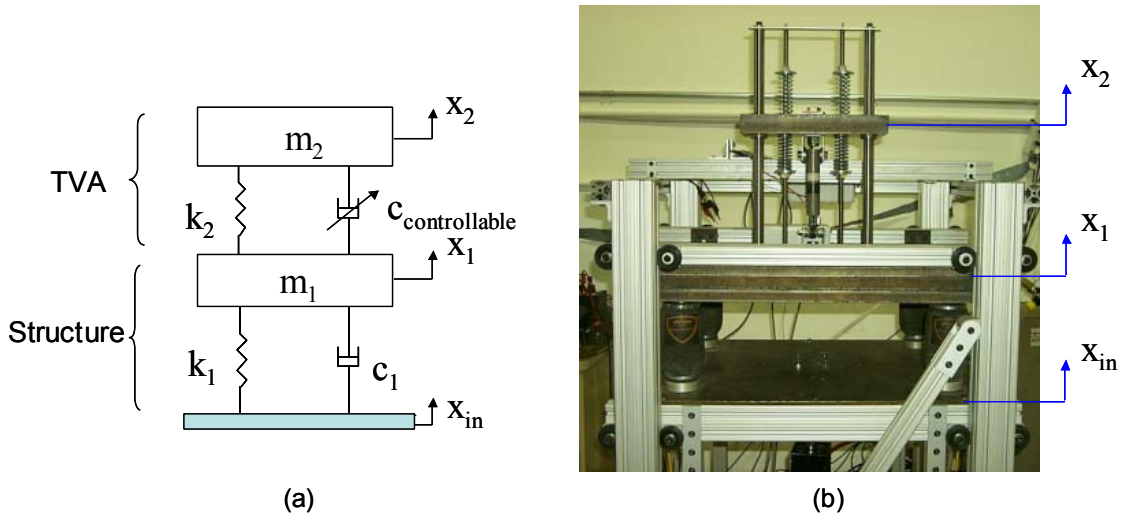

Figure 5-1. 2-DOF Test rig: (a) Mathematical Model; (b) Physical Model

Outlining the overall test rig setup, Figure 5-2 identifies the primary components of the test rig: the TVA mass, the primary structure (floor) mass, the air springs that represent primary structure (floor) stiffness, the coil springs that represent the TVA stiffness, the MR damper, the actuator, and the actuator plate. To help understand the test setup better, more detailed description of the components and their functions are provided next.

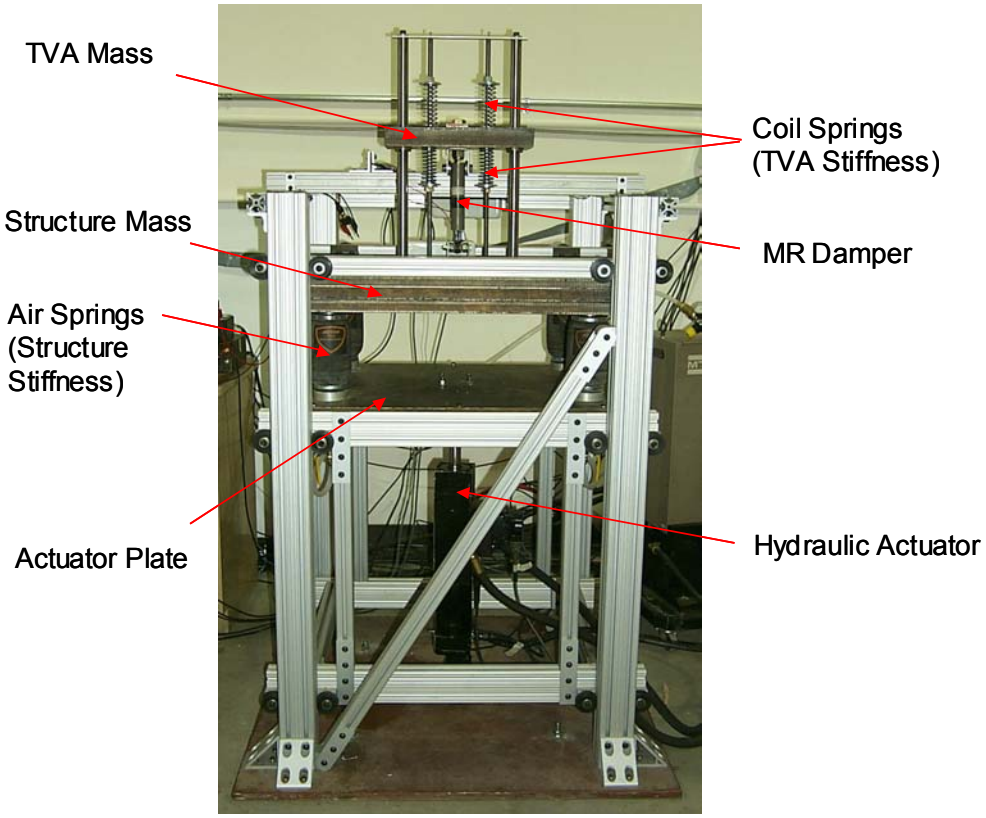

Figure 5-2. Test rig and Primary Components

With the use of extruded aluminum manufactured by 80/20 Inc., assembly and adjustments to the test rig are simplified. The main structure of the test rig is composed of four 3"x3" support posts that stand approximately 48" tall. Within these four posts, the actuator plate (which is connected to the hydraulic actuator) and structure mass are restricted to vertical motion by roller wheels. The roller wheels are used at all corners of the test rig and offer relatively friction-free motion. Figure 5-3 shows close-up of the roller wheels.

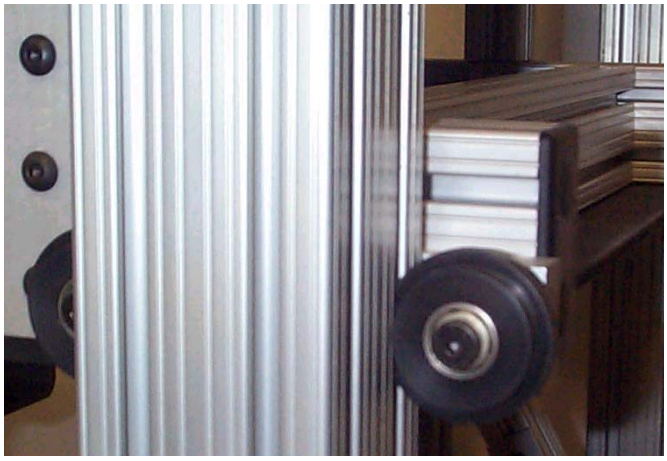

Figure 5-3. Close-up of Roller Wheels

The hydraulic actuator is mounted on the actuator plate which excites the structure mass through four air springs. In order to maintain the actuator plate as a rigid element, four 2”x3”x0.25” steel stiffeners are welded from the center of the plate to the four corners. The reinforced actuator plate is shown in Figure 5-4. Joining the actuator plate and the structure mass, the four air springs are networked and one air pressure is adjusted through only one regulator. The air pressure regulator is shown in Figure 5-5.

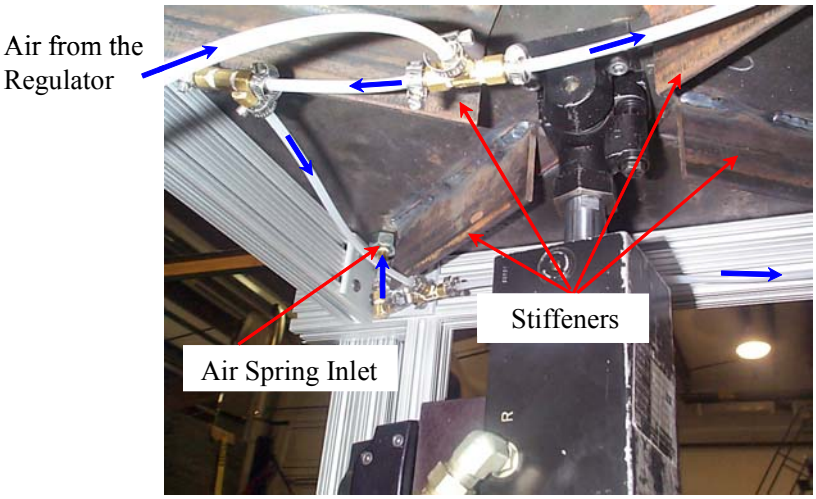

Figure 5-4. Actuator plate

Figure 5-5. Regulator

The bottom half of the test rig represents the structure mass and stiffness. The structure mass is modeled by three steel plates with a combined weight of 435 lb. Four Firestone model 7002 air springs represent the stiffness of the structure. The structure natural frequency is determined by the structure mass and the combined air springs' stiffness.

The TVA mass, made of a steel plate, is supported by an MR damper and four coil springs. The TVA is mounted atop the structure plates by harden linear bearing shafts. Linear bearings incorporated in the TVA plate eliminate lateral movements of the TVA mass, constraining the TVA to vertical motion only. The TVA weighs 30 lb. For fine tuning of the TVA, additional mass can be added on top of the TVA plate. Four coil springs are pre-compressed along the threaded rods with nuts and washers. The combined spring rate of the four coil springs represents the TVA stiffness. Again, several coil springs with different spring rates were available in order to fine tune the TVA. To prevent towering motion of the TVA, a cross bar secures the two linear bearing shafts. The TVA is shown in Figure 5-6

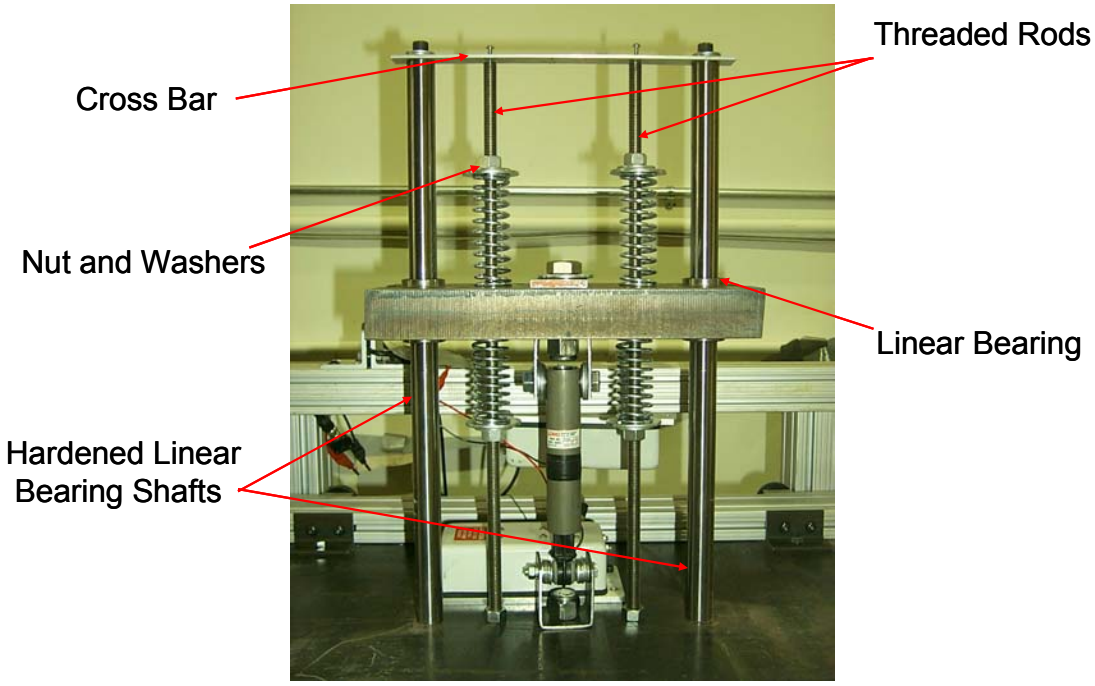

Figure 5-6. Semiactive Tuned Vibration Absorber

For the damping element of the semiactive TVA, an "MR sponge damper" is selected and is shown in Figure 5-7. As described in Chapter 2, an MR sponge damper is a new type of MR fluid device that contains MR fluid in an absorbent matrix. This MR sponge device is appropriate for the semiactive TVA application here because it provides the necessary on-state damping force when energized and has a reasonably low off-state damping.

Figure 5-7. The Magneto-Rheological Sponge Damper for Semiactive Tuned Vibration Absorber

In order to determine the damping characteristics of the MR sponge damper, it was tested in the Material Testing System (MTS) load frame, shown in Figure 5-8. The tests were conducted by collecting the peak force and velocities due to a sinusoidal input. Figure 5-9 shows the damper's force versus velocity curve.

Figure 5-8. MTS machine used for testing dampers

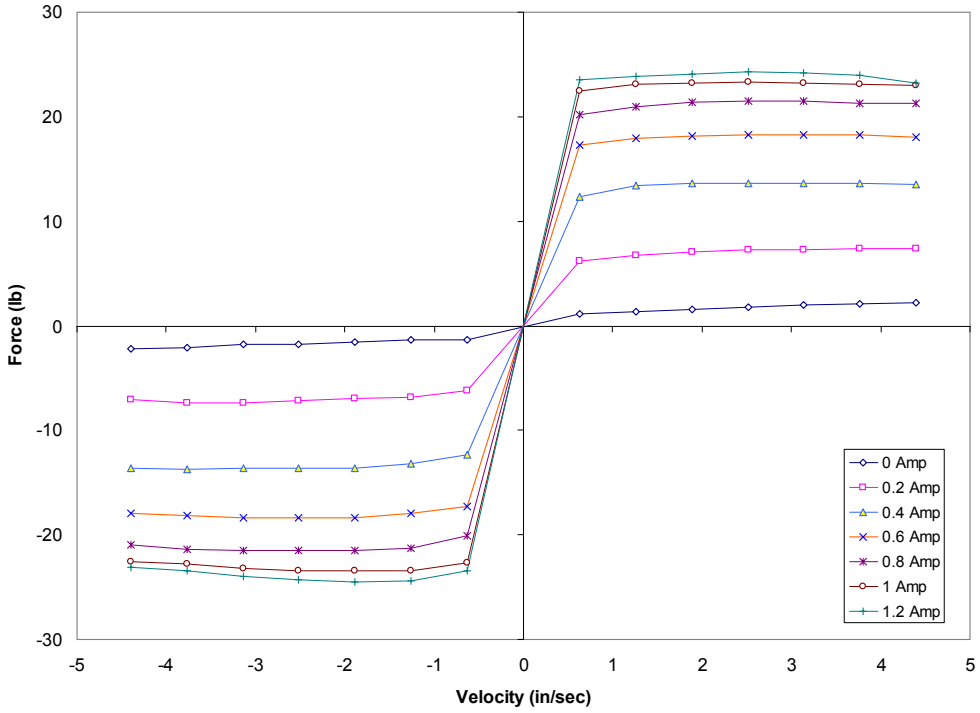

Figure 5-9. Force-Velocity Curve for the MR Sponge Damper

5.2 Hydraulic Actuation System

Input displacement excitations were provided by a hydraulic actuator manufactured by Material Testing Systems (MTS). The actuator is capable of inputs ranging from single frequency waveforms to multi-frequency signals as well as step and ramp inputs. The hydraulic actuator, shown in Figure 5-10, was one of four components included in the actuation system. This particular model, MTS model 242.09, has a dynamic stroke of ±2 inches (±5 cm) and a force capacity of ±2200 lb (±10 kN). An internal load cell and position sensor allow for force and position measurements. To avoid any lateral loading on the actuator, MTS swivel ends were incorporated into installation on both ends of the actuator.

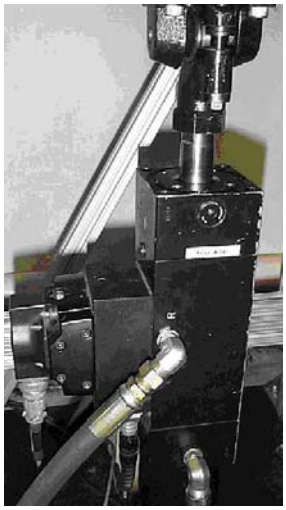

Figure 5-10. MTS 242 Series Hydraulic Actuator

The actuator is controlled by the MTS 407 Controller shown in Figure 5-11. Offering two modes of control, displacement or force, the 407 Controller is a single-channel, digitally supervised, servo controller. All input signals to the actuator, whether external or internal, must go through or be generated by the 407 Controller.

Figure 5-11. MTS 407 Controller

A SilentFlo Hydraulic Power Unit, MTS Model 505.20, is used to provide fluid to the actuation system. The hydraulic pump, shown in Figure 5-12, has a flow rate of 20 gal/min (75 L/min) and an operating pressure of 3000 psi (210 bar).

Figure 5-12. MTS SilentFlo Hydraulic Power Unit

Linking the hydraulic pump and the actuator, a MTS Model 263 Hydraulic Service Manifold is used to regulate the hydraulic pressure and flow to the actuator. The manifold is shown in Figure 5-13. The regulated flow is necessary to ensure proper dynamic response of the actuator.

Figure 5-13. MTS Hydraulic Service Manifold

5.3 Data Acquisition System

This section describes the data acquisition setup along with a comprehensive description of the hardware and software components. After an overview of the data acquisition, details of data acquisition components are described.

5.3.1 Overview of Data Acquisition

The MTS 407 hydraulic controller is used to control the actuator and monitor the actuator position and force. Excited by the actuator, the structure and TVA masses vibrate. Their motions are measured by an accelerometer and two LVDTs. The transducers collect the structure motions and relative motions between the structure mass and the TVA mass. The measured signals are then amplified and filtered using Frequency Devices model 9002 LP01. The dSPACE AutoBox provides digital signal processing of the transducer and actuator signals. These signals are then digitally converted and stored in a personal computer. Control signals to the MR damper, determined by the control policy, are converted to analog signals in the AutoBox. Then, the voltage signals are passed through the current driver and sent to the MR damper. The data acquisition flowchart shown in Figure 5-14 summarizes the above discussion.

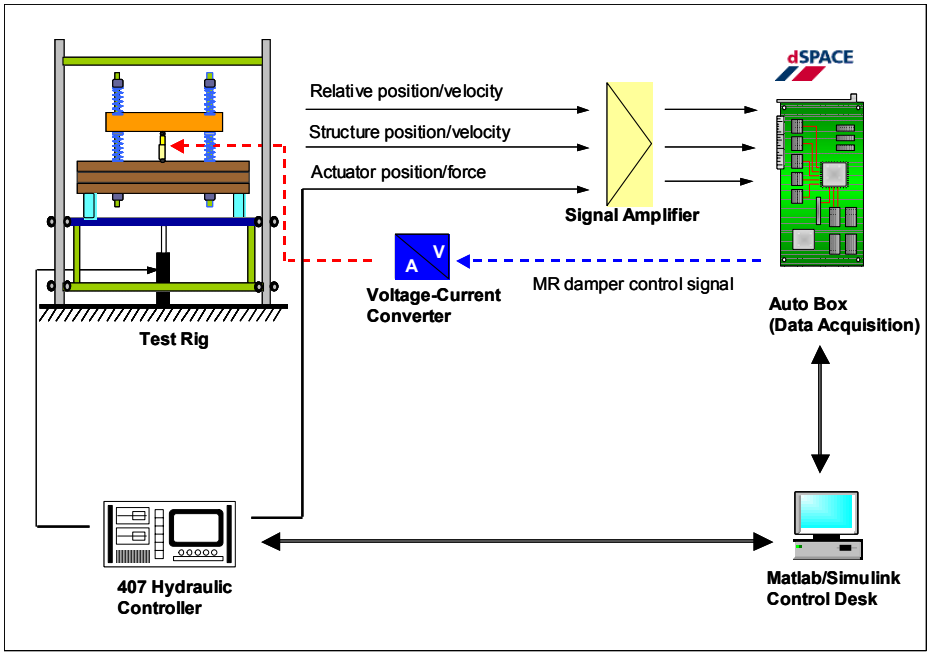

Figure 5-14. Schematic of Data Acquisition

5.3.2 Hardware Components of Data Acquisition

The hardware components of the data acquisition system included two LVDTs, an accelerometer, a signal conditioner, a dSPACE digital signal processor, the MTS 407 hydraulic controller, MR damper current driver, and two digital signal amplifiers. The MTS 407 controller sent input signals to the actuator and received the actuator's output signals. All the internal and external input signals to the actuator went through the MTS 407 controller. The embedded load cell and position sensors on the MTS hydraulic actuator measured both the actuator displacement and force.

The two LVDTs, (UniMeasure Velocity-Position Transducers Model VP510-10) measured the displacement and velocity of the system. UniMeasure Model VP510-10, shown in Figure 5-15, required a power supply for position measurements, while the velocity component of the transducer was self-energizing. With a sensitivity of 197 mV/in/sec and 999 mV/in for velocity and position respectively, these transducers were well suited to our applications and provided a clean signal for real-time control.

Figure 5-15. UniMeasure VP510-10 Velocity-Position Transducer

As seen in Figure 5-16, a UniMeasure Velocity-Position Transducer was mounted to a stationary reference above the structure mass. In this configuration, the velocity-position transducer measured both the absolute displacement and the absolute velocity of the structure mass with reference to the ground. A second UniMeasure Velocity-Position Transducer was mounted between the structure and the TVA mass to measure both the relative velocity and relative displacement.

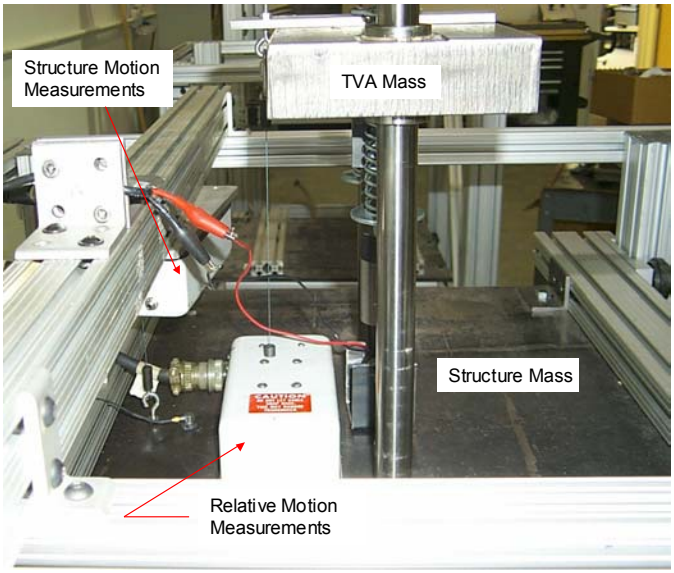

Figure 5-16. LVDT Mount

A PCB model U352L65 ICP accelerometer (sensitivity 97.9 mV/g) measured the acceleration of structure mass. It was placed on the structure mass as shown in Figure 5-17.

Figure 5-17. PCB Accelerometer

The acceleration measurement was conditioned using a PCB signal conditioner, shown in Figure 5-18, and gained by a factor of ten. The use of the gain at the signal conditioner preserved a good signal to noise ratio.

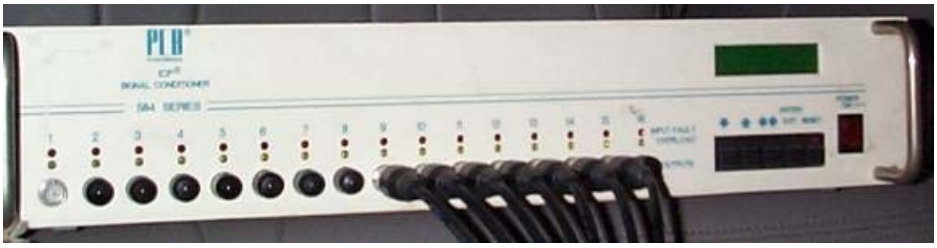

Figure 5-18. PCB Signal Conditioner

The two Frequency Devices Model 9002 LP01, shown in Figure 5-19, were used as an amplifier and a low pass filter. Representing human excitations, the amplitudes of actuator input were very small, as were the magnitudes of structure motions. These small signals only used a small portion of the A/D converter so the signals could not be completely expressed with a small number of A/D conversion bits. Thus, the Frequency Device units amplified these signals to fully realize the capacity of the A/D converter. The actuator input signal was gained by 25 (pre gain 5 and post gain 5), and the structure measurements were gained by 100 (pre gain 10 and post gain 10). The Frequency Devices unit is an 8-pole, 6-zero elliptic low pass filter. For current experiments, the cutoff frequency was set at 10 kHz.

Figure 5-19. Frequency Devices Model 9002 LP01 Units

All the measured transducer signals were routed to a custom built junction box as shown in Figure 20. Those signals then went to the AutoBox. Moreover, the out control

signals from the AutoBox come to the junction box before they went to the MR damper and the actuator.

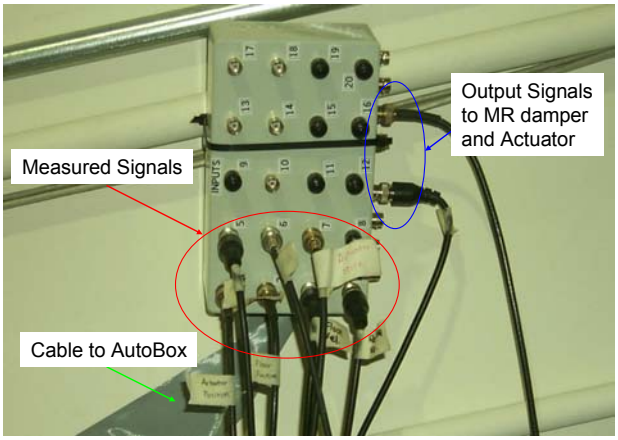

Figure 5-20. Junction Box

AutoBox is the hardware component of the dSPACE package. The AutoBox contains the DS 100e processor board with the DS2201ADC (analog to digital converter) and the DS2201DAC (digital to analog converter), an I/O card with twenty inputs, and eight outputs that were used to collect data and output control signals. Information flowed to and from the AutoBox via a dedicated Ethernet connection. The AutoBox is shown in Figure 5-21.

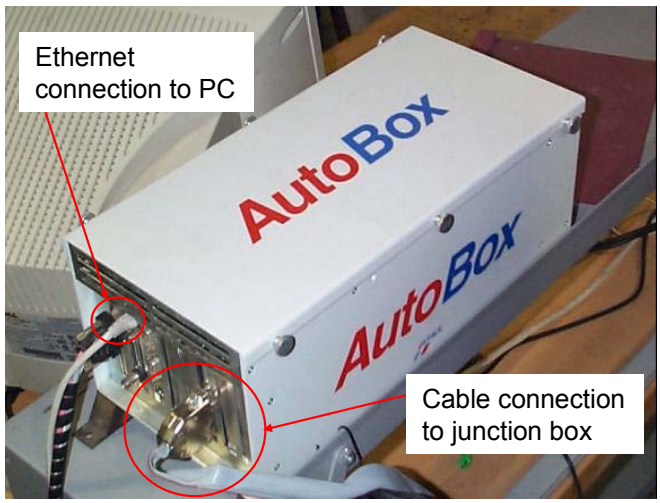

Figure 5-21. dSPACE AutoBox

It was necessary to use a current driver circuit because the MR damper dynamics were driven by current. The circuit shown in Figure 5-22 had to be used to amplify the current in the output signal of control policy coming from Control Desk. The circuit was designed such that the current to the damper was proportional to the control voltage coming from dSPACE. The first stage of the circuit converted the control voltage from dSPACE to a voltage referenced to the ground of the current driver circuit. The second stage of the circuit then routed the output from the first stage to a power transistor, which drove a proportional current through the MR damper [83]. Figure 1-22 shows the power supplies for the circuit (power supply one for 15V and power supply two for 12V), the circuit box, and the multimeter for monitoring current to the MR damper.

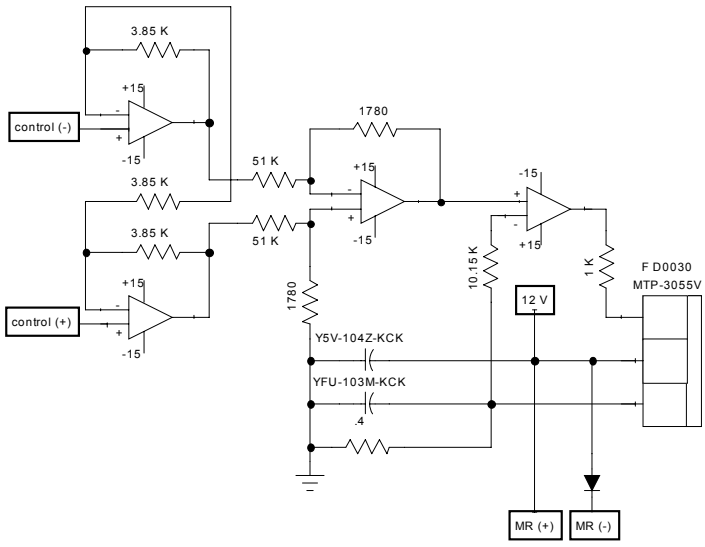

Figure 5-22. Current Driver Circuit for MR Damper [83]

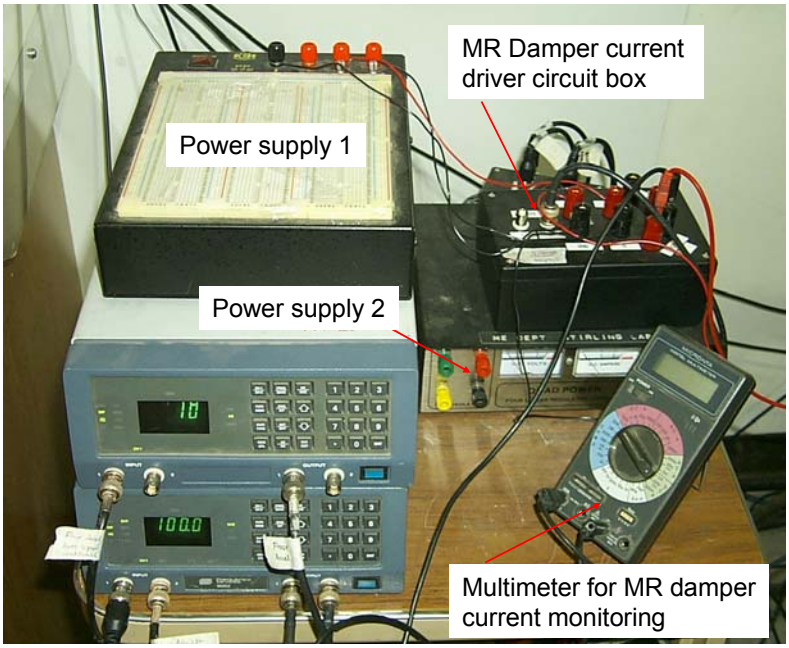

Figure 5-23. MR Damper Current Drive Circuit Box

5.3.3 Software Components of Data Acquisition

Testing software components included Matlab/Simulink and dSPACE Control Desk 3.0. MATLAB was the foundation for Simulink, which, through the Real Time Workshop toolbox, the three components were linked. All models for data acquisition and controller implementation were built within Simulink with inputs and outputs. dSPACE compiled these models and loaded them to the dSPACE DSP chip.

Figure 5-24 shows the block diagram used for all data acquisition, complete with real-time control outputs for each control policy. The signals measured on the test rig came into the AutoBox through the DS2201ADC (analog to digital converter). Within Simulink, the twenty input channels of the AutoBox were multiplexed into five ports with four input channels per port. For this reason, the signals had to pass through a demultiplexer that separated them. The DS2201DAC (digital to analog converter) allowed real-time control. In this case, the eight ports corresponded directly to the eight output channels on the AutoBox. The current study used seven input and two output channels.

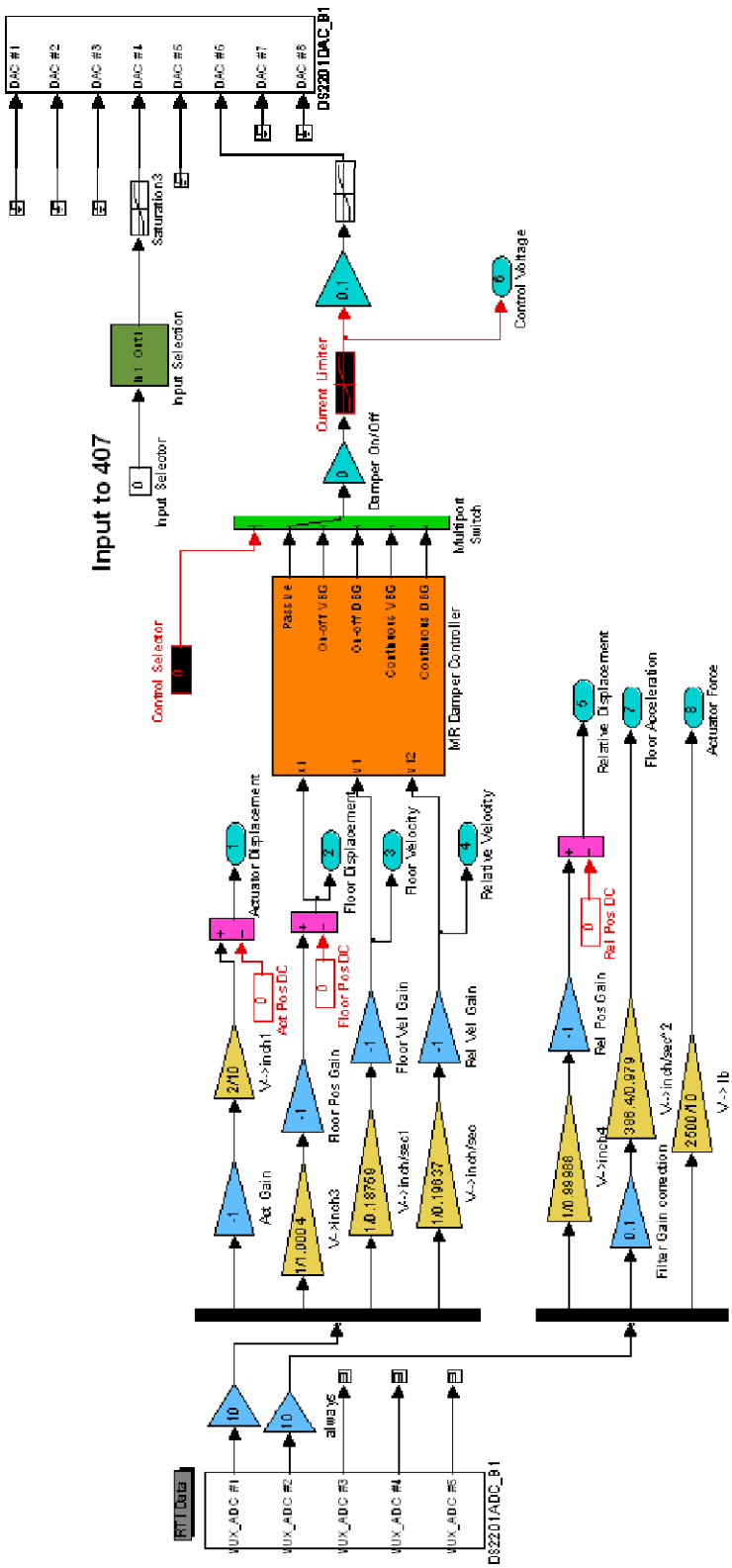

Figure 5-24. Data Acquisition and Control Block Diagram

Control Desk was the user interface software for this experiment. Within Control Desk, data could be viewed and model parameters could be tuned in real-time. The ability to adjust controller parameters real-time simplified controller development and made dSPACE a powerful tool for rapid prototyping. Signal processing systems were used to specify and manipulate output controller signals and input transducer signals. These block diagrams were then downloaded into the Control Desk software, which communicated with the AutoBox. MATLAB was the communicating language between Simulink and dSPACE. Subsequently, all data analysis occurred within MATLAB. Control Desk provided real-time analysis environment; its user interface is shown in Figure 5-25.

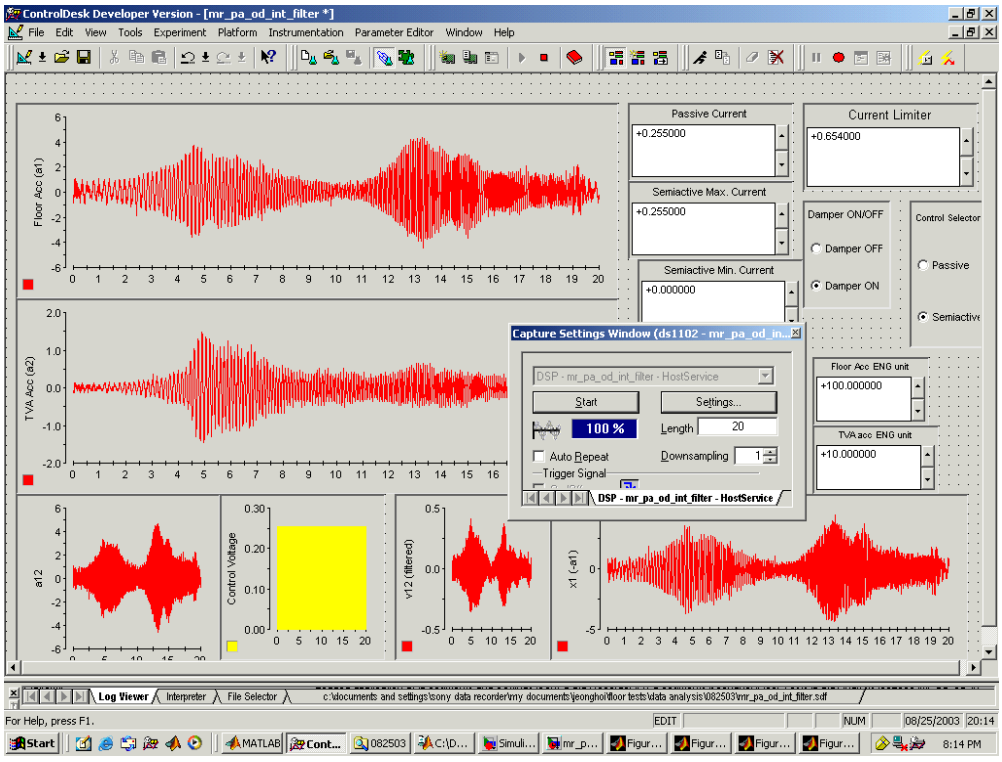

Figure 5-25 dSPACE Control Desk Software User Interface

5.4 Experimental Procedures

This section explains the input excitation used throughout the experiments. It also explains how the collected data was processed to analyze the experimental results.

5.4.1 Input Excitation

A chirp signal was chosen as the input in this study to identify the frequency dynamics of the MR TVA and to quantify the benefits of the control strategies in the frequency domain. The chirp signal that was used in the experiments was generated by Simulink. This chirp signal allowed the user to define the frequency range of the chirp as well as its duration. To enable continuous repetition, the user had the option of adding a period of zeros between the chirps to separate them. This function proved to be useful during testing. The parameters of the chirp signal for all testing are defined in Table 5-1. The input chirp signal is shown in Figure 5-26.

Table 5-1. Chirp Signal Parameters

Initial Frequency	0.5 Hz
Final Frequency	10 Hz
Target Time	64 sec
Zero Time	4 sec
Amplitude	0.01 in.

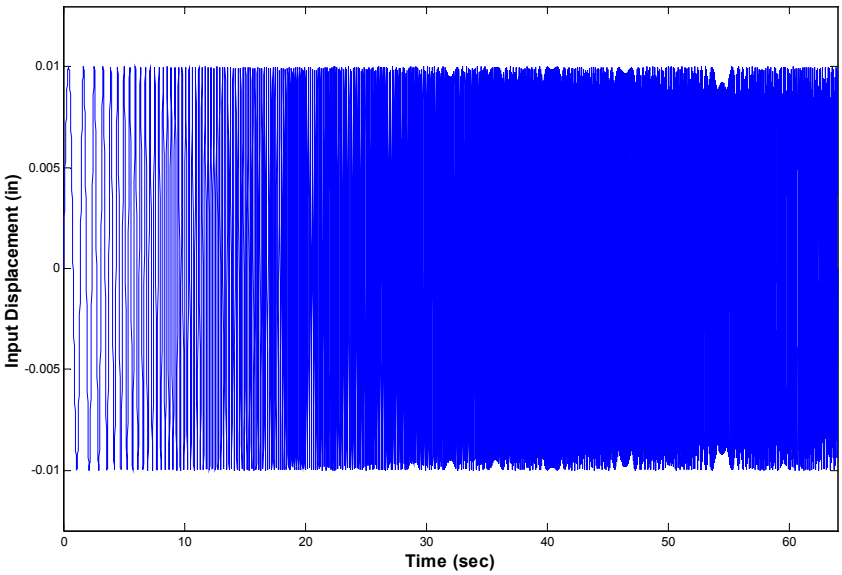

Figure 5-26. Chirp Input Signal

The frequencies (0.5-10 Hz) were chosen because humans are most susceptible to vibrations in the 2-4 Hz range [3], and the most problematic floor system's frequencies are less than 10 Hz [2]. With a target time of 64 seconds, the chirp signal slowly swept this frequency range. This slow sweeping-chirp signal preserved that the low frequency dynamics. The slow chirp also helped to minimize transient lag between the input and output. The four seconds of zero time aided in the data capturing and the data reduction processes. Each of the chirp signals was clearly separated by a period of zeros. This made the starting and ending points of the chirp easy to identify. The amplitude of the chirp signal was 0.01 inches. This small magnitude was used to represent realistic dynamic loading magnitudes of building floor systems.

5.4.2 Signal Processing Methods

Because the frequency content of the system dynamics was below 10 Hz, it was deemed acceptable to sample the time data at 100 Hz. A sample rate of 100 Hz was ten times faster than the fastest dynamics entering the system. This ensured that aliasing frequency content higher than the Nyquist frequency would not be an issue. Once the data was collected, it was loaded into Matlab. The data reduction took place within Matlab. The time traces collected using Control Desk were transformed into the frequency domain in order to generate transmissibilities and phase plots. The displacement transmissibilities of the structure mass and the input as well as the phase angles between the TVA and the structure masses were of particular interest. The transmissibilities and phase angles identified the dynamic characteristics of the semiactive TVAs, enabling comparison with those of the passive system. Conveniently, all of these displacement signals were available from the data acquisition system within Control Desk.

The frequency response function (FRF) was generated using the FRF estimator shown below,

$$H(\omega) = \frac{G_{XY}(\omega)}{G_{XX}(\omega)} = \frac{X^*(\omega) \cdot Y(\omega)}{X^*(\omega) \cdot X(\omega)} \tag{5.1}$$

where $G_{XY}(\omega)$ is the cross spectrum from input to output, and $G_{XX}(\omega)$ is the auto spectrum of the input. The displacement signals, conditioned to remove the zero-time offset, were transformed into the frequency domain using the FFT algorithm. Once they were in the frequency domain, the cross spectrums and auto spectrums were generated. Using equation 5.1, the transmissibilities were plotted to show the output/input ratio between the structures and the input displacements.

Chapter 6 Experimental Results

A series of tests were performed on the test setup, evaluating the passive and the semiactive TVA in the same manner as the simulation study. This chapter presents the experimental results and performance evaluations of the TVAs. It begins with identifying the primary system parameters before the TVA was mounted on the system by performing a single-degree-of-freedom and static tests. After identifying the primary system, the dynamic properties of the passive TVA were analyzed. Following the passive TVA analysis, the subsequent sections discuss the dynamics of the semiactive TVA based on the results of parametric studies. The parametric studies considered the effects of on-state/off-state current and control gain changes. The parametric studies were then extended to off-tuning tests, which evaluated the performance of the semiactive TVA with varying the primary structure mass (mass off-tuning). This chapter ends with concluding remarks regarding the benefits of semiactive TVAs.

6.1 System Identification

This section presents the system identification of the primary structure before adding the TVA. Identifying the primary system is important in tuning the TVAs. The section describes a single-degree-of-freedom (SDOF) modal test used to characterize the primary system. The section also discusses a static test that was performed to validate the use of air springs in the primary system as its stiffness element.

6.1.1 SDOF Test

Before any TVA tests, an experimental modal test was performed on the primary structure. The purpose of this test was to identify the structure's natural frequency and damping ratio. Figure 6-1 shows the result of the SDOF test. The maximum transmissibility (equal to fifteen) occurs at the frequency of 5.1 Hz. This indicates the natural frequency of the primary structure. The transmissibility of fifteen implies that the output displacement of the structure is fifteen times larger than that of the input. One of

the primary goals of this research is to reduce this transmissibility by using semiactive TVAs. The half-power method was employed to identify the system's damping ratio. A detailed discussion of the half-power method can be found in reference [84]. The system damping ratio was found to be 0.03 (3%) as shown below:

$T_{peak} = 15$

$T_{3dB} = 0.707 \times T_{peak} = 10.6$

$\omega_a = 4.95$ Hz

$\omega_b = 5.28$ Hz

$\omega_n = 5.1$ Hz

$$\zeta_1 = \frac{\omega_b - \omega_a}{2\omega_n} = \frac{5.28 - 4.95}{2 \times 5.1} = 0.03\ (3\ \%)$$

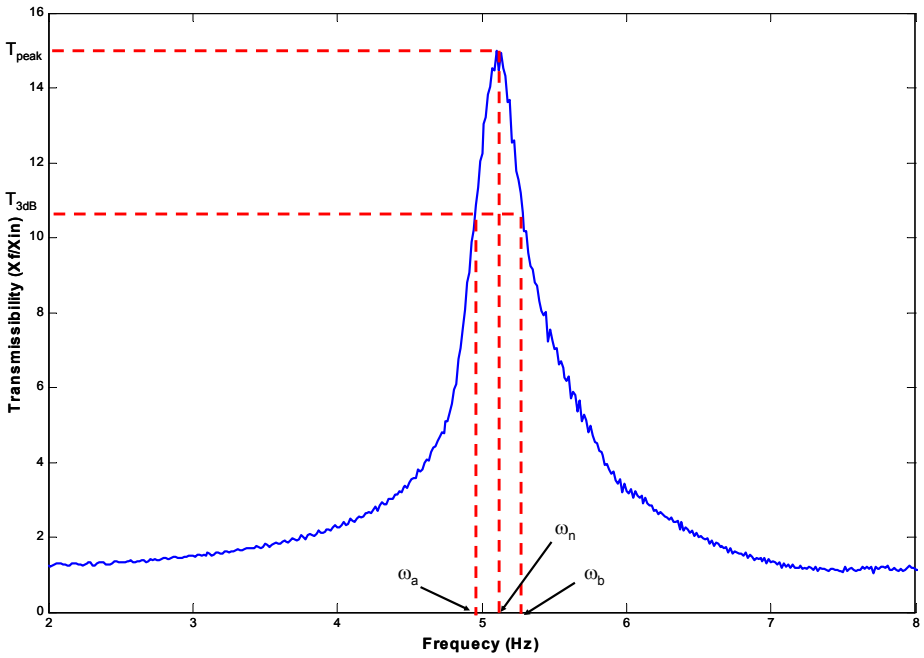

Figure 6-1. System Identification with single-degree-of-freedom (SDOF) Test

Recalling the equation for natural frequency,

$$\omega_{n1} = \sqrt{\frac{k_1}{m_1}}$$

where k_1 is stiffness of the system, and m_1 is the mass of the system.

The mass of the structure is 575 lb (base plates + added mass) and the stiffness can be calculated. Table 6-1 summarizes the system parameters for the primary system.

Table 6-1. Parameters of the primary system

Structure Mass (m_1)	575 lb
Structure Stiffness (k_1)	1,528 lb/in
Structure Damping Ratio (ζ_1)	3 %
Natural Frequency (ω_{n1})	5.1 Hz

6.1.2 Static Test

The stiffness element of the primary system was composed of four air springs. A static test was performed to validate that the experiments were performed in the linear region of air springs. For the static test, up to 300 lb of external mass were added to the nominal mass of the structure, and its deflections were measured. The maximum weight of 300 lb was chosen in the static test because it exceeded the maximum additional mass that would be added to the original structure mass for the mass off-tuning test. Figure 6-2 shows a linear relationship between the added weight and the deflection of air springs. The results validated the use of the linear region of air springs for the scope of the experiments.

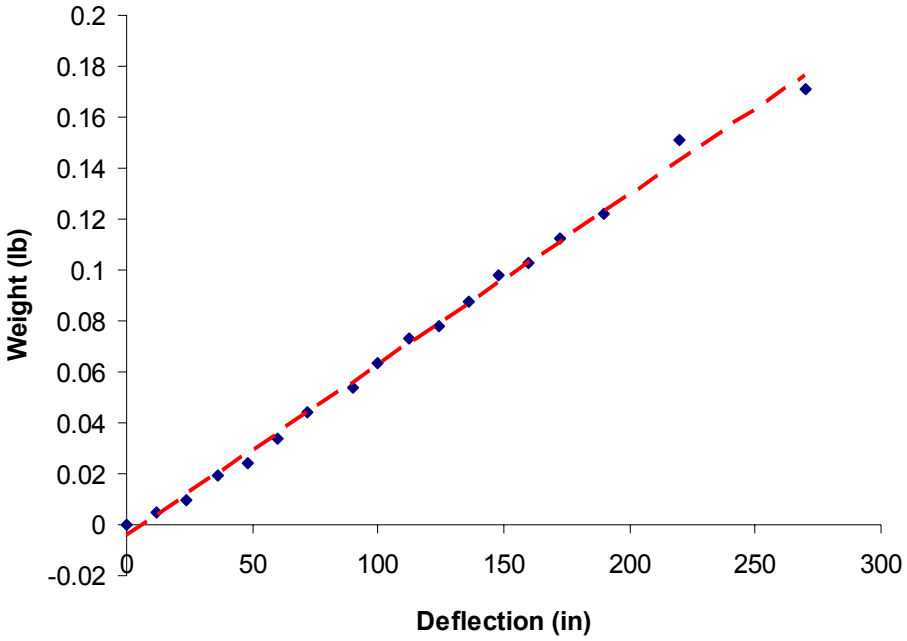

Figure 6-2. Results of Static Test

6.2 Passive Test

This section presents the dynamic behavior of the passive TVA, which will then be compared with those of the semiactive TVA. After first estimating TVA parameters based on the simulation results, the TVA was then fine tuned experimentally. For passive TVA testing, the MR damper was used in a passive mode. In other words, the current to the MR damper was constant throughout the test, making the damper behave like a passive damper.

6.2.1 Design of Passive TVA (Tuning Passive TVA)

Typically, three parameters need to be determined to design a TVA; its mass, stiffness, and damping ratio. This experimental study uses a fixed TVA mass (m_2), which weighs 32 lb (the TVA plate mass + fixture mass). It was used to calculate the mass ratio (μ) of the system:

$$\mu = \frac{m_2}{m_1} = \frac{32}{575} = 0.056$$

This mass ratio is very close to the recommended mass ratio ($0.02 \leq \mu \leq 0.05$) of TMDs for building applications [85].

Based on the simulation results, each coil spring rate was estimated. The passive TVA was tuned by fine tuning the parameters experimentally. Table 6-2 summarizes the tuned parameters.

Table 6-2. Parameters for Passive TVA

TVA Mass (m_2)	32 lb
Mass Ratio (μ)	5.56 %
Each Spring Stiffness (k_{cs})	26 lb/in
Current (i)	0.12 Amps

6.2.2 Dynamic Analysis of Passive TVA

The dynamic analysis was performed using the chirp signal described earlier. The response of the system to the chirp was used to generate the transmissibilities of the structure. Time histories of the structure and the TVA are not directly used to analyze the dynamic performance of the system. As an example of the time traces, however, Figure 6-3 is included. Figure 6-3a shows the displacement of structure mass, and Figure 6-3b shows the displacement of TVA mass. As expected, the amplitude of the TVA is much larger than that of the structure, indicating that the TVA is working effectively.

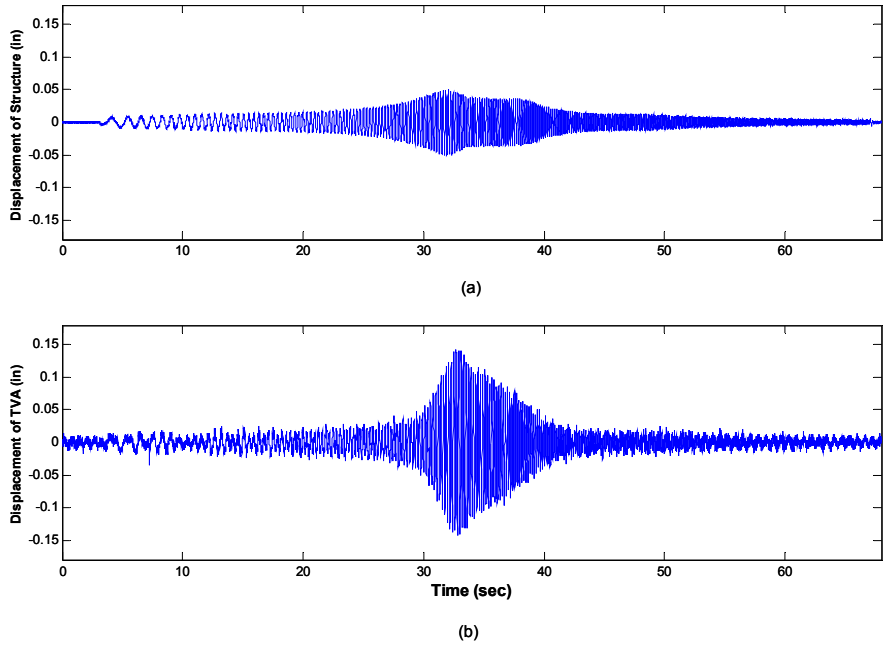

Figure 6-3. Time Responses of Passive TVA (a) Displacement of Structure (x_1); (b) Displacement of the TVA (x_2)

The dynamic analysis is performed through the use of the frequency domain response. Figure 6-4 shows a transmissibility plot and a phase plot of the passive TVA testing. Transmissibility, which is the ratio between output displacement of the structure and the input, was used as a performance index. As the transmissibility increased, the magnitude of vibrations in the primary structure also increased. Thus, the purpose of using a TVA was to reduce transmissibility. Before adding a TVA to the primary system, there was one resonant peak with a maximum transmissibility of fifteen as shown in Figure 6-4a, indicating a single-degree-of-freedom system (SDOF). The SDOF resonant peak indicates that the primary system's natural frequency was 5.1 Hz. Mounting a TVA on the structure reduced the transmissibility as shown in Figure 6-4a. When the current was 0.0 Amps, there were two resonant peaks, indicating that the TVA mass added one more degree of freedom to the system. Increasing the current from 0.0 Amps to 0.1 Amps reduced the two resonant peaks. However, this occurred at the expense of increasing the transmissibility at the valley. As the damping was further increased (by increasing current), the two resonant peaks merged into one peak, and the peak grew.

This indicates that the TVA mass and the primary mass were linked, disabling the TVA and magnifying the vibrations. At a high current (i.e. 0.6 Amps in this experiment), the coupled system acted much like a SDOF system, showing one distinct resonant peak (see Figure 6-4 a). However, the frequency of the new SDOF peak was lower than that of the no-TVA-attached SDOF peak. This was because the effective mass of the coupled system became the sum of the TVA mass and the structure mass and reduced the natural frequency.

Figure 6-4b further shows the dynamics of the passive system with phase angles. A phase angle is the angle between the TVA and the structure. When the current was 0.0 Amps or 0.1 Amp, the phase angle was close to 90 degrees around the resonant frequency of the structure. This indicates that the TVA mass and the structure mass were 90 degrees out of phase, and the TVA counteracted the motions of the structure. Consequently, the transmissibility decreased, implying a reduction of structure vibrations. However, when the current was 0.3 Amps, the phase angle dropped below 90 degrees. With a current of 0.6 Amps, the phase angle became about 10 degrees, implying that the TVA and the structure were highly coupled. Thus, the benefits of using the TVA were negated at this high current.

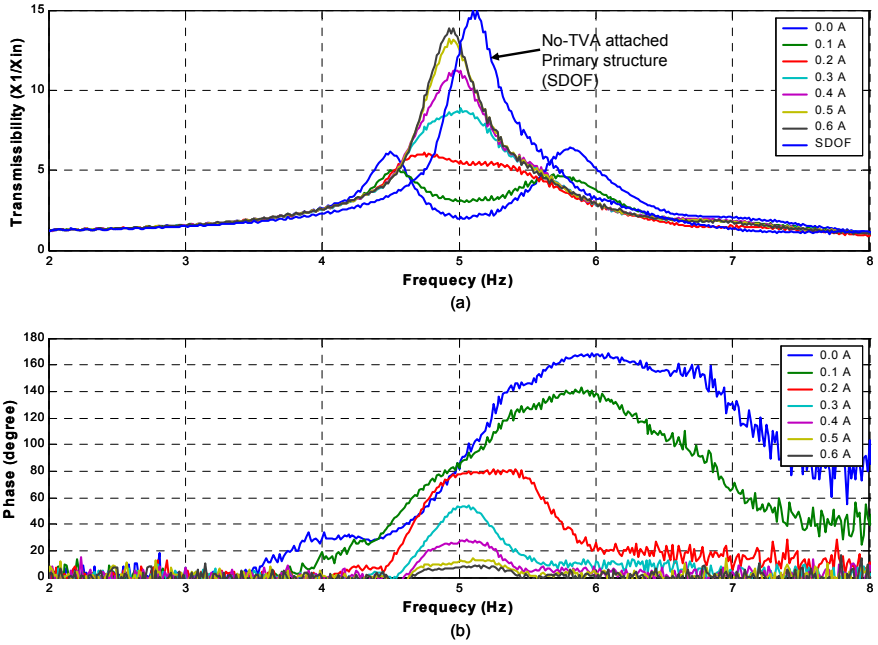

Figure 6-4. Passive Test Results: (a) Transmissibility between the input and the structure displacement and (b) Phase angles between the structure and the TVA

6.3 Semiactive Test

The subsequent sections study the dynamics of semiactive TVAs by performing parametric studies. The primary purpose of the parametric studies is to understand the dynamics of each semiactive TVA. The parametric studies look into the effects of on-state/off-state currents as well as control gains. The sections also offer a damper lock-up dynamics to explain the experimental results and to dissect the implementation. Furthermore, the sections compare the dynamic performances between the passive and semiactive systems to analyze the relative benefits of the semiactive systems. After understanding dynamics of semiactive TVAs in this section, the next section (section 6.4) will perform off-tuning tests to evaluate the robustness of semiactive TVAs.

6.3.1 Design of Semiactive TVAs (Tuning Semiactive TVAs)

Semiactive TVAs were tuned in the same manner as the passive TVA case. Simulation results were used to estimate the initial coil spring rate (k_{cs}), on-state and off-state currents. Table 6-3 summarizes the parameters for each semiactive TVA after fine tuning. The subsequent sections use these tuned semiactive TVAs for parametric studies.

Table 6-3. Parameters for Semiactive TVAs

Parameters	On-off VBG	Continuous VBG	On-off DBG	Continuous DBG
Coil spring rate (in/sec)	25	25	25	25
On-state Current (Amps)	0.2	0.6	0.6	0.6
Off-state Current (Amps)	0	0	0	0
Gain	N/A	0.1	N/A	1000

6.3.2 Effect of On-state Current

This section evaluate the effect of on-state current changes on the on-off VBG controlled semiactive TVA and the on-off DBG controlled semiactive TVA.

6.3.2.1 On-off Velocity-Based Groundhook TVA

For this case, the off-state current was set to 0.0 Amps. The on-state current was then increased discretely from 0.1 Amps to 0.6 Amps with an increment of 0.1 Amps. Assessing the dynamics of the test rig with on-off VBG control begins with an evaluation of the transmissibilities of the structure mass with respect to the input. Figure 6-5 shows the transmissibility and phase plots of the on-off VBG controlled semiactive TVA. As Figure 6-5a demonstrates, the benefits of controlling the structure mass at the valley come at the expense of poor control of the two resonant peaks. With an on-state current above 0.3 Amps, the semiactive TVA experiences coupling of the two masses, which is similar to the passive TVA dynamics shown in Figure 6-4a. However, the rate of transmissibility growth at the valley occurs slowly when compared with that of the passive TVA. This indicates that the coupling of the two masses in the on-off VBG case

is less than in the passive case. The phase plot shown in Figure 6-5b supports this finding. As the on-state current increases, the phase angle decreases from about 90 degrees to 60 degrees, while the phase angle is dropped to close to 10 degrees in the passive case.

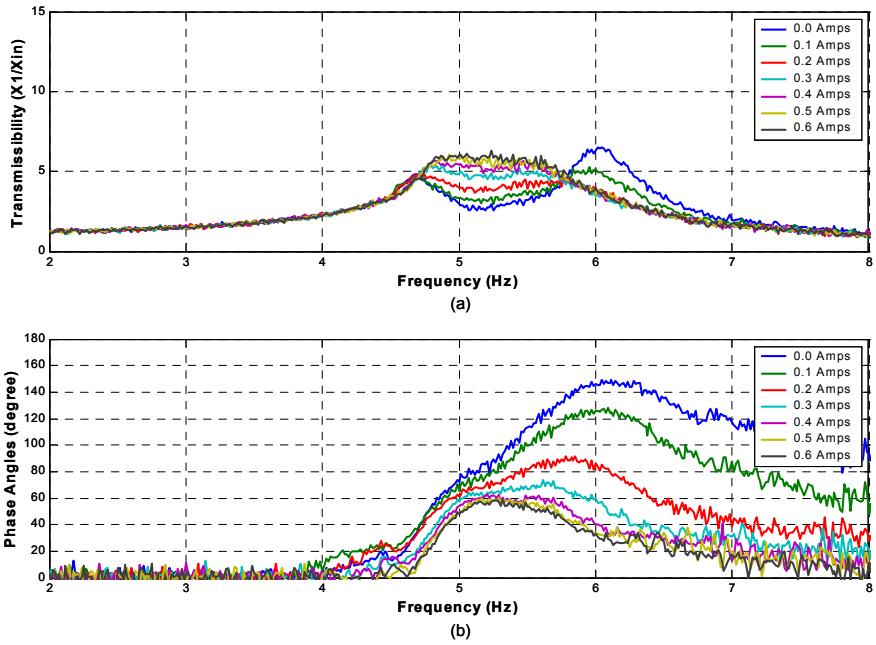

Figure 6-5. Effect of On-State Current of the On-Off VBG TVA: (a) Transmissibility (X1/Xin) and (b) Phase Angles Between the TVA and the Structure

6.3.2.2 On-off Displacement-Based Groundhook TVA

To study the effect of on-state currents, the on-state currents were discretely set 0.0, 0.1, 0.3, and 0.6 Amps, while the off-state current was set to 0.0 Amps. The lowest off-state current (0.0 Amps) ensured the MR damper's lower boundary current limit and offered a wider range of force envelopes. Figure 6-6 shows the results of the on-state currents changes of the on-off DBG TVA. As the on-state current increased, the two resonant peaks decreased. Unlike the passive system, the reduction in the magnitudes of two resonant peaks occurred without the expense of raising the isolation valley. In other words, the isolation valley maintained the minimum transmissibility around the resonance of the structure, keeping the two masses decoupled at high on-state currents. This observation highlights one of the relative merits of the semiactive system.

The phase plot, shown in Figure 6-6b, supports the above discussion. It shows that the phase angle around the resonant frequency of the structure (5.1Hz) was close to 90 degrees, regardless of on-state currents. This indicates that the TVA effectively counteracted the motions of the structure, reducing transmissibility. Again, unlike the passive case, the semiactive system's phase angle with high currents did not drop, enabling the TVA to work effectively.

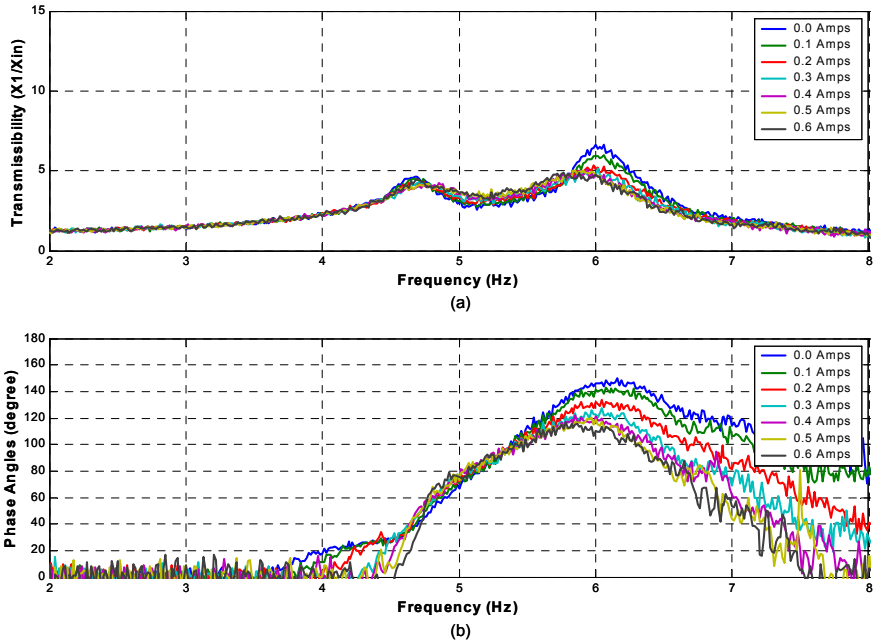

Figure 6-6. Effect of On-State Current of the On-Off DBG TVA: (a) Transmissibility (X1/Xin) and (b) Phase Angles Between the TVA and the Structure

6.3.3 Damper Lock-up Analysis

The previous section showed one of the benefits of semiactive TVAs, namely maintaining isolation with high damping. Before further evaluating the dynamics of the semiactive TVAs, this section intends to explain the experimental results by investigating the damper-switching and lock-up dynamics in the TVAs. This investigation is important because it will help to interpret the dynamics of the passive and the semiactive TVAs. Moreover, this investigation will reveal the impact of the implementation of the various semiactive policies used here.

Lock-up is a condition under which the two masses (i.e., structure mass and TVA mass) become coupled, and their dynamics approach that of a single-degree of freedom system. Theoretically, the amplitudes, phases, and frequencies of the structure mass and the TVA mass should be the same at the point of lock-up. Once lock-up occurs, there is small or no relative motion across the damper. In essence, the MR damper effectively becomes a rigid link between the two masses.

While a passive system has no control on the damper state, the semiactive cases adjust the current, based on the control logic. In other words, the passive system provides a constant current to the MR damper, but a semiactive system continuously changes the current to the damper. Therefore, a closer look at the time histories of current state changes in the MR damper reveals the lock-up dynamics of the semiactive system.

In order to simplify this investigation, three representative cases were considered: the passive system, the on-off VBG system, and the on-off DBG system. All three cases used a current of 0.6 Amps. The passive case immediately exhibited lock-up; the on-off VBG case slowly approached lock-up; and the on-off DBG case did not lock-up. Obviously, the passive case had no control, so it provided a constant current of 0.6 Amps to the MR damper. Because this current exceeds the lock-up current, the damper effectively became a rigid link between the two masses. The linked system then acted like a SDOF system as shown in Figure 6-4. However, the semiactive cases adjusted the current to the damper based on the control logic. Thus, the damper state switching dynamics for each of the semiactive on-off control are evaluated. The damper state

switching dynamics will show the actual implementation of the semiactive control, which led to the damper lock-up analysis.

6.3.3.1 Damper State Switching Dynamics with the On-off VBG Control

As noted in Chapter 3, the on-off VBG control law is:

$$v_1 v_{12} \geq 0 \qquad c_{controllable} = c_{on}$$
$$v_1 v_{12} < 0 \qquad c_{controllable} = c_{off}$$

Figure 6-7 illustrates the execution of the on-off VBG control as the damper follows the control law. The time trace for the velocity of the structure mass (v_1) is plotted along with the relative velocity between the structure and the TVA (v_{12}) and damper current. Note that the amplitudes of the time traces are adjusted to show them on the same axis. This is justified because the signs of the structure velocity and the relative velocity time traces are what determine the damper state. When the product of v_1 and v_{12} is positive, the damper current is set to the maximum damping or on-state current. Otherwise, the damper current is zero, offering minimum damping. Figure 6-7 shows a sample execution of the on-off VBG control. The time traces and the current history are captured around the resonant frequency of the structure. Under on-off VBG logic, the current is continuously switching between the maximum (on-state) and minimum (off-state) levels, as shown in Figure 6-7. In the passive case, the damping level is always set at the maximum level. On-off VBG's current level is at the maximum state for less time than in the passive case. For this reason, on-off VBG approached lock-up at a slower rate than the passive case did.

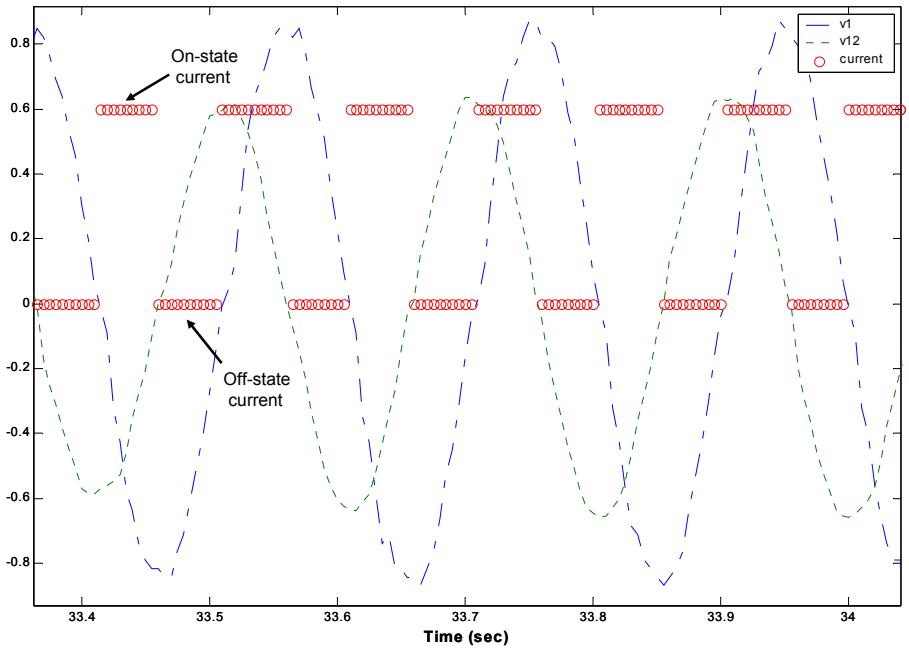

Figure 6-7. Sample Time Traces of On-off VBG Control Policy Execution

6.3.3.2 Damper State Switching Dynamics of On-off DBG control

This section looks into the execution of on-off DBG control. Given that the displacement of structure is multiplied by the relative velocity, and the quantity determines the damper switching for the on-off DBG case, the control law is:

$$x_1 v_{12} \geq 0 \qquad c_{controllable} = c_{on}$$
$$x_1 v_{12} < 0 \qquad c_{controllable} = c_{off}$$

Figure 6-8 shows time histories of the structure displacement and the relative velocity across the damper, along with the damper state changes of the on-off DBG semiactive system. These time traces were also captured around the resonance of the structure, where lock-up occurred for the passive case. The time traces are scaled to conveniently evaluate the control logic; this is valid because the signs of the signals determine the damping state. Unlike passive and on-off VBG cases, under on-off DBG control logic, the current level was at the off-state for most of the time. In other words,

when the system approached lock-up, the on-off DBG control switched the current level to the minimum state. Because the product of the structure displacement (x_1) and the relative velocity (v_{12}) was less than zero (Figure 6-8), the current state of the semiactive case was at off-state (0.0 Amps) for most of the time, preventing damper lock-up. Because the semiactive system can offer low damping around the structure's natural frequency, the lock-up condition can be avoided, enabling the semiactive system to perform better than either the passive system or the on-off VB G case. Figure 6-8 also shows that the current of the passive system was at the set current (0.6 Amps) all the time, providing high damping to the damper and contributing to lock-up.

The damper switching analysis indicates that the on-off DBG's control logic prevented the MR damper from locking-up. The analysis further indicates that the on-off DBG control can offer the benefits of high damping at the resonant peaks, while still maintaining good isolation around the natural frequency of the structure.

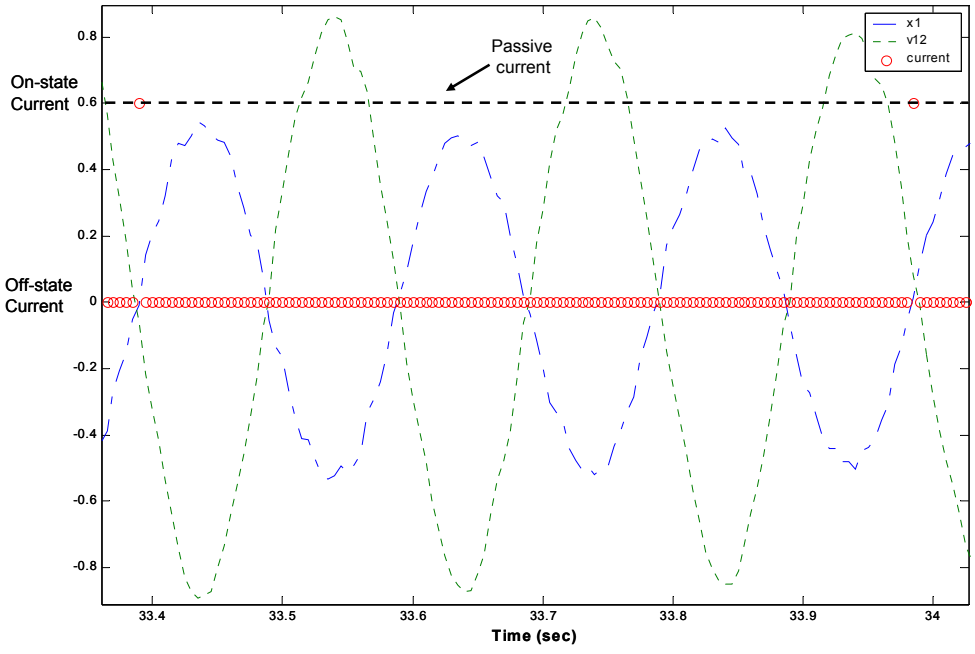

Figure 6-8. Sample Execution of On-off DBG Control

6.3.4 *Effect of Off-state Current*

To further evaluate the dynamics of the semiactive system, this section looked into the effect of changing the off-state currents of the MR damper.

6.3.4.1 On-off Velocity-Based Groundhook TVA

In this case, the on-state current was set to the optimal level, which was 0.2 Amps. The off-state current varied discretely from 0.0 Amps to 0.1 Amps. Figure 6-9a shows that as the off-state current increased, the two resonant peaks came together and the isolation valley grew. This indicates that the dynamics of the on-off VBG system with high off-state currents slowly approached those of the passive system. The phase plot (see Figure 6-9b) shows that the phase angles around the resonance of the structure decreased, as off-state currents increased. The results suggest that the semiactive TVA should keep the off-state current as low as possible to obtain its performance gains.

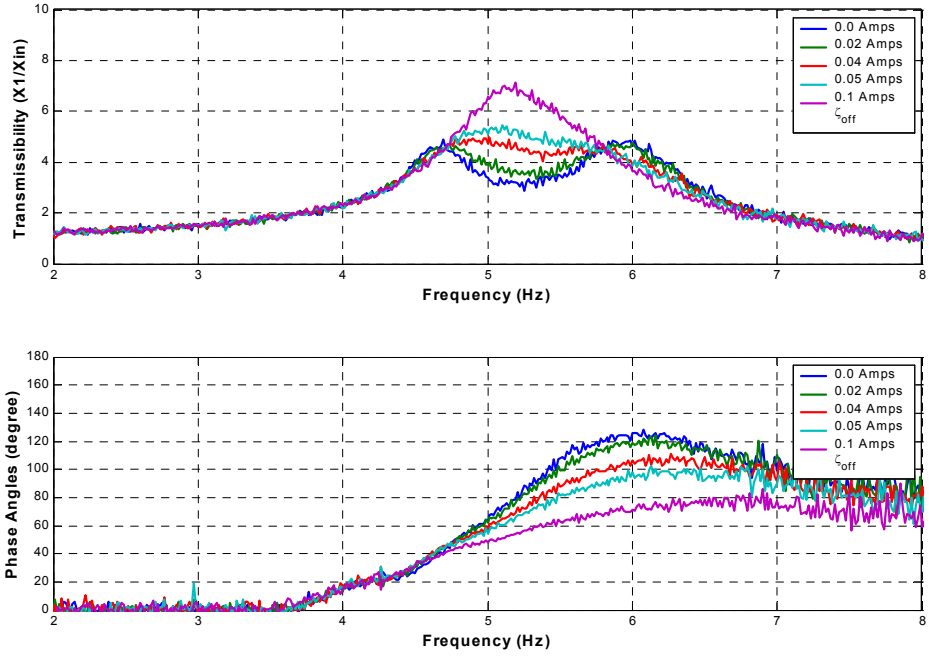

Figure 6-9. Effect of Off-State Current of the On-Off VBG TVA: (a) Transmissibility (X1/Xin) and (b) Phase Angles Between the TVA and the Structure

6.3.4.2 On-off Displacement-Based Groundhook TVA

In this case, the on-state current was set to the maximum operation level, which was 0.6 Amps. This maximum on-state current provided a wider force envelope for the study. The off-state current varied discretely from 0.01 Amps to 0.2 Amps. Figure 6-10a shows that as the off-state damping (current) increased, the amplitudes of the two resonant peaks also increased and the isolation valley grew. This indicates that the dynamics of the semiactive system with high off-state currents slowly approached those of the passive system. The phase plot, shown in Figure 6-10b, confirms the observations. As off-state currents increased, the phase angles around the resonance of the structure decreased, indicating the two masses were becoming coupled. The results suggest that the semiactive TVA should keep the off-state current as low as possible (if not optimal) to obtain its performance gains.

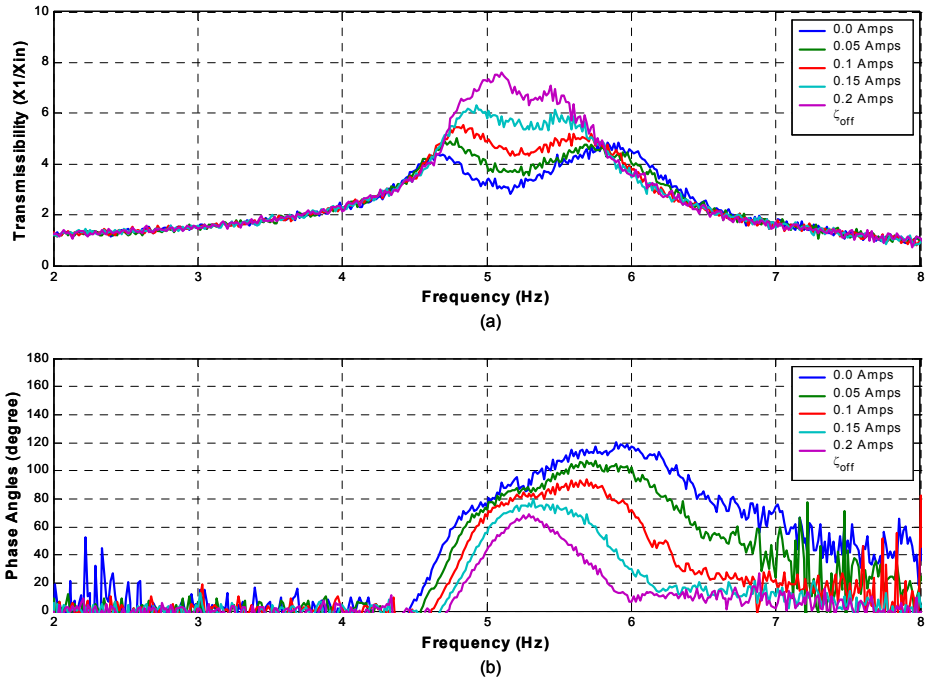

Figure 6-10. Effect of Off-State Current of the On-Off DBG TVA: (a) Transmissibility (X1/Xin) and (b) Phase Angles Between the TVA and the Structure

6.3.5 Effect of Gains

This section presents the effects of control gains for the continuous semiactive TVAs. For this parametric study, the on-state and off-state currents were fixed, such that they limited the upper and lower boundaries of the damping (current) range, respectively. The control gain then changed discretely.

6.3.5.1 Continuous Velocity-Based Groundhook TVA

To study the dynamics of the continuous, velocity-based, groundhook-controlled, semiactive TVA, the on-state current was set at the maximum operation current (i.e., 0.6 Amps) and the off-state current was set at 0.0 Amps. The on-state and the off-state currents are the maximum and the minimum damping boundaries, respectively. To change the dynamics of the continuous VBG case, the gain was adjusted. The gain, the constant parameter 'G' in equation 3.17, varied discretely from 0 to 1000. This gain determined the distribution of damping (current) levels between the two boundaries. A lower gain indicates that damping levels are more closely distributed in the lower boundary (or off-state); conversely, a higher gain indicates that the damping levels are more distributed in the upper boundary. As the gain increased, the continuous groundhook control followed the on-off damping control. This is because the large gain pushed the damping distribution up to the maximum (or on-state) damping limit. Figure 6-11 shows the results of continuous VBG control. When the gain increased, the two peaks came together and the peak grew, exhibiting similar dynamics to those of passive and on-off VBG control. The phase plots followed the similar trends of passive and on-off VBG cases, approaching zero phase angles as the gain increased. It is note worthy that the phase angles significantly decrease as the gain increases larger than one, indicating that the continuous VBG control is very sensitive to gain control and that the two masses are coupled.

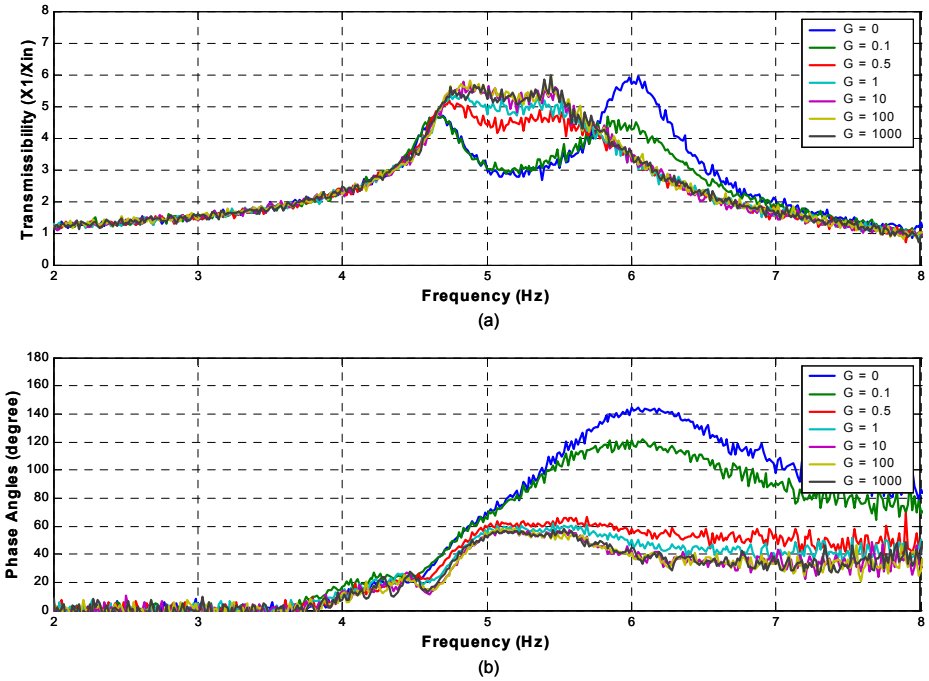

Figure 6-11. Effect of gains of the Continuous VBG TVA: (a) Transmissibility (X1/Xin) and (b) Phase Angles Between the TVA and the Structure

6.3.5.2 Continuous Displacement-Based Groundhook TVA

The continuous DBG control case was studied the same manner as the continuous VBG case. Again, the on-state current of 0.6 Amps limited the upper boundary, and the off-state current of 0 Amps limited the lower boundary. Also, the gain discretely varied from 0 to 1000. Figure 6-12 shows the results of the continuous DBG controlled semiactive TVA. As the gain increases, the two peaks come down, but the valley rises slightly. For the most part, the dynamics of continuous DBG are the same as on-off DBG. Both displacement-based semiactive controls outperform the passive and velocity based controls in reducing the resonant vibrations of the primary structure.

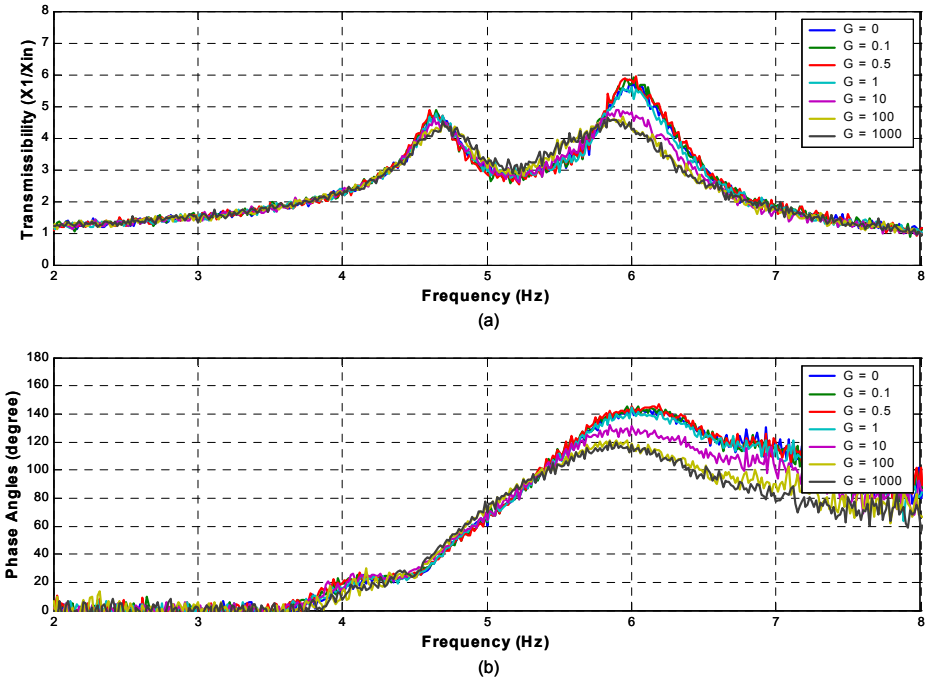

Figure 6-12. Effect of gain of the Continuous DBG TVA: (a) Transmissibility (X1/Xin) and (b) Phase Angles Between the TVA and the Structure

6.4 Off-tuning Test

This section offers the results and analyses of the experimental off-tuning test, which looked into the structure's mass changes (mass off-tuning). It begins with a brief overview of the mass off-tuning test, explaining the procedures of the test. It then presents the results of both passive and semiactive TVAs. After evaluating the relative benefits of semiactive TVAs as compared with an equivalent passive system, this section provides a guideline for the practical use of semiactive TVAs in floor vibration applications.

6.4.1 Overview of the Test

Often for a building, mistuning of a TVA occurs due to changes in the primary mass (floor system). Adding or removing external mass to an existing floor, such as people and furniture, will change the floor mass. This change is responsible for TVA off-tuning or mistuning. Thus, a TVA that is being considered for floor vibration applications must be able to robustly adapt to changes in the floor mass. Although a passive TVA can be optimally designed, it only offers benefits at a narrow band of frequency (around the tuned frequency). Therefore, the major problem with using a passive TVA on a floor system is mistuning, which sharply reduces the performance of a TVA. This section evaluates the effect of changing the floor mass (mass off-tuning) in passive and semiactive TVA systems. In order to justify the benefits of practical use of a semiactive TVA, the off-tuning experiments must show that the semiactive TVA robustly adapts to changes in system parameters.

In order to study the effect of changing in the structure mass, twenty additional steel plates were used to vary the structure mass of the test setup. Each of the plates weighed ten pounds. The sum of the nominal structure mass and ten plates served as a baseline mass. This enabled the subtraction and addition of 100 pounds, which make it possible to vary –23 % to +23 % of the baseline mass. Figure 6-13 shows the test rig with the additional steel plates, which changed the structure mass.

Figure 6-13. Structure mass with additional masses

6.4.2 Passive Case

This section presents the off-tuning analysis for the passive case. Figure 6-14 shows the transmissibility and the phase changes as the primary mass decreases. Up to 100 pounds were reduced from the baseline mass by gradually removing two steel plates, which weighed twenty pounds. When the structure mass decreased, the second resonant peak increased, indicating the shift in natural frequency because of the structure mass reduction.

Figure 6-15 shows that transmissibility and the phase changes as the primary mass increases. In this case, two steel plates were added to the baseline mass, up to 100 pounds. As the structure mass increased, the natural frequency of the structure decreased, increasing the frequency ratio. Thus, the adding external mass to the baseline mass raised the first resonant peak.

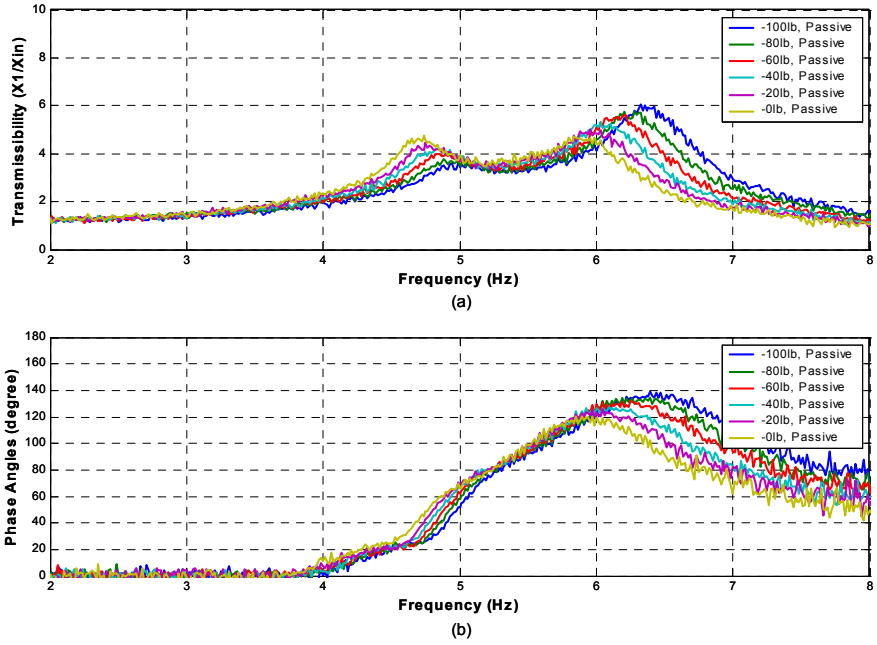

Figure 6-14. Passive (Subtracting Mass)

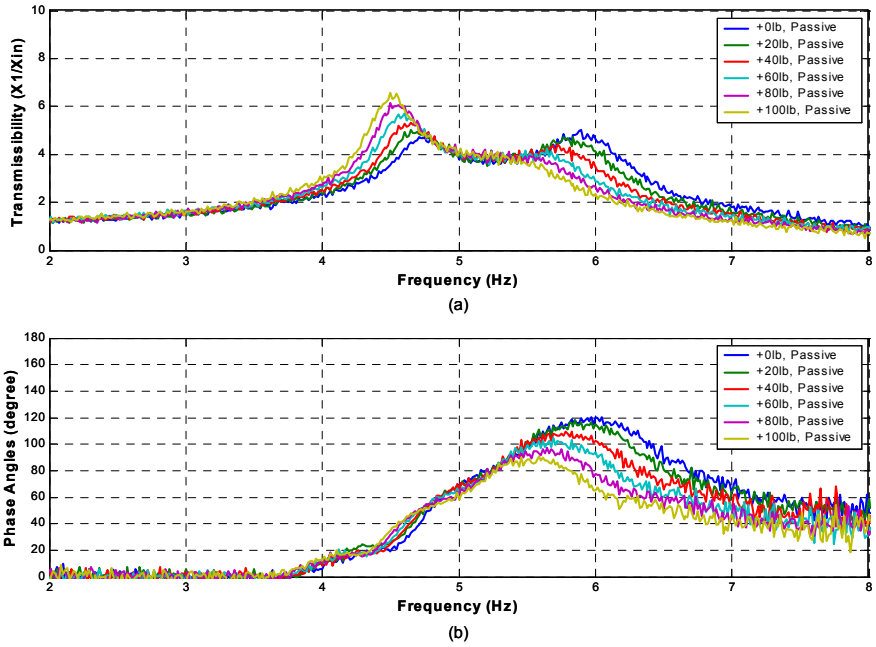

Figure 6-15. Passive (Adding Mass)

6.4.3 Semiactive Case

This section analyzes the mass off-tuning for the semiactive case with on-off DBG control, which is identified as the "best" control among the four policies. This analysis used the same process as the passive case. Two steel plates were added and removed from the baseline structure mass at a time; ultimately, 100 pounds of mass was adjusted.

Figure 6-16 shows the transmissibility and the phase changes resulting from the primary mass decrease. When the structure mass decreased, the second resonant peak increased, indicating the shift in natural frequency because of the structure mass reduction. This trend was similar to that of the passive case. However, the rate increase of the second peak was slower in the on-off DBG case, suggesting that the on-off DBG system more robustly adapted to the primary system's mass change.

Figure 6-17 shows that transmissibility and the phase changes resulting from the primary mass increase. As the structure mass increased, the natural frequency of the structure decreased, increasing the frequency ratio. Thus, the adding external mass to the baseline mass raised the first resonant peak. In this case, the peak increase was still less than that of the passive TVA. The next section will compare the changes of the maximum transmissibility of the passive and the on-off DBG TVAs with regard to the structure mass change, and will graphically evaluate the relative benefits of the semiactive case.

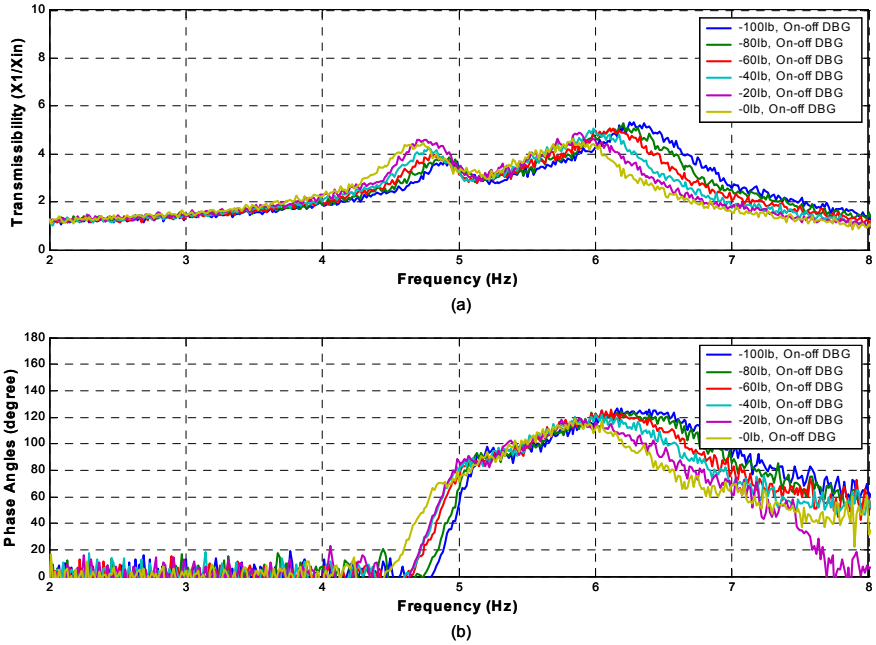

Figure 6-16. On-off DBG (Subtracting Mass)

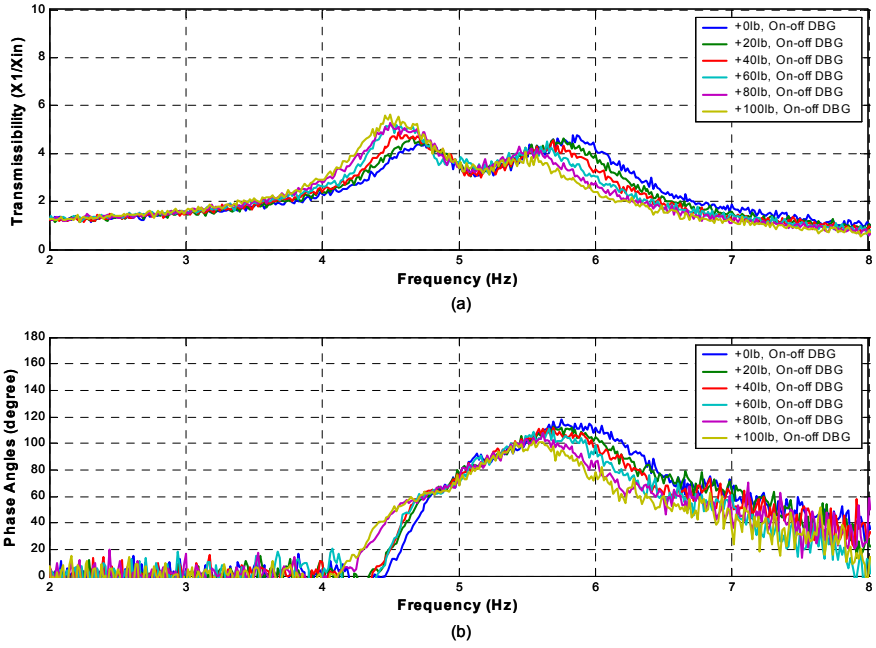

Figure 6-17. On-Off DBG (Adding Mass)

6.4.4 Comparisons

This section presents the experimental results again to directly compare the performance of the passive and semiactive TVAs. This comparison will allow us to analyze the relative benefits of the semiactive system.

Figure 6-18 shows transmissibility changes of passive and semiactive TVAs as the structure mass decreased. The second resonant peak of the passive TVA increased as the structure mass decreased as shown in Figure 6-18a. Similarly, the semiactive TVA's second resonant peak increased (see Figure 6-18b). However, the rate increase of the second peak was slower in the semiactive case, suggesting that the semiactive system was more robust to the primary system's mass change.

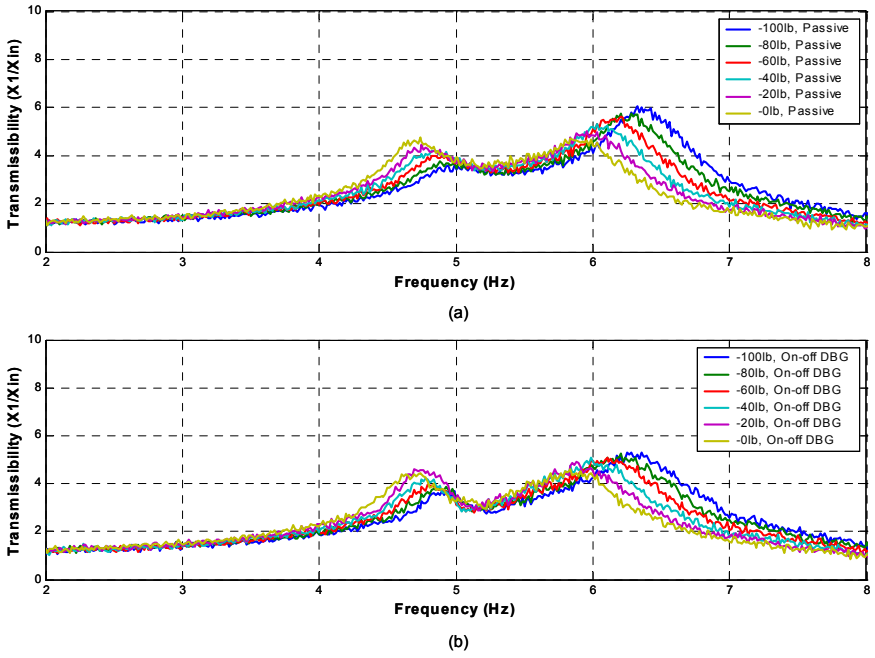

Figure 6-18. Removing Mass from the Structure: (a) Passive TVA and (b) Semiactive TVA

Figure 6-19 compares transmissibility changes of passive and semiactive TVAs as the structure mass increased. As external mass added to the baseline structure mass, the first resonant peak increased for both the passive and the semiactive cases. The rate increase of the first peak, however, was higher in the passive case than that of the

semiactive case. This indicates that the semiactive TVA was more robust to the mass off-tuning than the passive TVA. Moreover, the maximum transmissibility of the semiactive TVA was lower than that of the passive TVA, indicating that the semiactive outperforms the passive in reducing the maximum vibrations of the structure.

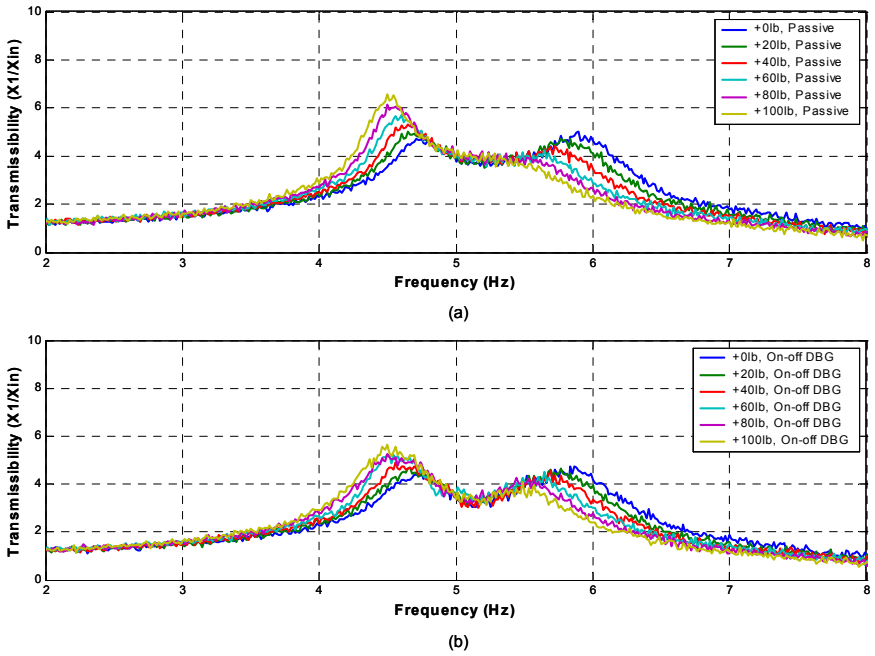

Figure 6-19. Adding Mass to the Structure: (a) Passive TVA and (b) Semiactive TVA

6.4.5 Design Guide for Floor Vibration Applications

This section summarizes the mass off-tuning analysis and suggests a practical guide for the use of TVAs in floor structures. Figure 6-20 shows that the peak transmissibility changes of the passive and semiactive systems as the structure mass varied from –100 lb to + 100 lb of its baseline mass. The slope of the semiactive TVA is less than that of passive, indicating that the semiactive system was more robust to changes in the structure mass. The results show that the slope is greater for increases than for decreases in the structure mass. This means that TVAs are more robust to decreases in the structure mass or decreases in the frequency ratio.

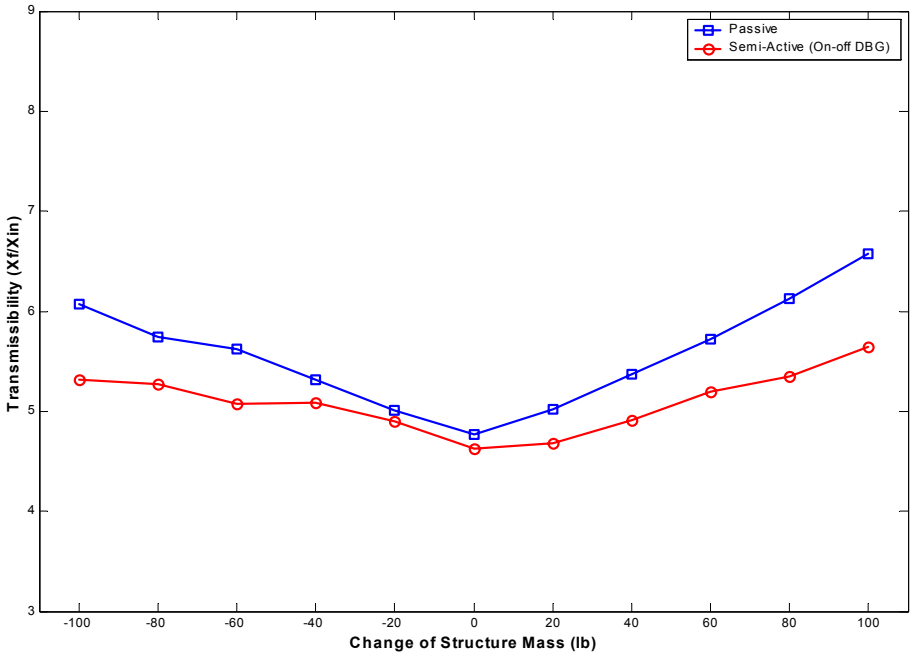

Figure 6-20. Peak Transmissibility Variations as the Structure Mass Changes

Based on the mass off-tuning tests, it is recommended to install slightly off-tuned TVAs (below the optimum TVAs) in practice. In the case of a floor structure, its effective mass tends to increase with the presence of occupants, who feel annoying floor vibrations. If TVAs are optimally tuned at first, the vibration levels always increase above those of optimal TVAs with the presence of people. On the other hand, if TVAs are off-tuned slightly lower than the optimum TVAs, the vibration levels can reach those of the optimum TVAs with the presence of the occupants, attaining the maximum benefits of TVAs. Of course, one must estimate the effective mass changes of floor systems, which varies by applications, to determine how much to off-tune the TVAs.

6.5 Remarks on Simulation and Experimental Results

The purpose of this section is to provide a brief comparison between numerical simulation and experimental results. However, it is not the intent of this section to provide an all inclusive comparison between the numerical simulation and experimental results. The scope of this research is not to develop a model that exactly describes the experimental system. Rather, in this research, the simulation is primarily used to understand the dynamic behaviors of MR TVAs and identify semiactive control techniques that are well suited for the experiments. The numerical simulations were conducted with a linear damper model. They were mainly intended to aide us in selecting the most promising semiactive control techniques for the MR TVA, in order for us to perform our experiments more efficiently. The experimental results that were described earlier are intended to provide the main assessment of the effectiveness of MR TVAs for structural vibration applications, such as floor vibrations. Nonetheless, we feel compelled to provide a brief comparison between the numerical and experimental results, as is traditionally done.

To this end, we will provide a comparison between the structure that is used in our experimental set up and the model that is used in simulation. As is shown in Figure 6-21, the simulated structure closely matches the experimental structure. The slight difference in the structure's resonant peak can be attributed to the difference between the structure damping that was modeled and the damping that existed in our experiments.

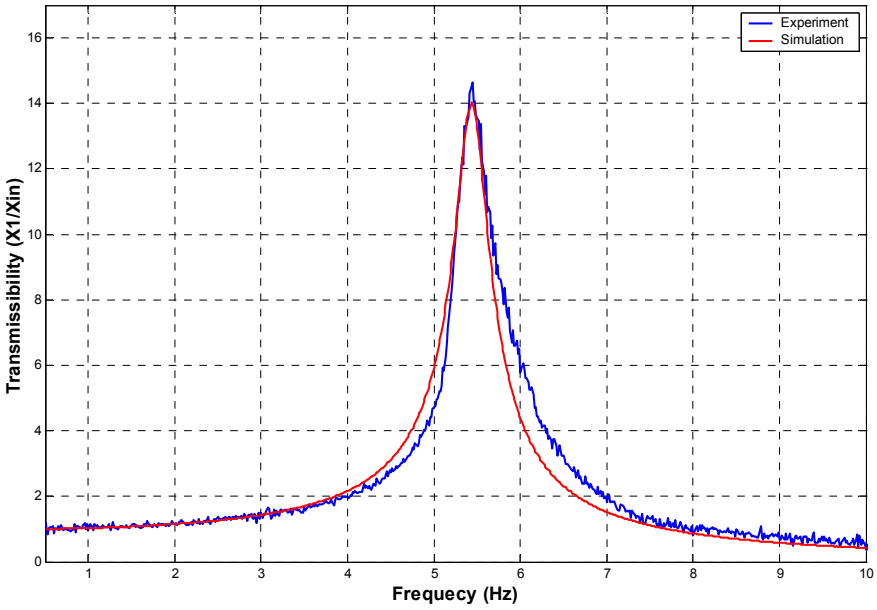

Figure 6-21. Transmissibility Comparison between Simulation and Experiment for SDOF Structure

Figure 6-22 shows a comparison between the optimally tuned structure, as obtained experimentally, and a simulation case. Both results are obtained using the on-off DBG semiactive control method. Here, only case is considered as an example. The amplitudes of the resonant peaks in the simulation match the experiments. However, there is a slight shift in frequency which can be attributed to the difference in the stiffness used in the simulation and the stiffness of the TVA springs.

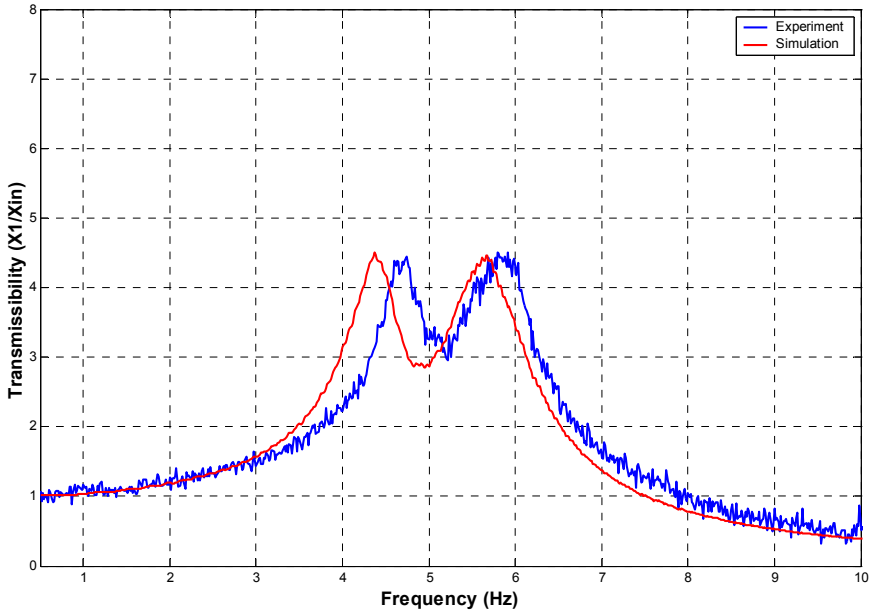

Figure 6-22. Transmissibility Comparison between Simulation and Experiment for Tuned MR TVA

Both Figure 6-21 and Figure 6-22 show that the numerical model with the linear damper could be "tuned" to closely match the experimental results, which includes a non-linear MR damper. The MR damper force-velocity characteristics are described in Figure 5-9. Again, the reader is cautious not to interpret Figure 6-21 and Figure 6-22 to conclude that our intention was to have a numerical model that will exactly duplicate the experimental results.

Chapter 7 Conclusions

This chapter summarizes the work has done in this dissertation, highlighting important findings. It also suggests recommendations for future research to extend this work.

7.1 Summary

This research proposed a novel semiactive tuned vibration absorber for controlling vibrations in structures. Typically, semiactive systems have provided excellent solutions in many engineering problems because they comprise the pros and cons of passive and active systems. Thus, this study used a versatile Magneto-Rheological (MR) damper in a conventional TVA to realize a semiactive TVA system. This study evaluated this new semiactive TVA system, assessing its dynamic performance both numerically and experimentally.

The first phase of this study was the numerical simulation in which optimal tuning of the TVAs and parametric studies were performed. To control damping in the proposed, semiactive TVA, two basic groundhook control strategies (velocity-based on-off/continuous control) were investigated and two modified strategies (displacement-based on-off/continuous control) were proposed. After each TVA model was optimized using numerical optimization techniques, the performance of the four control strategies were compared along with the passive TVA. The optimization results performed on a 2-DOF model indicated that the displacement-based groundhook control policies outperformed passive and velocity-based groundhook schemes in reducing vibration levels of the main structure. The off-tuning study showed that the semiactive TVA was more robust than the passive case to changes in parameters of the structure. Particularly, displacement-based, on-off control (On-off DBG) showed the best robustness to mass off-tuning, which commonly occurs in building floors and sharply degrades the performance of TVAs. Based on these results, on-off DBG was identified as the best control method among the four control strategies.

The second phase of this study consisted of a series of experimental investigations on a 2-DOF test model representing the primary system coupled with an MR TVA. Using this test setup, a number of tests were conducted to evaluate the effectiveness of various semiactive control policies, to compare the performance of semiactive systems with the passive system, and to analyze the relative benefits of semiactive TVAs over the passive TVA. Overall, the experimental results agreed with the simulation results, confirming the effectiveness of semiactive TVAs. The best performance was attained with the displacement-based, on-off groundhook control. This policy exhibited the lowest transmissibility, indicating that it reduced the vibrations of the system the most. It also showed that on-off DBG was robust to changes in the structure mass. These results corresponded to the simulation results which identified the on-off DBG as the best control policy. Based on the mass off-tuning analysis, a practical guideline for installing the TVA in floor systems can be adopted; because the floor mass tends to increase with the presence of occupants, TVAs should be tuned slightly less than their optimum.

In conclusion, the study showed that the performance of the proposed semiactive MR TVA outperformed the equivalent passive TVA in reducing the maximum vibration levels. It further showed that the semiactive system is more effective when subjected to changes in system parameters.

7.2 Recommendations for Future Research

While completing the objectives of this research initially, several subjects have been identified for future research. This section presents these ideas.

7.2.1 Development of New Type of MR Devices

Based on the results of this study, semiactive MR TVAs had better performance gains with low off-state damping and high on-state damping. Thus, developing MR dampers that can offer these characteristics are desirable to maximize performance of the MR TVAs. Modification of double-ended type MR dampers rather than mono-tube MR dampers would be a good start. The accumulators in the mono-tube MR dampers are filled with gas and act like spring (stiffness) in the systems; hence, they add complexity when tuning TVAs. Thus, further studies might try to develop a double-ended damper for MR TVAs so that the complexity of the accumulator can be eliminated. One might also consider developing new types of semiactive dampers that have a large dynamic force range. Moreover, other modes of MR dampers (such as squeeze mode) may be considered for semiactive MR TVAs.

7.2.2 Laboratory Floor Test

Although the 2-DOF test rig was quite effective for establishing the fundamental aspects of this study due to its simplicity, it represents a test condition that can differ from practice. In order to bridge this gap and yet maintain the test repeatability that can be enjoyed in a laboratory environment, it is recommended to perform a series of tests with a full scale laboratory floor system.

7.2.3 Other Recommendations

Other recommendations are summarized as follows:

- Developing alternative damping control algorithms that are not considered here.

- Incorporating analytical MR damper models, such as Bouc-Wen model, that can more closely relate analytical parameters with experimental parameters. It will also help the development of new control policies.
- Extending the 2-DOF model to multiple-degree-of-freedom models and/or continuous systems. This will examine one or multiple MR TVAs in beam and plate models (which represent bridges and building structures) for global vibration control of such systems.
- Exploring other applications of MR TVAs is a possibility. MR TVAs can be used (but not limited) in earthquake engineering to protect bridges and building structures from seismic hazards and wind engineering to mitigate wind-induced vibrations on high-rise buildings to enhance occupants comfort.

References

1. Alvis, S. R., (2001), "An Experimental and Analytical Investigation of Floor Vibrations," M.S. Thesis, Virginia Polytechnic Institute and State University, Blacksburg, Virginia.
2. Murray, T. M., (1991), "Building Floor Vibrations," *Engineering Journal,* American Institute of Steel Construction, 28 (3), pp.102-109.
3. Griffin, M. J., (1990), *Handbook of Human Vibration*, Academic Press, San Diego, CA, USA.
4. *Popular Mechanics*, January, 2002. p. 24.
5. Eriksson, P-E, (1994), "Vibration of Low-Frequency Floors-Dynamic Forces and Response Prediction," Ph.D. Dissertation, Chalmers University of Technology, Goteborg, Sweden.
6. Murray, T. M., Allen, D. E., and Ungar, E.E., (1997), "Floor Vibrations Due to Human Activity," *AISC Steel Design Guide Series 11*, American Institute of Steel Construction, Chicago.
7. Webster, A. and Vaicaitis, R., (1992), "Application of Tuned Mass Dampers to Control Vibrations of Composite Floor Systems," *Engineering Journal,* American Institute of Steel Construction, 29 (3), pp.116-124.
8. Hanagan, L.M., and Murray, T. M., (1997), "Active Control Approach For Reducing Floor Vibrations," *Journal of Structural Engineering*, ASCE, Vol. 123, No. 11, pp. 1497-1505.
9. Hanagan, L. M., (1994), "Active Control of Floor Vibrations," Ph.D. Dissertation, Virginia Polytechnic Institute and State University, Blacksburg, Virginia.
10. Hanagan, L.M., and Murray, T. M., (1995), "Active Control of Floor Vibration: Implementation Case Studies," *American Control Conference*, June 22-23, Seattle, Washington.
11. Den Hartog, J. P., (1956), *Mechanical Vibrations*, McGraw-Hill Book Company, Inc: New York.
12. Warburton, G. B., (1982), "Optimum Absorber Parameters for Various Combinations of Response and Excitation Parameters," *Earthquake Engineering and Structural Dynamics*, 10, pp. 381-401.
13. Tsai, H. C. and Lin, G, C., (1993), "Optimum tuned-mass dampers for minimizing steady-state response of support-excited and damped systems," *Earthquake Engineering and Structural Dynamics*, 22, pp. 957-973.
14. Sun, J. Q., Jolly, M. R., and Norris, M. A., (1995), "Passive, Adaptive and Active Tuned Vibration Absorbers – A survey," *Transactions of the ASME, 50th Anniversary of the Design Engineering Division*, Vol. 117, pp.234-242.
15. Housner, G. W., Bergman, L. A., Caughey, T. K., Chassiakos, A. G., Claus, R. O., Masri, S. F., Skelton, S.E., Soong, T. T., Spencer, B.F., and Yao, J. T. P., (1997),

"Structural Control: Past, Present, and Future," *Journal of Engineering Mechanics*, 123(9), pp. 897-971.

16. Symans, M. D. and Constantinou, M. C., (1999), "Semiactive control systems for seismic protection of structures: a state-of-art review," *Journal of Engineering Structures*, 21, pp. 469-487.
17. Soong, T. T. and Spencer, B.F. Jr., (2002), "Supplemental energy dissipation: state-of-the-art and state-of-the-practice," *Journal of Engineering Structures*, 24, pp. 243-259.
18. Pan, T.-C., Mita, LA., and Li, J., (2001), "Vehicle-Induced Floor Vibration in a Multistory Factory Building," *Journal of Performance of Constructed Facilities*, Vol. 15, No. 2, pp. 54-61.
19. Patten, W. N., Sack, R. L., and He, Q., (1996), "Controlled Semiactive Hydraulic Vibration Absorber for Bridges," *Journal of Structural Engineering*, Vol. 122, No. 2, pp. 187-192.
20. Hrovat, D., Barak, P., and Rabins, M., (1983), "Semi- Active versus Passive or Active Tuned Mass Dampers for Structural Control," *Journal of Engineering Mechanics*, Vol. 109, pp. 691-705.
21. Soong, T. T. and Reinhorn, A. M., (1993), "Observed Response of Actively Controlled Structures," *Proceedings of Structural Engineering in Natural Hazards Mitigation*, pp. 187-192.
22. Gordaninejad, F. and Kelso, S. P., (2000), "Magneto-Rheological Fluid Shock Absorbers for HMMWV," *Proceedings of SPIE*, Vol. 3989, pp. 266-273.
23. Ahmadian, M. and Marjoram, R. H., (1989), "Effects of Passive and Semiactive Suspensions on Body and Wheelhop Control," *Journal of Commercial Vehicles*, Vol. 98, pp. 496-604.
24. Dyke S. J. and Spencer, B. F. Jr., (1996), "Seismic Response Control Using Multiple MR dampers," *Proceedings of the 2nd International Workshop on Structural Control*, Hong Kong, December, pp. 163-173.
25. Lenzen, K. H., (1966), "Vibration of Steel Joist Concrete Slab Floors" *Engineering Journal*, American Institute of Steel Construction 2(3), pp. 133-136.
26. Allen, D. L. and Swallow, J. C., (1975), "Annoying Floor Vibrations-Diagnosis and Therapy," *Sound and Vibration*, March, pp. 12-17.
27. Allen, D. E. and Pernica, G., (1984), "A Simple Absorber for Walking Vibrations," *Canadian Journal of Civil Engineering*, Vol. 11, pp. 112-117.
28. Thornton, C. H., Cuoco, D. A., and Velivasakis, E. E., (1990), "Taming Structural Vibrations," *Civil Engineering*, November, pp. 57-59.
29. Setareh, M., and Hanson, R.D., (1992a), "Tuned Mass Dampers for Balcony Vibration Control," *Journal of Structural Engineering*, ASCE, Vol. 118, No.3, pp. 723-740.

30. Setareh, M., and Hanson, R.D., (1992b), "Tuned Mass Dampers to Control Floor Vibration form Humans," *Journal of Structural Engineering*, ASCE, Vol. 118, No.3, pp. 741-762.

31. Setareh, M., Hanson, R.D., and Peek, R., (1992), "Using Component Mode Synthesis and Static Shapes for Tuning TMDs," *Journal of Structural Engineering*, ASCE, Vol. 118, No.3, pp. 763-782.

32. Webster, A. C. and Vaicaitis, R., (1992), "Application of Tuned Mass Dampers to Control Vibrations of Composite Floor Systems," *Engineering Journal*, American Institute of Steel Construction, 3rd Quarter, pp. 116-124.

33. Bell, D. H., (1994), "A Tuned Mass Damper to Control Occupant Induced Floor Motion," *Proceedings of the 18th Annual Meeting of the Vibration Institute*, Willowbrook, Illinois, pp. 181-185.

34. Shope, R. L. and Murray, T. M., (1994), "Using Tuned Mass Dampers to Eliminate Annoying Floor Vibrations," *Proceedings of Structures Congress XIII*, ASCE, Vol. I, No.3, pp. 339-348.

35. Rottmann, C. E., (1996), "Use of Tuned Mass Dampers to Control Annoying Floor Vibrations," M.S. Thesis, Virginia Polytechnic Institute and State University, Blacksburg, Virginia.

36. Matsumoto, Y., Nishioka, T., Shiojiri, H., and Matsuzaki, K., (1978), "Dynamic Design of Footbridges," *International Association for Bridge and Structural Engineering*, 3, August, pp. 1-15.

37. Bachmann, H. and Weber, B., (1995), "Tuned Vibration Absorbers for 'Lively' Structures," *Structural Engineering International*, January, pp. 31-36.

38. Wirsching, P. H. and Campbell, G. C., (1974), "Minimal Structure Response Under Random Excitation Using the Vibration Absorber," *Earthquake Engineering and Structural Dynamics*, Vol. 2, pp. 303-312.

39. Kitamura, H., Fujita, T., Teramoto, T., and Kihara, H., (1988), "Design and analysis of a tower structure with tuned mass damper," *Proceedings 9th World Conference of Earthquake Engineering, Tokyo-Kyoto, Japan*, VIII, pp. 415-420.

40. Clark, A. J., (1988), "Multiple passive tuned mass dampers for reducing earthquake induced building motion," *Proceedings of 9th World Conference on Earthquake Engineering*, August 2-9, Tyoko-Kyoto, Japan, V, 779-784.

41. Soto-Brito, R. and Ruiz, S. E., (1999), "Influence of Ground Motion Intensity on the Effectiveness of Tuned Mass Dampers," *Earthquake Engineering and Structural Dynamics*, Vol. 28, pp. 1255-1271.

42. Gupta, Y. P., and Chandrasekaren, (1969), "Absorber system for earthquake excitation," *Proceedings 4th World Conference of Earthquake Engineering, Santiago, Chile*, II, pp.139-148.

43. Kaynia, A. M., Venerziano, D., and Biggs, J. M., (1981), "Seismic Effectiveness of Tuned Mass Dampers," *Journal of Structural Division*, ASCE, Vol. 107, No. 8, pp. 1465-1484.

44. Sladek, J. R. and Klinger, R. E., (1983), "Effect of Tune-Mass Dampers of Seismic Response," *Journal of Structural Division*, ASCE, Vol. 107, pp. 2004-2009.

45. Chowdhury, A. H., Iwuchukwu, M. D. and Garske, J. J., (1987), "The past and future of seismic effectiveness of tuned mass dampers," *Proceedings of 2nd International Symposium Structural Control (Leipholz, H.H.E. ed)*, Martinus Nijhoff Publishers, pp.105-127.

46. Villaverde, R., (1985), "Reduction in seismic response with heavily-damped vibration absorbers," *Earthquake Engineering and Structural Dynamics*, 13, pp. 33-42.

47. Villaverde, R. and Koyama, L. A., (1993), "Damped resonant appendages to increase inherent damping in buildings," *Earthquake Engineering and Structural Dynamics*, 22, pp. 491-507.

48. Villaverde, R., (1994), "Seismic control of structures with damped resonant appendage," *Proceedings 9th World Conference of Structural Control, Los Angeles, California, USA*, WP-4, pp. 113-119.

49. Sadek, F., Mohraz, J., Taylor, A. W., and Chung, R. M., (1997), "A Method of Estimating the Parameters of Tuned Mass Dampers for Seismic Application," *Earthquake Engineering and Structural Dynamics*, 26, pp. 617-635.

50. Gnec, S., (2002), "Synthesis and Properties of Magnetorheological (MR) fluids," Ph. D. Dissertation, University of Pittsburgh.

51. Jolly, M. R., Bendar, J. W., and Carlson, J. D., (1998), "Properties and Applications of Commercial Magnetorheological Fluids," *SPIE 5th Annual Symposium on Smart Structures and Materials*, March, San Diego, CA.

52. http://www.mrfluid.com

53. Poynor, J. C., (2001), "Innovative Design for Magneto-Rheological Dampers," M.S. Thesis, Virginia Polytechnic Institute and State University, Blacksburg, Virginia.

54. Ahmadian, M., (1999), "Design and Development of Magneto-Rheological Dampers for Bicycle Suspensions," *ASME Dynamical Systems & Control Division*, DSC-Volume 67, pp. 737-741.

55. Ahmadian, M., Poynor, J. C,., and Gooch, J. M., (1999), "Application of Magneto-Rheological Dampers for Controlling Shock Loading," *ASME Dynamical Systems & Control Division*, DSC-Volume 67, pp. 731-735.

56. Dyke, S. J., Spencer Jr. B. F., Sain, M. K., and Carlson, J. D., (1996), "Seismic Response Reduction Using Magnetorheological Dampers," *Proceedings of the IFAC World Congress*, June 30 –July 5, San Francisco, CA.

57. Housner, G. W., Bergman, L. A., Caughey, T. K., Chassiakos, A. G., Claus, R. O., Masri, S. F., Skelton, S.E., Soong, T. T., Spencer, B.F., and Yao, J. T. P., (1997), "Structural Control: Past, Present, and Future," *Journal of Engineering Mechanics*, 123 (9), pp. 897-971.

58. Symans, M. D. and Constantinou, M. C., (1999), "Semiactive control systems for seismic protection of structures: a state-of-art review," *Journal of Engineering Structures*, 21, pp. 469-487.

59. Soong, T. T. and Spencer, B.F. Jr., (2002), "Supplemental energy dissipation: state-of-the-art and state-of-the-practice," *Journal of Engineering Structures*, 24, pp. 243-259.

60. Spencer, B. F. Jr., Dyke, S. J., Sain, M. K., and Carlson, J. D., (1997), "Phenomenological Model of a Magnetorheological Damper," *Journal of Engineering Mechanics*, Vol. 123, No. 3, pp. 230-238.

61. Dyke, S. J., Spencer, B. F. Jr., Sain, M. K., and Carlson, J. D., (1996), "Modeling and Control of Magnetorheological Dampers for Seismic Response Reduction," *Smart Materials and Structures*, Vol. 5, pp. 565-575.

62. Dyke, S. J., Spencer, B. F. Jr., Sain, M. K., and Carlson, J. D., (1998), "An Experimental Study of MR dampers for Seismic Protection," *Smart Materials and Structures*, Vol. 7, pp. 693-703.

63. Hiemenz, G. J., Choi, Y. T., and Wereley, N. M., (2000), "Seismic Control of Civil Structures Utilizing Semiactive MR Bracing Systems," *Proceedings of SPIE*, Vol. 3988, pp. 217-228.

64. Yi, F., Dyke, S. J., Caicedo, J. M., and Carlson, J. D., (2001), "Experimental Verification of Multinput Seismic Control Strategies for Smart Dampers," *Journal of Engineering Mechanics,* Vol. 127, No. 11, pp. 1152-1164.

65. Yoshioka, H., Ramallo, J. C., and Spencer, B. F., (2002), ""Smart" Base Isolation Strategies Employing Magnetorheological Dampers," *Journal of Engineering Mechanics,* Vol. 128, No. 5, pp. 540-551.

66. Abe, M. and Igusa, T. (1996), "Semiactive Dynamic Vibration Absorbers for Controlling Transient Response," *Journal of Sound and Vibration*, 198(5), pp. 547-569.

67. Hidaka, S., Ahn, Y. K., and Morishita, S., (1999), "Adaptive Vibration Control by a Variable-Damping Dynamic Absorber Using ER Fluid," *Journal of Vibration and Acoustics*, vol. 121, July, pp. 373-378.

68. Pinkaew, T. and Fujino, Y., (2001), "Effectiveness of Semiactive Tuned Mass Dampers Under Harmonic Excitation," *Engineering Structures*, 23, pp. 850-856

69. Koo, J. H., Ahmadian, M., Setareh, M., and Murray, T., "An Experimental Evaluation of Magneto-Rheological Dampers for Semiactive Tuned Vibration Absorbers," *SPIE 2003 Smart Structures and Materials/NDE*, Paper No. 5052-12, March 2-6, 2003 in San Diego, CA, USA.

70. Koo, J. H., Ahmadian, M., "A Qualitative Analysis of Groundhook Tuned Vibration Absorbers for Controlling Structural Vibrations," *Proceedings of the IMECHE Park K, Journal of Multibody Dynamics*, Vol. 216, No. 4, pp. 351-359.

71. Koo, J. H., Ahmadian, M., and Setareh, M., "Adaptability Analysis of Semiactive Tuned Vibration Absorbers for Controlling Floor Vibrations," *US-Korea Conference on Science, Technology, and Entrepreneurship*, July 8-11, 2002, Seoul, Korea

72. Koo, J. H., Ahmadian, M., Setareh, M., and Murray, T., "In Search of Suitable Control Methods for Semiactive Tuned Vibration Absorbers," *Journal of Vibration and Control*. (in press)

73. Agrawal, A. K. and Yang, J. N., (2000), "Semiactive control strategies for building subject to near-field earthquakes," *Proceedings of SPIE*, Vol. 3988, pp. 359-370.

74. Abe, M. and Igusa, T., (1996), "Semiactive Dynamic Vibration Absorbers for Controlling Transient Response," *Journal of Sound and Vibration*, 198(5), pp. 547-569.

75. Hidaka, S., Ahn, Y. K., and Morishita, S., (1999), "Adaptive Vibration Control by a Variable-Damping Dynamic Absorber Using ER Fluid," *Journal of Vibration and Acoustics*, Vol. 121, pp. 373-378.

76. Pinkaew, T. and Fujino, Y., (2001), "Effectiveness of Semiactive Tuned Mass Dampers Under Harmonic Excitation," *Engineering Structures*, 23, pp. 850-856.

77. Karnopp, D. C., and Crosby, M. J., (1974), "System for Controlling the Transmission of Energy Between Spaced Members," U.S. Patent 3,807,678.

78. Karnopp, D. C., Crosby, M. J., and Harwood, R. A., (1974), "Vibration Control Using Semiactive Force Generators," *American Society of Mechanical Engineers, Journal of Engineering for Industry*, May, pp. 619-626.

79. Crosby, M. J., and Karnopp, D. C., (1973), "The Active Damper," *The Shock and Vibration Bulletin* 43, Naval Research Laboratory, Washington D. C.

80. Miller, L. R., (1988), "An Approach to Semiactive Control of Multi-Degree-of-Freedom Systems," Ph.D. Thesis, North Carolina State University, Raleigh, N.C.

81. Carter, A. K., (1998), "Transient Motion Control of Passive and Semiactive Damping for Vehicle Suspensions," M.S. Thesis, Virginia Polytechnic Institute and State University, Blacksburg, Virginia.

82. Ahmadian, M. and Pare, C., (2000), "A Quarter-Car Experimental Analysis of Alternative Semiactive Control Methods," *Journal of Intelligent Material Systems and Structures*, Vol. 11, pp. 604-612.

83. Simon, D. E., (2001), "An Investigation of the Effectiveness of Skyhook Suspensions for Controlling Roll Dynamics of Sport Utility Vehicles Using Magneto-Rehological Dampers," Ph. D. Dissertation, Virginia Polytechnic Institute and State University, Blacksburg, Virginia.

84. Inman, D. J., (2001), *Engineering Vibration*, 2nd edition, Prentice-Hall, Inc., New Jersey.

85. Bachmann H., et al., (1995), *Vibration Problems in Structures: Practical Guidelines*, Birkhäuser Verlang, Basel; Boston; Berlin.

Vita

Jeong-Hoi Koo is originally from HongSung, Korea. He graduated from Chungnam National University (CNU), Teajon, Korea in February 1998 with B. Eng. degree. In order to broaden his academic career, he began his graduate study at South Dakota State University (SDSU), in Brookings, SD. He worked as a graduate exchange student from the fall of 1998 to July of 1999. After completing his Master's degree, he moved to Blacksburg, VA to pursue a Ph. D degree in Mechanical Engineering at Virgina Tech in the fall of 1999. He earned his Ph.D in summer 2003. He is currenlty working as a post-doctoral researcher at the Advance Vehicle Dynamics Laboratoty at Virgina Tech, and an adjuct faculty at a local college. He married Eunsun Yook in May 2000, and they are expecting their first baby in May 2004.